
ETD Archive

2012

Gain-of-Function Mutations in SCN5A Gene Lead to Type-3 Long QT Syndrome

Fang Fang
Cleveland State University

Follow this and additional works at: <https://engagedscholarship.csuohio.edu/etdarchive>

 Part of the [Chemistry Commons](#)

[How does access to this work benefit you? Let us know!](#)

Recommended Citation

Fang, Fang, "Gain-of-Function Mutations in SCN5A Gene Lead to Type-3 Long QT Syndrome" (2012). *ETD Archive*. 94.

<https://engagedscholarship.csuohio.edu/etdarchive/94>

This Dissertation is brought to you for free and open access by EngagedScholarship@CSU. It has been accepted for inclusion in ETD Archive by an authorized administrator of EngagedScholarship@CSU. For more information, please contact library.es@csuohio.edu.

GAIN-OF-FUNCTION MUTATIONS IN SCN5A GENE LEAD TO TYPE-3 LONG QT
SYNDROME

FANG FANG

Bachelor's of Science in Chemistry

Zhengzhou University

August 2004

Master's of Science in Chemistry

Cleveland State University

December 2009

submitted in partial fulfillment of requirement for the degree

DOCTOR OF PHILOSOPHY IN CLINICAL AND BIOANALYTICAL CHEMISTRY

at the

CLEVELAND STATE UNIVERSITY

NOV 2012

@COPYRIGHT BY FANG FANG 2012

This dissertation has been approved for
the Department of Chemistry and for the College of Graduate Studies of
Cleveland State University

By

Dr. Qing Wang, Department of Molecular Cardiology/CCF
Major Advisor
Date _____

Dr. Yan Xu, Department of Chemistry/CSU
Academic Advisor
Date _____

Dr. Xue-long Sun, Department of Chemistry/CSU
Advisory Committee Member
Date _____

Dr. Robert Wei, Department of Chemistry/CSU
Advisory Committee Member
Date _____

Dr. Yuping Wu, Department of Mathematics/CSU
External Examiner
Date _____

ACKNOWLEDGEMENTS

I would like to take this opportunity to express my sincere appreciation to everyone who has helped me in the past six years. I would especially thank my research advisor, Dr. Qing Wang, who gave me opportunities to study these interesting projects. During my five years of study in Dr. Wang's lab, not only did he have provided all the possible experimental environment and let me finish my research study, but he also showed his patience, encouragement and financial support.

Besides, I would like to thank Dr. Teng Zhang and Dr. Sandro Yong in our lab who gave me a lot of advices and trained me to learn experiment techniques I used in my research. I would like to thank Dr. Carlos Oberti and Xiaofen Wu, the experts in Cardiology, to give me a lot of advice in Electrocardiogram (ECG) readings.

I also would like to thank all my committee members, Dr. Yan Xu, Dr. Robert Wei, Dr. Xue-long Sun and Dr. Yuping Wu for their revision and suggestion of this dissertation.

Finally, I would like to thank my husband, Dr. Xiaopeng Li and my parents. Without their support, I cannot complete this dissertation. I would also like to thank my son, Yifang Li, being such a wonderful boy and using his sweetest smile to support me.

GAIN-OF-FUNCTION MUTATIONS IN SCN5A GENE LEAD TO TYPE-3 LONG QT SYNDROME

FANG FANG

ABSTRACT

Type-3 long QT syndrome, which is related to type 5 voltage-gated sodium channel alpha subunit (*SCN5A*) mutation, has been identified since 1995. LQTS mutation in *SCN5A* is a gain-of-function mutation producing late sodium current, $I_{Na,L}$. Brugada mutation in *SCN5A* is a loss-of-function causing I_{Na} decrease. Whereas, the mechanism for Dilated Cardiomyopathy mutations in *SCN5A* is still not fully understood.

N1325S is one of the first series of mutations identified for type-3 LQTS. Our lab created a mouse model for LQTS by expressing *SCN5A* mutation N1325S in the mouse hearts (TG-NS) and a matched experimental control line with overexpression of wild-type *SCN5A* (TG-WT). There are some interesting findings in TG-NS mice: (i) Intracellular sodium (Na^+) level is higher in TG-NS myocytes compared with TG-WT myocytes. (ii) Ca^{2+} handling is abnormal in TG-NS myocytes, but not in TG-WT myocytes. (iii) Apoptosis was also found in TG-NS mouse heart tissue, but not in TG-WT hearts. These results provoke the hypothesis that gain-of-function mutation N1325S in *SCN5A* leads to LQTS through abnormal cytosolic Ca^{2+} homeostasis.

Another LQTS mutation in *SCN5A* R1193Q was identified in 2004 and the electrophysiological property is similar to other gain-of-function *SCN5A* mutations. The transgenic mouse model for this mutation was also established and the surface

Electrocardiogram (ECG) results indicate longer corrected QT interval also present in transgenic mice carrying R1193Q mutation. Besides, quinidine, an anti-arrhythmic medication, can cause arrhythmic symptoms such as premature ventricular contraction (PVC), premature atrial contraction (PAC) and atrioventricular (AV) block in R1193Q transgenic mice.

In order to further study the relationship between abnormal Ca^{2+} handling and the type of *SCN5A* mutation, either gain-of-function or loss-of-function, we have chosen HL-1 cells, a cell line with indefinite passages in culture with all the adult cardiac phenotypes. The similar abnormal Ca^{2+} handling was also identified in HL-1 cells expressing N1325S mutation but not in those cells expressing wild-type *SCN5A* gene. Since we hypothesized that the abnormal Ca^{2+} handling is caused by $\text{I}_{\text{Na,L}}$ created by gain-of-function mutation, either in HL-1 cells or in isolated TG-NS myocytes, I then use $\text{I}_{\text{Na,L}}$ blocker ranolazine, a clinical trial medication for LQT patients, to specifically block $\text{I}_{\text{Na,L}}$. After the blockage of $\text{I}_{\text{Na,L}}$, the abnormal Ca^{2+} handling was rescued in both isolated myocytes from TG-NS mice and HL-1 cells expressing N1325S mutation. Finally, several different types of *SCN5A* mutations related to different types of heart diseases were selected and the Ca^{2+} handling was tested in transfected HL-1 cells.

TABLE OF CONTENTS

ABSTRACT	v
LIST OF TABLES	xiii
LIST OF FIGURES	xiv
LIST OF ABBREVIATIONS.....	xv
CHAPTER	
I. INTRODUCTION	1
1.1 Voltage-Gated Sodium Channel Gene <i>SCN5A</i>	1
1.1.1 The Family of Voltage-Gated Sodium Channels	1
1.1.2 Type 5 Voltage-Gated Sodium Channel $Na_v1.5$ and <i>SCN5A</i> Gene	5
1.2 Cardiac Disease and Mutations in <i>SCN5A</i> Gene	6
1.2.1 Long QT Syndrome	7
1.2.2 Dilated Cardiomyopathy	9
1.2.3 Brugada Syndrome	9
1.2.4 Progressive Cardiac Conduction Defect (PCCD).....	11
1.2.5 Sick Sinus Syndrome (SSS)	13
1.2.6 Atrial Fibrillation	14
1.2.7 Overlapping Syndromes	15
1.3 Cardiovascular System	15
1.3.1 The Structure of the Cardiovascular System	15

1.3.2 Electrical Conduction in the Heart and Electrocardiogram	
(ECG)	17
1.4 HL-1 Atrial Cells	17
1.4.1 Development of HL-1 Cardiomyocytes	17
1.4.2 Studies of Cardiac Muscle Cell Structure and Function	
Using HL-1 Cardiomyocytes	18
1.5 Regulation of Na _v 1.5 Function in Cardiac Cells	19
1.5.1 Ankyrin Proteins	19
1.5.2 Caveolin-3	19
1.5.3 Na _v 1.5 β-Subunits	20
1.5.4 Protein Kinase A (PKA)	21
1.5.5 Tyrosine Phosphorylation of Na _v 1.5	22
1.5.6 Glycerol-3-Phosphate Dehydrogenase Like Protein (<i>GPD1-L</i>)...	23
1.5.7 Calmodulin (CaM)	23
1.5.8 Ca ²⁺ /Calmodulin-Dependent Protein KinaseII (CaMKII).....	24
1.5.9 <i>MOG1</i>	25
1.5.10 Fibroblast Growth Factor Homologous Factor 1B (<i>FHF1B</i> or	
<i>FGF12-1b</i>)	25
1.5.11 14-3-3η Protein	26
1.5.12 Ubiquitin-Protein Ligases of the <i>Nedd4/Nedd4</i> -Like Family...	26
1.6 Anti-Arrhythmic Medications and Their Side Effects	27

1.6.1 Quinidine	27
1.6.2 Mexiletine	28
1.6.3 Ranolazine	29
1.6.4 Other Anti-Arrhythmic drugs.....	30
1.7 Cardiac Excitation-Contraction Coupling (ECG) and Ca^{2+} Handling in	
Cardiac Cells	30
1.7.1 The Importance of Ca^{2+} in Cardiomyocytes	30
1.7.2 The Process of Excitation-Contraction Coupling	31
1.7.3 Cardiac Ion Channels and Cardiac Action Potential	33
1.7.4 The Cellular Relaxation and the Removal of Cytosolic Ca^{2+}	33
1.7.5 Dysfunction of $\text{Na}^{+}/\text{Ca}^{2+}$ Exchanger Causes Ca^{2+} Overload and	
Arrhythmias	33
1.7.6 Intracellular Ca^{2+} Transient and Excitation-Contraction	
Coupling	36
II CARDIAC EXPRESSION OF <i>SCN5A</i> SNP R1193Q IN TRANSGENIC MICE	
PRLONGS QT INTERVAL	38
2.1 Abstract	38
2.2 Introduction	39
2.3 Materials and Methods	40
2.3.1 Preparation of Experimental Animals.....	40
2.3.2 Western Blot Analysis	42

2.3.3 Semi-Quantitative Real-Time PCR (RT-PCR) Analysis.....	43
2.3.4 Telemetry ECG Recordings	43
2.3.5 Echocardiographic Assessment of Cardiac Structure and Function in Transgenic Mice	44
2.3.6 Data Analysis	44
2.4 Results	45
2.4.1 Generation and Identification of Transgenic Mice with Cardiac Specific Overexpression of Mutant Human <i>SCN5A</i> Gene with SNP R1193Q.....	45
2.4.2 Development of Long-QT Syndrome in TG-RQ Mice.....	47
2.4.3 Quinidine Prolonged QTc, and Increased the Frequencies of PACs, PVCs, and Sinus Atrial Exit Block in TG-RQ Mice.....	49
2.4.4 Echocardiographic Assessment of Cardiac Structure and Function in the Mice	54
2.5 Discussion	56
III LQTS MUTATION N1325S IN <i>SCN5A</i> CAUSES DISRUPTION OF CYTOSOLIC CALCIUM HOMEOSTASIS IN MOUSE VENTRICULAR MYOCYTES	59
3.1 Abstract	59
3.2 Introduction	60
3.3 Methods and Materials	62

3.3.1 Isolation of Mouse Ventricular Myocytes	62
3.3.2 Measurements of Ca^{2+} Transient Signals	64
3.4 Results	65
3.5 Discussion	69
IV LATE SODIUM CURRENT PRODUCED BY GAIN-OF-FUNCTION LQTS	
MUTATIONS IN CARDIAC SODIUM CHANNEL LEADS TO ABNORMAL	
CALCIUM HANDLING IN CARDIAC CELLS	72
4.1 Abstract	72
4.2 Introduction	73
4.3 Materials and Methods	75
4.3.1 HL-1 Cardiac Cell Culture	75
4.3.2 Na^{+} Channel Cloning and Site-Directed Mutagenesis	76
4.3.3 HL-1 Cell Transfection	76
4.3.4 Intracellular Ca^{2+} Transient Measurements	77
4.3.5 Data Analysis	77
4.4 Results	78
4.4.1 N1325S Mutant Sodium Channels Lead to Irregular	
Ca^{2+} Handling in HL-1 Cells	78
4.4.2 Ranolazine Can Reduce the SR Ca^{2+} Content and Strengthen	
the Ability of Removing Extra Cytosolic Ca^{2+} in HL-1 Cells	
Expressing N1325S Mutant <i>SCN5A</i>	81

4.4.3 Mexiletine Can Reduce the SR Ca^{2+} Content in HL-1 Cells	
Expressing N1325S Mutant <i>SCN5A</i>	85
4.4.4 Classification of Different <i>SCN5A</i> Mutations	87
4.4.5 Ranolazine Effect in Various <i>SCN5A</i> Mutations.....	89
4.5 Discussion	91
BIBLIOGRAPHY	94

LIST OF TABLES

Table	page
I. Different Types of Voltage-Gated Sodium Channel Alpha Subunit	3
II. Overlapping Syndrome of Cardiac Sodium Channelopathy	16
III. Ionic Currents and Different Phases of AP	35
IV. Effects of Quinidine Treatment on PACs, PVCs and SAEB in TG-RQ Mice and Control NTG Mice.....	53
V. Echocardiographic Assessment of Cardiac Structure and Function in the Mice.....	55

LIST OF FIGURES

Figure	Page
1. Schematic Diagram of Cardiac Excitation-Contraction Coupling (ECG) Events in Ventricular Myocytes	32
2. A schematic Diagram Showing that Different Ionic Currents Contribute to Different Phases of a Cardiac Action Potential	34
3. Generation and Genotyping of TG-RQ Mice	46
4. ECG Recordings of Non-Transgenic(NTG), Transgenic Wild-Type (TG-WT) and Transgenic R1193Q (TG-RQ) Mice	48
5. Quinidine Treatment Prolonged QTc in Both NTG and TG-RQ Mice.....	50
6. Quinidine Treatment Induced Increased PVCs, PACs and SAEB in TG-RQ mice.....	52
7. Ca ²⁺ Transients Signals in Isolated TG-NSL3 Mice Myocytes	67
8. Ca ²⁺ Transients Signals in Isolated TG-NSL12 Mice Myocytes	68
9. Ca ²⁺ Transient Signals in Transfected HL-1 Cells	80
10. Effect of Ranolazine Treatment in HL-1 Cells Expressing the N1325S Mutation	84
11. Effect of Mexiletine treatments in HL-1 Cells Expressing the N1325S Mutation.....	86
12. Effects of Different <i>SCN5A</i> Mutations on Ca ²⁺ Transients	88
13. Effect of Ranolazine in Various <i>SCN5A</i> Mutations	90

LIST OF ABBREVIATIONS

AF	Atrial Fibrillation
AP	Action Potential
AV node	Atrioventricule node
BDM	2,3-Butanedione Monoxime
BrS	Brugada Syndrome
CaM	Calmodulin
CaMKII	Ca ²⁺ /Calmodulin-Dependent Protein Kinase II
CCD	Cardiac Conduction Disturbance
CICR	Ca ²⁺ Induced Ca ²⁺ Release
CNS	Central Nerve System
DAD	Delayed Afterdepolarization
DCM	Dilated Cardiomyopathy
DRG	Dorsal Root Ganglion
EAD	Early Afterdepolarization
ECC	Excitation-Contraction Coupling
ECG	Electrocardiogram
EGF	Epidermal Growth Factor
EGFR	Epidermal Growth Factor Receptor
ER	Endoplasmic Reticulum

FHF1B	Fibroblast Growth Factor Homologous Factor 1B
GPD1-L	Glycerol-3-Phosphate Dehydrogenase Like Protein
IQ	Isoleucine-Glutamine
IVF	Idiopathic Ventricular Fibrillation
LQTS	Long QT Syndrome
MHC	Myosin Heavy Chain
MOG1	Multicopy Suppressor of gsp1 Mutants
NCX	Na ⁺ /Ca ²⁺ Exchanger
PACs	Premature Atria Contractions
PCCD	Progressive Cardiac Conduction Defect
PKA	Protein Kinase A
PKC	Protein Kinase C
PVCs	Premature Ventricle Contractions
PVDF	Polyvinylidene Difluoride
RT-PCR	Real-Time Polymerase Chain Reaction
SA node	Sinoatrial node
SERCA	Sarcolemmal Ca ²⁺ -ATPase
SIDS	Sudden Infant Death Syndrome
SND	Sinus Node Dysfunction
SNP	Single Nucleotide Polymorphism

SR	Sarcoplasmic Reticulum
SSS	Sick Sinus Node Syndrome
TN-C	Troponin Complex
TTX	Tetrodotoxin
VF	Ventricular Fibrillation
VT	Ventricular Tachycardias

CHAPTER I

INTRODUCTION

1.1 Voltage-Gated Sodium Channel Gene *SCN5A*

1.1.1 The Family of Voltage-Gated Sodium Channels

Voltage-gated sodium channels are large membrane proteins which produce depolarization and initiate action potentials in neurons, cardiomyocytes and skeleton muscle cells (Andavan and Lemmens-Gruber 2011). The sodium channels are composed of a large pore forming α subunit and one or several small β subunits (Abriel 2007). To date, there are at least twelve different α subunit isoforms and four β subunit isoforms that have been cloned for voltage-gated sodium channels in mammals.

Voltage-gated sodium channel α subunit contains four homologous domains (DI to DIV), and each domain is composed of six transmembrane segments (S1 to S6) (Abriel 2007). The fourth transmembrane segment (S4) carries positively charged amino acids and plays an important role as a voltage sensor (Abriel and Kass 2005). The pore is

formed by the extracellular loop between S5 and S6 (Schroeter et al 2010). The site-directed mutation study in the sodium channel α subunit indicates that the activation of the channel is regulated by S6 (Hanlon and Wallace 2002). The fast inactivation involves the linker between DIII and DIV; whereas the slow inactivation is modulated by the conformational change of the extracellular region of the channel (Hanlon and Wallace 2002, Ragsdale et al 1994).

Twelve isoforms of voltage-gated sodium channel α subunits are expressed in different tissues (Table I). The dysfunction of sodium channels causes a variety of human diseases. *SCN1A*, *SCN2A* and *SCN3A* are mainly expressed in neurons, and the mutations in these three sodium channels can cause seizures and epilepsy, especially in infants (Baulac et al 1999, Bender et al 2012, Kearney et al 2001, Saitoh et al 2012, Wallace et al 2001). Mutations in skeleton muscle sodium channel gene *SCN4A* cause hyperkalemic periodic paralysis and paramyotonia congenital (Meyer-Kleine et al 1994, Plassart et al 1994). Mutations in cardiac sodium channel gene *SCN5A* produce persistent late sodium current ($I_{Na,L}$) and are the main cause of long-QT syndrome (LQTS), ventricular fibrillation (VF) and Brugada syndrome (Baroudi et al 2000, Bezzina et al 1999, Chen et al 2002, Deschênes et al 2000, Tian et al 2004, Tian et al 2007, Wan et al 2001, Wang et al 1995a, Wang et al 2004, Zhang et al 2011). In 1990, *SCN6A* was identified in human heart and uterus (George et al 1994). Later, *SCN7A* was assigned although the authors symbolized this gene as *SCN6A*, and the localization of *SCN7A* (*SCN6A*) was obtained using chromosome microdissection-PCR method (George et al 1994, Han et al 1991). The single nucleotide polymorphism in human *SCN7A* gene was found to be associated with essential hypertension in the Chinese population (Zhang et al 2003). *SCN8A*

Table I. Different Types of Voltage-Gated Sodium Channel Alpha Subunit

Gene	Chromosome Localization	Tissue	Mutation and Disease	References
<i>SCN1A</i>	2q23-q24	Brain	Epilepsy and Dravet's syndrome	(Saitoh et al 2012) (Bender et al 2012) (Wallace et al 2001)
<i>SCN2A</i>	2q22-q23	Brain	Seizures	(Kearney et al 2001)
<i>SCN3A</i>	2q24-q31	Brain and dorsal root ganglion (DRG)	Epilepsy	(Baulac et al 1999)
<i>SCN4A</i>	17q23.1-q25.3	Skeletal muscle	Paramyotonia and congenita	(Plassart et al 1994) (Meyer-Kleine et al 1994)
<i>SCN5A</i>	3p21	Heart	LQTS	(Wang et al 1995b) (Bezzina et al 1999)
<i>SCN6A</i>	2q21-q23	Uterus and heart	Essential hypertension	(George et al 1994) (Zhang et al 2003)
<i>SCN7A</i>	2q21-q23	Glial cells and DRG	N/A	(Potts et al 1993)
<i>SCN8A</i>	12q13	Brain, DRG and spinal cord	Cerebellar atrophy, ataxia and mental retardation	(Trudeau et al 2006)
<i>SCN9A</i>	2q24	DRG, brain and spinal cord	Insensitive to pain	(Nilsen et al 2009)
<i>SCN10A</i>	3p22-p24	DRG and heart	Longer PR on ECG	(Chambers et al 2010)
<i>SCN11A</i>	3p21-p24	DRG	N/A	(Jeong et al 2000)
<i>SCN12A</i>	3p23-p21.3	Central nerve system (CNS) and DRG	N/A	(Jeong et al 2000)

was found in fetal brains and the protein contains 1,980 amino acids. Interestingly, human *SCN8A* shares 98.5% sequences with the same mouse gene (Plummer et al 1998). *SCN8A* gene was first studied in mutant mice. Mutations in *SCN8A* in mice caused dysfunction in motor units such as “motor endplate disease” and mutant jointing (Burgess et al 1995, Kohrman et al 1996). A patient with a heterozygous two base pairs deletion mutation in exon 24 of *SCN8A* was found to have cerebellar atrophy, ataxia, and mental retardation (Trudeau et al 2006). Higher resistance to seizures in two mutant *Scn8a* mouse lines, *Scn8a* (med) and *Scn8a* (med-jo) suggests that mutant *Scn8a* can reduce the neural excitability (Martin et al 2007). Mutations in *SCN9A* were found in patients insensitive to pain, which is termed as “channelopathy -associated insensitivity to pain” (Nilsen et al 2009). Genome wide association studies of *SCN10A* indicated that SNPs in this gene can lead to longer PR interval on electrocardiograms (ECG) (Chambers et al 2010). *Scn11a* was first identified in the mouse and expressed in the small sensory neurons of dorsal ganglia (DRG) and trigeminal ganglia (Dib-Hajj et al 1998, Dib-Hajj et al 1999). Later, *SCN11A*, which was called *SCN12A*, was identified in the human brain and found to be expressed in the central nervous system (CNS) especially in the gray matter of the hippocampus, cerebellum and olfactory bulb (Jeong et al 2000).

Although different types of sodium channels are expressed in different species and tissues, they are highly conserved evolutionarily. Cardiac sodium channel gene, *SCN5A*, is especially highly homologous to *SCN8A* and *SCN9A* which are primarily expressed in neurons (Kerr et al 2004, Plummer and Meisler 1999). *SCN6A* and *SCN7A* are actually orthologs in the human and mouse (George et al 1990, George et al 1994, Han et al 1991). *SCN1A*, *SCN2A* and *SCN3A* are form a gene cluster on chromosome 2q24 (Mulley et al

2005). *SCN5A*, *SCN10A* and *SCN11A* are evolutionally more closely related because they are tetrodotoxin-sensitive, and all located on chromosome 3p21 (Plummer and Meisler 1999). The sequence of *SCN8A* is also highly similar to different domains in *SCN2A*, *SCN4A* and *SCN5A*. For example, the second domain in *SCN8A* is 93%, 89% and 80% homologous to *SCN2A*, *SCN4A* and *SCN5A*, respectively. However, the cytoplasmic loop between Domain I and Domain II in *SCN8A* is less identical to the other three genes (Plummer and Meisler 1999).

The β subunits for voltage-gated sodium channels are glycoproteins which are not only the accessory part for alpha subunits, but also modulate Na^+ current (I_{Na}) (Patino and Isom 2010). In addition, they function in cell aggregation, migration, invasion and neurite outgrowth when working as cell adhesion molecules (CAM) (Schroeter et al 2010). There are at least four types of voltage-gated sodium channel β subunits referred to as $\beta 1$ - $\beta 4$, which are encoded by *SCN1B*-*SCN4B*, respectively (Patino and Isom 2010).

1.1.2 Type 5 Voltage-Gated Sodium Channel $\text{Na}_v1.5$ and *SCN5A* Gene

Type 5 voltage-gated sodium channel, $\text{Na}_v1.5$, is an integrated membrane protein which mediates the rapid upstroke of the action potential (AP) in cardiac cells. $\text{Na}_v1.5$ is the pore forming subunit of human cardiac sodium channel. The entrance of Na^+ through $\text{Na}_v1.5$ into a cardiac cell initiates the action potential in both ventricular and atrial cardiac cells (Schroeter et al 2010). $\text{Na}_v1.5$ is encoded by the *SCN5A* gene which is located on chromosome 3p21 and is composed of 22 introns and 28 exons (George et al 1995). $\text{Na}_v1.5$ is a large protein containing 2,016 amino acids with an estimated molecular weight of 227 kDa (Wang et al 1996b). Northern blot analysis showed that this

gene was mainly expressed in the heart (Gellens et al 1992).

Currently, there are several alternatively spliced $\text{Na}_v1.5$ variants in different species and tissues. $\text{Na}_v1.5a$ was first observed in rat brain, and was the first cardiac sodium channel splice variant. Later, $\text{Na}_v1.5a$ was found in diverse tissues in rodents, but was not expressed in human heart (Schroeter et al 2010). $\text{Na}_v1.5c$ and $\text{Na}_v1.5d$ are two splice variants in human hearts. The expression of $\text{Na}_v1.5c$ is more abundant than $\text{Na}_v1.5d$. In $\text{Na}_v1.5c$, an extra glutamine residue is introduced at codon position 1077 on the 5'-end of exon 18. The transcriptional ratio of $\text{Na}_v1.5c$: $\text{Na}_v1.5$ is around 1:2, and there is no obvious functional differences in $\text{Na}_v1.5c$ compared with $\text{Na}_v1.5$ (Makielski et al 2003). In $\text{Na}_v1.5d$, a 120 bp fragment is deleted from exon 17, and as a result, 44 amino acids are missing on the intracellular loop II between the second segment DII and the third segment DIII. Electrophysiological study has demonstrated that the channel kinetics is significantly changed in $\text{Na}_v1.5d$ (Camacho et al 2006, Gellens et al 1992).

1.2 Cardiac Diseases and Mutations in *SCN5A* Gene

In 1995, the first mutation in the *SCN5A* gene was identified and linked to an inherited cardiac arrhythmia, long QT syndrome (LQTS) (Wang et al 1995b). Since then, various mutations in this gene have been found and associated with numerous arrhythmic syndromes, such as Brugada syndrome (BrS), progressive cardiac conduction defect (PCCD), sick sinus node syndrome (SSS), atrial fibrillation (AF) and dilation cardiomyopathy (DCM) (Beggs 1997, Chen et al 1998, Lei et al 2008, Makiyama et al 2008, Tan et al 2001).

1.2.1 Long QT Syndrome

LQTS is a cardiac disorder characterized by the prolonged QT interval on the surface electrocardiogram (ECG), syncope and sudden death as a result of a polymorphic ventricular tachycardia, *torsade de pointes* (Wang et al 2004). Both genetic and acquired or environmental factors contribute to the pathogenesis of LQTS. To date, LQTS is known to be caused by mutations in at least thirteen genes, including the cardiac potassium channel genes *KvLQT1* or *KCNQ1* (11p15.5, LQT1) (Neyroud et al 1997, Splawski et al 1997a, Wang et al 1996a), *HERG* or *KCNh2* (7q35-36, LQT2) (Curran et al 1995), the cardiac sodium channel gene *SCN5A* (3p21-24, LQT3) (Wang et al 1995a), the non-ion channel ankyrin-B gene encoding a protein that links ion channels to the cytoskeleton (4q25-27, LQT4) (Mohler et al 2003), cardiac potassium channel gene *KCNE1* (21q22, LQT5) (Schulze-Bahr et al 2003, Splawski et al 1997b), *KCNE2* (21q22, LQT6) (Abbott et al 1999), *KCNJ2* (17q24.3, LQT7) (Tristani-Firouzi et al 2002), L-type Ca²⁺ channel *CACNA1C* (12p13.3, LQT8) (Navedo et al 2010), scaffolding protein caveolin-3 *CAV3* (3p25, LQT9) (Balijepalli and Kamp 2008), the cardiac sodium channel gene *SCN4B* (11q22.3, LQT10) (Vincent 2003), A-kinase-anchoring protein-9 (*AKAP9*) (7q21.2, LQT11) (Chen et al 2007), alpha-1 syntrophin gene (*SNTA1*) (20q11.21, LQT12) (Ueda et al 2008), and potassium channel gene *KCNJ5* (11q24, LQT13) (Yang et al 2010).

In 1995, Wang et al. reported that mutations in the cardiac sodium channel gene *SCN5A* caused type 3 LQTS. To date, there are more than 45 mutations in *SCN5A* that have been identified to be causative to LQTS. These mutations span the entire sodium channel from the 9th amino acid (G9V) to the last amino acid (P2006A) (Wang et al 2007).

The first gain-of-function mutation Δ KPQ in *SCN5A* produced late Na^+ current (I_{NaL}) and was first identified in two unrelated LQTS families. Δ KPQ is a three amino acids deletion at position 1505-1507 locating at the intracellular loop between DIII and DIV (Wang et al 1995b). Because of the persistent late Na^+ current (I_{NaL}), which is caused by the fluctuation of this mutant channel between normal and non-inactivating modes, the cardiac action potential is prolonged, which provides a potential mechanism for this type of congenital LQTS (Bennett et al 1995). N1325S is another gain-of-function mutation in *SCN5A* gene causing type 3 LQTS. A transgenic mouse model which expressed mutant human N1325S *SCN5A* gene was established and showed prolonged QT interval on ECG, spontaneous ventricular tachyarrhythmia (VT) and ventricular fibrillation (VF) (Tian et al 2004).

In 2004, a missense mutation in *SCN5A*, R1193Q, was found in one of seven patients with drug-induced acquired LQTS. This mutation can destabilize inactivation gating and generate a persistent, non-inactivating current in both human kidney (HEK-293) cells and *Xenopus* oocytes. The biophysical defects of R1193Q are almost identical to two well-characterized *SCN5A* mutations, N1325S and R1644H (Wattanasirichaigoon et al 1999), which can cause type 3 LQTS. One group reported that *SCN5A* R1193Q is a polymorphism in a Chinese family that is associated with progressive cardiac conduction defects and long QT syndrome (Sun et al 2008). Another group reported that *SCN5A* R1193Q is a common polymorphism in general Chinese population. They pointed out that about 12% (11/94) of the subjects carried the R1193Q mutation. They analyzed clinical data from 9 of the 11 patients with the mutation. Although none of the carriers had Brugada syndrome, one had prolonged QTc and

another had borderline QTc appeared to be homozygous for R1193Q (Hwang et al 2005).

1.2.2 Dilated Cardiomyopathy

Patients with idiopathic dilated cardiomyopathy (DCM) usually have clinical features of an increased ventricular size and reduced ventricular systolic function (Beggs 1997). Most mutations causing DCM are thought to have either structural defects or dysfunction in electrical excitation-contraction in cardiac cells. The structural defects caused by DCM mutations usually result in contractile filament disarray and cell death, and further lead to fibrosis which is the characteristics of DCM (Asahi et al 2003, Chen and Chien 1999, Kane et al 2005, Schmitt et al 2003).

In 1996, *SCN5A* was first related to DCM after the study of a family with DCM associated with sinus node dysfunction, supraventricular tachyarrhythmias, conduction delay, and stroke (Olson and Keating 1996). Although *SCN5A* mutations related to DCM are not as common as to other cardiac diseases, the high percentage of prevalence of familial DCM indicates that gene defects play an important role in this cardiac disorder. To date, around ten mutations in *SCN5A* that cause DCM have been reported. However, the molecular mechanism by which these mutations can cause DCM is still not clear (Ruan et al 2009). It was also suggested that some mutations in *SCN5A* such as N1325S can cause both LQTS and DCM, and this result has already been confirmed in transgenic mouse model expressing N1325S mutant *hSCN5A* (Yong et al 2007, Zhang et al 2011).

1.2.3 Brugada Syndrome

Brugada syndrome (BrS) is a cardiac disease that is characterized by elevated

ST-segment in right precordial leads (V1-V3) on ECG, and it is a common form of idiopathic ventricular fibrillation (IVF). Patients with BrS will have increased risk in cardiac arrhythmias and sudden death caused by episodes of rapid polymorphic ventricular tachycardias (VT) or ventricular fibrillation (VF) (Brugada and Brugada 1992). Although some patients with BrS have no symptoms on their ECG (IVF with normal ECG), their symptoms can be accentuated by the administration of some medications such as sodium channel blocker flecainide (Brugada et al 2002).

Cardiac sodium channel *SCN5A* related to type 1 BrS. In 1998, the first series of *SCN5A* mutations were identified in BrS patients. T1620M is a missense mutation on the extracellular loop between S3 and S4 on DIV (Chen et al 1998). Nowadays, more than 90 mutations in *SCN5A* are identified to be linked to BrS (Ruan et al 2009). Opposite to gain-of-function LQTS mutations in *SCN5A*, BrS mutations are loss of function mutations. Chen *et al.* stated that missense mutation T1620M locating on the extracellular loop between S3 and S4 on DIV exhibited a significantly faster recovery compared with wild-type channels. Later, the trafficking of sodium channel α subunit is also considered as another potential mechanism for BrS. In 2000, a missense mutation R1432G was reported to reduce the membrane sodium channel expression and sodium current density (Deschênes et al 2000).

Besides the *SCN5A* gene, there are six other genes that are related to BrS. *GPD1L* (3p21-23) encoding a protein that interacts with sodium channel α subunit can cause type 2 BrS (BrS2). *CACNA1C* (12p13.3) encoding calcium channel α subunit ($\text{Ca}_v1.2$) can cause BrS3. *CACNB2* encoding calcium channel β subunit ($\text{Ca}_v\beta2$) causes BrS4. *SCN1B* (19q13.1) encoding one of the sodium channel β subunit ($\text{Na}_v\beta$) causes BrS5. *KCNE3*

(11q13-q14) encoding β subunit of I_{Ks}/I_{to} (MiRP2) causes BrS6. *SCN3B* (11q23.3) encoding type 3 β subunit of sodium channel ($Na_v\beta3$) causes BrS7 (Hedley et al 2009).

It is estimated that the prevalence of BrS is about 5:10,000 (Blangy et al 2005). BrS is also thought to be responsible for at least 4% of all sudden deaths and 20% of all sudden deaths in patients without any heart structural abnormality (Antzelevitch et al 2007). As a result, the study of BrS mechanism is very essential. Since the BrS mutations in *SCN5A* are caused by the decreased membrane channel expression, rescuing the trafficking defect might be a potential treatment for BrS (Bezzina and Tan 2002, Valdivia et al 2002).

1.2.4 Progressive Cardiac Conduction Defect (PCCD)

Progressive cardiac conduction defect (PCCD), also known as Lev-Lenegre disease, is one of the most common cardiac conduction disturbances (CCD) and characterized by progressive alteration of cardiac conduction through the blockage of left and right His-Purkinje bundles and QRS complex widening (Schott et al 1999). Patients with PCCD ultimately develop chronic atrio-ventricular block due to the abnormal His-Purkinje system. As a result, pacemaker implantation is the most common treatment for patients with PCCD (Royer et al 2005).

Cardiac conduction disturbance has been linked to the *SCN5A* gene and two other chromosomal locations (19q13.2-13.3 and 16q23-24) where no genes have been identified yet (Bezzina et al 2003, Brink et al 1995, de Meeus et al 1995, Schott et al 1999, Tan et al 2001). In 1999, Schott first reported two mutations in two families with PCCD. In a large French family, a mutation of T→C substitution at position +2 of the

splicing donor site of intron 22 was found and expected to lead to in-frame skipping of exon 22, producing an impaired protein without the voltage-sensor S4 in DIII. The young individuals with this mutation did not show severe symptom. However, with aging and the increases of fibrosis, patients will develop the PCCD phenotype. In another small Dutch family, a deletion of a single nucleotide G at position 5280 was detected. The mutation results in a frameshift which produces a premature stop codon. Individuals with this mutation presented with a congenital conduction defect from birth, indicating that the effect of this premature stop codon is immediate (Schott et al 1999). Later, a missense mutation of G514C was identified in a 3-year old girl who experienced episodes of fainting during a febrile disease. Her ECG revealed typical cardiac conduction defect with slow conduction such as broad P waves, prolonged PR intervals and a wide QRS complex. The electrophysiological study in TSA201 cells expressing the G514C mutation showed an opposite effect on sodium current (I_{Na}) during activation and inactivation. The more rapidly decay of G514C channel reduces the I_{Na} accessible for cardiac impulse conduction. The positive shift (+7mV) of the normalized current-voltage (IV) curve suggested the destabilized close-state inactivation, which would increase I_{Na} (Tan et al 2001).

There are some PCCD mutations in *SCN5A* that can also cause Brugada syndrome, which was described as cardiac sodium channel overlap syndromes (Remme et al 2008). For example, a missense mutation G1406R was identified in a 45-member family. This mutation can either cause Brugada syndrome or isolated cardiac conduction defect (Kyndt et al 2001).

1.2.5 Sick Sinus Syndrome (SSS)

Sick sinus syndrome (SSS), also known as sinus node dysfunction (SND), is characterized by variable manifestations that include inappropriate sinus bradycardia, sinus arrest, atrial standstill, chronotropic incompetence and tachycardia bradycardia syndrome. Patients with SSS always have symptoms such as dizziness or syncope (Benson et al 2003, Dobrzynski et al 2007)

Besides atria and ventricles, *SCN5A* is also expressed in some pacemaker cells in sinoatrial (SA) node. Although the function of I_{Na} is still not very clear, some evidence suggests that $Na_v1.5$ defects are the possible reason for some SA node dysfunction. To date, at least 14 mutations in *SCN5A* associated with SSS have been recognized (Lei et al 2008, Ruan et al 2009). In 2003, six loss-of-function *SCN5A* mutations were identified in five SSS patients. Two of these six mutations are completely nonfunctional (G1408R and R1623X) and the other four are partially dysfunctional (T220I, P1298L, delF1617 and R1632H) (Benson et al 2003). The study of *SCN5A*^{+/-} knockout mice, which develop symptoms such as sinus bradycardia, slowed SA conduction and SA exit block, indicates that the loss-of-function of $Na_v1.5$ is the mechanism for SSS (Papadatos et al 2002). There are also some gain-of-function mutations in *SCN5A* that can cause mixed symptoms including SSS, LQTS, BrS and DCM. In 2003, a gain-of-function mutation 1795insD was found to produce both persistent sodium current and a negative shift in inactivation. It is concluded that the effects of this persistent sodium current and the negative shift reduce the sinus rate, thus explaining the mechanism for QT-prolongation and sinus bradycardia and sinus pauses (Veldkamp et al 2003). Thus, both loss-of-function and gain-of-function mutations can cause the dysfunction of sinus node.

1.2.6 Atrial Fibrillation

Atrial fibrillation (AF) is the most common cardiac disorder that is characterized by rapid and irregular activation of the atria. About 15% of all strokes are caused by AF. One third of patients with strokes are over 65 years of age, thus as the population ages, AF is responsible for the potential economic cost for the public health care system (Fatkin et al 2007, Matsusue et al 2012, Wang et al 2003).

At least 11 genes are related to AF and they include both ion channel genes and non-ion channel genes. Mutations in both potassium channels and sodium channels can cause AF. The ion channel genes are *KCNQ1* (α -subunit of I_{Ks} channel), *KCNE2* (β -subunit of I_{Ks} channel), *KCNE5* (β -subunit of I_{Ks} channel), *KCNJ2* (Kir2.1 channel), *KCNA5* ($K_v1.5$ channel), *SCN5A* (sodium channel α -subunit), *SCN1B* (sodium channel β -subunit), *SCN2B* (sodium channel β -subunit), and *SCN3B* (Chen et al 2003, Das et al 2009, Hong et al 2005, Makiyama et al 2008, Olson et al 2005, Olson et al 2006, Otway et al 2007, Ravn et al 2008, Wang et al 2010, Watanabe et al 2009, Yang et al 2004). The non-ion channel genes are *NUP155* (nucleoporin), *GJA5* (connexin-40) and *NPPA* (atrial natriuretic peptide (mANP)) (Gollob et al 2006, Hodgson-Zingman et al 2008, Oberti et al 2004, Zhang et al 2008).

In 2008, a *SCN5A* mutation M1875T was found in a Japanese family with only AF. This family has no symptoms of structural heart disease or ventricular arrhythmias. The electrophysiological study showed that M1875T is a gain-of-function mutation without producing persistent inward Na^+ currents. The characteristic of this mutation is obviously different from the LQT-type gain-of-function mutations which produce persistent late sodium current (Makiyama et al 2008).

1.2.7 Overlapping Syndromes

The effects of mutations in *SCN5A* are usually complicated. As a result, patients carrying certain mutations will display not only one type of symptom, but a mixed syndromes. Numerous *SCN5A* mutations lead to mixed phenotypes, known as a overlapping syndrome of cardiac sodium channelopathy (Remme et al 2008).

In 1999, Bezzina et al. first revealed that a single *SCN5A* mutation could cause multiple cardiac disorders within the same family. They found out that the family carrying 1795insD mutation in *SCN5A* presenting ECG features of sinus node dysfunction, bradycardia, BrS and LQTS (Bezzina et al 1999). Later, another deletion mutation Δ K1500 was reported to cause LQTS, BrS and conduction disease (Grant et al 2002). To date, more than 30 mutations in *SCN5A* can cause different combination of cardiac diseases. Most of these combinations are cardiac conduction dysfunction (CCD) and Brugada syndrome (BrS) (Table II).

1.3 Cardiovascular System

1.3.1 The Structure of the Cardiovascular System

The cardiovascular system is composed of the heart and blood vessels, which supply oxygen and nutrition throughout the body. The heart is a muscular organ that propels blood while contracting. There are four chambers in the human heart: left and right atria and ventricles. There are two types of blood circulation systems in the human body. Pulmonary circulation carries oxygen-deprived blood from the right ventricle through the pulmonary artery to lungs, and then returns it back to the left atrium with oxygenated blood through the pulmonary vein. Systematic circulation carries oxygenated

Table II. Overlapping Syndrome of Cardiac Sodium Channelopathy

SCN5A Mutation	Clinical Phenotype					References
	LQTS	BrS	CCD	SSS	Other	
E161K		+	+	+		(Smits et al 2005)
T187I		+		+		(Makiyama et al 2005)
P336L		+	+			(Cordeiro et al 2006)
D365N		+	+			(Makiyama et al 2005)
R367H		+	+			(Takehara et al 2004)
R376H		+	+			(Rossenbacker et al 2004)
N406S		+	+			(Itoh et al 2005)
G752R		+	+			(Potet et al 2003)
F861fs951X		+	+			(Schulze-Bahr et al 2003)
E867X		+	+			(Schulze-Bahr et al 2003)
D1114N	+	+				(Splawski et al 2000)
W1191X		+	+			(Shin et al 2007)
E1225K		+	+	+		(Schulze-Bahr et al 2003)
D1275N			+		AF/DCM	(McNair et al 2004)
G1319V		+	+			(Casini et al 2007)
P1332L	+		+			(Ruan et al 2007)
I1350T		+	+			(Juang et al 2003)
G1406R		+	+			(Kyndt et al 2001)
G1408R			+	+		(Kapplinger et al 2010)
Δ K1479		+	+	+		(Schulze-Bahr et al 2003)
Δ K1500	+	+	+			(Grant et al 2002)
Δ KPQ	+		+			(Wang et al 1995b)
Δ F1617	+	+		+		(Chen et al 2005)
R1623X			+	+		(Makiyama et al 2005)
R1632H			+	+		(Benson et al 2003)
I1660V		+	+			(Cordeiro et al 2006)
S1710L		+	+			(Akai et al 2000)
V1763M	+		+			(Chang et al 2004)
M1766L	+		+			(Valdivia et al 2002)
V1777M	+		+			(Lupoglazoff et al 2002)
1795insD	+	+	+			(Bezzina et al 1999)
S1812X		+	+			(Schulze-Bahr et al 2003)
P2005A	+		+			(Shim et al 2005)

blood from the left ventricle through the aorta to the rest of the body, and then returns it back to the right atria with oxygen-deprived blood (Luca et al 2009). The cardiac muscle contraction is caused by the electrical signal turned by excitation-contraction coupling in cardiac muscle cells.

1.3.2 Electrical Conduction in the Heart and Electrocardiogram (ECG)

The electrical signal arisen by cardiac action potentials starts at the sinoatrial node (SAN), which is located in the upper side of the right atrium. SAN sends the impulse to the right atrium, to the left atrium through Bachmann's bundle, and then to the atrioventricle (AV) node. The electrical signal of left and right atria generates the P wave on the electrocardiogram (ECG). The AV node plays an important role in delaying the ventricle contraction. Without the delay of AV node, ventricles and atria would beat at the same time. Two branches of His bundles in AV node, left and right branches, activate two ventricles, respectively and generate the PR segment on the ECG. The His bundles then branch to produce a bunch of Purkinje fibers, which spread the electrical impulse in ventricles, and form the QRS complex on the ECG (Klabunde 2012).

1.4 HL-1 Atrial Cells

1.4.1 Development of HL-1 Cardiomyocytes

In 1998, William C Claycomb successfully derived a cardiac muscle cell line, named HL-1, from the AT-1 mouse atrial cardiomyocyte tumor lineage. HL-1 cells can be passed infinitely, and still maintain the phenotype of cardiomyocytes. With specific culture media, HL-1 cells can be cultured beyond 30 passages and still remain beating

and contain no other cell types. With immunochemistry tests, HL-1 cells were confirmed to have perinuclear ANF-containing granules, cardiac-specific myosin and muscle-specific desmin intermediate filaments. These immunochemistry observations confirmed that HL-1 cells possess cardiac morphological properties. The gene expression analysis using RT-PCR (reverse transcription PCR) identified the presence of adult isoform of myosin (α -MHC) and contraction proteins such as α -cardiac actin, *ANF* and connexin43 (*CX43*). The gene expression results revealed that HL-1 cells retained biochemical characteristics of cardiac cells. Finally, Claycomb reported that HL-1 cells showed spontaneous action potentials and repolarizing K^+ currents using whole cell patch-clamp technique (Claycomb et al 1998).

1.4.2 Studies of Cardiac Muscle Cell Structure and Function Using HL-1 Cardiomyocytes

Before the development of HL-1 cardiomyocytes, isolated embryonic or neonatal rat and mouse cardiomyocytes were most widely used for cardiac studies. However, embryonic or neonatal cardiomyocytes lack the adult myocyte phenotypes. Some labs are also using isolated adult cardiomyocytes, but these adult cardiomyocytes cannot be cultured, and they are difficult to be transfected. The technique of adult cardiomyocytes isolation also highly depends on the quality of enzymes. The invention of HL-1 cells, the only cardiac cell line that can be continuously divided and still maintain the adult cardiac phenotypes in culture, provides a model for the study of cardiac diseases (White et al 2004).

HL-1 cardiomyocytes were first used to study the change of gene expression in

cardiac cells under pathophysiological stress such as hypoxia, hyperglycemia, and hyperinsulinemia (Collier et al 2002, Nguyen and Claycomb 1999). HL-1 cells were also used to study cellular signaling pathways and different types of receptors in cardiomyocytes.

1.5 Regulation of Na_v1.5 Function in Cardiac Cells

1.5.1 Ankyrin Proteins

There are three ankyrin proteins encoded by *ANK1*, *ANK2* and *ANK3* genes. Ankyrin-B (encoded by *ANK2*) and ankyrin-G (encoded by *ANK3*) are expressed in the heart (Cunha and Mohler 2006). Although in ankyrin-B knockout mice, late opening of Na_v1.5 was observed in isolated neonatal myocytes, there is no evidence showing that ankyrin-B directly interacts with Na_v1.5 (Chauhan et al 2000). However, ankyrin-G was found to directly interact with Na_v1.5 on the loop between DII and DIII on a 9 amino acid conserved motif (Lemaillet et al 2003). In 2004, a BrS mutation in Na_v1.5, E1053K, was reported by Mohler et al. This mutation is in the ankyrin-G binding motif and disrupts the interaction between ankyrin-G and Na_v1.5. As a result, Na_v1.5 cannot be transferred to plasma membrane, and tracked in the cytoplasm. These findings suggest that ankyrin-G functions as a helper for Na_v1.5 trafficking and sorting (Mohler et al 2004).

1.5.2 Caveolin-3

The cell membrane is composed of lipids and proteins. According to Singer and Nicholson's fluid-mosaic model about the cell membrane, proteins can float in the

phospholipid bilayers freely (Brown and London 1998). The less fluid liquid-order phase (Lo) is created by phospholipids with longer saturated acyl chains of the fatty acids and cholesterol pack, and the more fluid liquid-disorder phase (Ld) is composed of phosphoglycerolipids with polyunsaturated fatty acids (Binder et al 2003). Lo microdomains, called lipid rafts, function as signal transduction and protein-protein interactions to adapt the environmental changes. Caveolae, the best characterized lipid raft, is small embolic membrane structures (Palade 1953). Caveolae is rich in cholesterol and sphingolipids with cholesterol-binding proteins called caveolin. Caveolins are small proteins with several isoforms. Among these isoforms, caveolin-3 is highly expressed in myocytes, and it is encoded by *CAV3* gene (Song et al 1996, Tang et al 1996, Williams and Lisanti 2004). The co-immunoprecipitation and immunochemistry studies for caveolin-3 indicate that $\text{Na}_v1.5$ interacts and co-localizes with caveolin-3 (Yarbrough et al 2002).

1.5.3 Na_v 1.5 β -Subunits

Sodium channels are composed of one pore forming α subunit and one or several auxiliary β subunits that regulate the channel function (Meadows and Isom 2005). There are four genes encoding human sodium channel β subunits: $\beta 1$ (*SCN1B*) (Isom et al 1992), $\beta 2$ (*SCN2B*) (Isom et al 1995), $\beta 3$ (*SCN3B*) (Morgan et al 2000), and $\beta 4$ (*SCN4B*) (Maier et al 2003). These four β subunits have different regulatory functions for $\text{Na}_v1.5$. Coexpression of $\beta 1$ and $\text{Na}_v1.5$ results in a current density increase (Qu et al 1995). Coexpression of $\beta 3$ and $\text{Na}_v1.5$ increases current density, depolarizes shifts in the voltage-dependence of inactivation, and increases the rate of recovery from inactivation (Fahmi et al 2001). However, another group claimed that $\beta 3$ causes hyperpolarizing shifts

in inactivation and slows the recovery from inactivation (Ko et al 2005). As a result, the study about the effect of $\beta 3$ on $\text{Na}_v1.5$ is controversial. Coexpression of $\beta 2$ and $\beta 4$ with $\text{Na}_v1.5$ has no obvious effect on the current (Dhar Malhotra et al 2001, Yu et al 2003), though one group found that when expressed in HEK 293 cells, a mutation (L179F) in *SCN4B* increases the late sodium current, which is similar to gain-of-function mutations in *SCN5A* such as ΔKPQ (Medeiros-Domingo et al 2007).

It appears that the effect of β subunits on $\text{Na}_v1.5$ is inconclusive and controversial due to the possibility that the interaction between a β subunit and $\text{Na}_v1.5$ α subunit is complicated and that different groups used in different cell types. $\beta 1$ and $\beta 2$ subunits are associated with ankyrin, another important $\text{Na}_v1.5$ regulation protein discussed above. The localization of $\beta 1$ -ankyrin complex is controlled by the phosphorylation of the tyrosine on $\beta 1$ carboxyl-terminus (Y181) (Malhotra et al 2002). Using a phosphorylated antibody, tyrosine phosphorylated $\beta 1$ -ankyrin complex was found to colocalize with $\text{Na}_v1.5$ at the intercalated disk (Malhotra et al 2004).

1.5.4 Protein Kinase A (PKA)

In cardiac cells, the β -adrenergic receptor activates a GTP-binding protein (Gs). This GTP-binding protein then stimulates adenylyl cyclase and leads to the increase of intracellular cAMP, which will activate PKA (Li et al 2000). It is found that PKA activation can increase I_{Na} by at least 30% in normal canine cardiomyocytes, but can only increase I_{Na} by 17% in the cells at infarcted zone. Since it was hypothesized that PKA activator could either increase the current by direct phosphorylation of the α subunit or facilitate the channel trafficking from ER to plasma membrane (Frohnwieser et al 1997,

Murphy et al 1996, Zhou et al 2000), chloroquine, an inhibitor of cell trafficking, was used to distinguish the two hypotheses. After the administration of chloroquine, the peak I_{Na} did not change much in infarcted cells, but increased only 10% in the noninfarcted cells (Baba et al 2004). This result indicates that PKA activator increases I_{Na} by pushing more sodium channels to plasma membranes. Later, another group used GFP tagged $Na_v1.5$ to provide direct evidence that PKA helped the trafficking of cardiac sodium channels. They demonstrated that in the stable cell line expressing GFP- $Na_v1.5$, more sodium channels localized onto the membrane, and the peak I_{Na} increased after applying PKA activators (Hallaq et al 2006).

1.5.5 Tyrosine Phosphorylation of $Na_v1.5$

Many ion channels are the targets for protein phosphorylation and dephosphorylation, which then alter the electrophysiological properties and activities of the excitable cells. It was proved that voltage-gated sodium channel α subunit can be negatively regulated by PKA phosphorylation on Ser⁵⁷³ located on the intracellular loop between DI and DII (Cantrell et al 1997). Sodium channel α subunit can also be regulated by PKC so that the peak current was reduced by a negative shift of steady-state inactivation in the hyperpolarized direction (Qu et al 1994).

The study of tyrosine phosphorylation is more recent. One group suggested that cardiac sodium channels can be phosphorylated by Src family tyrosine kinases. Using the anti-phosphotyrosine antibody, the immunoprecipitated $Na_v1.5$ was increased in cells expressing constitutively activated Src family tyrosine kinase Fyn. The phosphorylated residue (Y1495) in $Nav1.5$ was also found (Ahern et al 2005). Another group studied the

effect of tyrosine kinases on I_{Na} in guinea pig ventricular myocytes. In their study, I_{Na} increased when being treated with epidermal growth factor (EGF). The increased I_{Na} can be inhibited by epidermal growth factor receptor (EGFR) kinase inhibitor tyrphostin AG556 and enhanced by orthovanadate (a protein kinase phosphatase inhibitor) (Liu et al 2007). Jespersen T. et al found that $Na_v1.5$ interacts with protein tyrosine phosphatase PTPH1 and concluded that tyrosine phosphorylation destabilizes the inactivated state of $Na_v1.5$ (Jespersen et al 2006).

1.5.6 Glycerol-3-Phosphate Dehydrogenase Like Protein (*GPD1-L*)

In 2002, a locus on chromosome 3 was described in a large family with BrS, but no mutation was found in *SCN5A* gene, which is located nearby (Weiss et al 2002). Later, a missense mutation in *GPD1-L*, the glycerol-3-phosphate dehydrogenase like protein, was found in this BrS family. As a result, it brought attentions about the interaction between *GPD1-L* and *SCN5A* which is an important BrS gene. When co-expressed with *SCN5A* in HEK293 cells, this BrS mutation in *GPD1-L* can reduce I_{Na} (London et al 2007). Three more mutations in *GPD1-L* were found in some patients died of sudden infant death syndrome (SIDS). The expression of these mutant *GPD1-L* variants in mouse neonatal cardiomyocytes decreases I_{Na} (Van Norstrand et al 2007).

1.5.7 Calmodulin (CaM)

Calmodulin (CaM) is a Ca^{2+} sensor protein and can undergo a Ca^{2+} -induced conformational change. This small ubiquitous intracellular Ca^{2+} -binding protein with only 147 amino acids participates in numerous signaling pathways and cellular processes

such as growth, proliferation and movement (Chin and Means 2000). During the cardiac excitation-contraction coupling, Ca^{2+} handling is crucial for many physiological events (Saimi and Kung 2002). When interacting with other proteins, CaM usually binds to the isoleucine-glutamine (IQ) CaM binding motif on these proteins (Herzog et al 2003). In 2002, Tan HL and co-workers found the IQ motif on the C-terminus of $\text{Na}_v1.5$. The binding of CaM significantly potentiates slow inactivation (Tan et al 2002). It is also found that Ca^{2+} concentrations can modulate Na^+ channel through CaM (Kim et al 2004), but recent studies suggest that this modulation is caused by the Ca^{2+} binding motif on the proximal part of $\text{Na}_v1.5$ C-terminus (Shah et al 2006, Wingo et al 2004).

1.5.8 Ca^{2+} /Calmodulin-Dependent Protein Kinase II (CaMKII)

CaMKII, a serine/threonine protein kinase, is activated by intracellular $[\text{Ca}^{2+}]$ changes. There are four CaMKII isoforms: α , β , δ , and γ , and each isoform is encoded by a specific gene. All the CaMKII isoforms have similar core structures including a regulatory domain, an N-terminal catalytic domain, and a C-terminal association domain (Braun and Schulman 1995). CaMKII δ is predominantly expressed in the heart (Couchonnal and Anderson 2008). Using immunoprecipitation and immunostaining, it has been confirmed that CaMKII δ_c interacts and co-localizes with $\text{Na}_v1.5$ in mouse myocytes. By overexpressing CaMKII δ_c in rabbit myocytes, Stefan Wagner et al. successfully proved that CaMKII δ_c was able to enhance the steady-state inactivation of I_{Na} (Wagner et al 2006). The mice overexpressing CaMKII δ_c in the hearts developed chronic heart failure and episodes of ventricular tachycardia. Not only does CaMKII interact with $\text{Na}_v1.5$ and regulate I_{Na} in the myocytes, it is also an important protein

linking Ca^{2+} and Na^{+} in the cardiac cells. As a result, CaMKII is a potential drug target for arrhythmia treatment (Abriel et al 2000).

1.5.9 *MOGI*

MOGI was first identified as a multi-copy suppressor of the yeast nuclear transport factor *GSP1* or *scRan*. It is a small protein encoded by *RANGRF* gene with molecular weight of 29 kDa (Marfatia et al 2001, Oki and Nishimoto 1998)). Yeast two-hybrid and *in vitro* binding experiments indicate that *MOGI* binds to the GTP-binding nuclear protein *Ran*. As a result, *MOGI* is thought to regulate nuclear protein trafficking (Marfatia et al 2001). In 2008, Ling Wu et al. found that *MOGI* interacts with $\text{Na}_v1.5$ on the intracellular loop between DII and DIII by a yeast two hybrid screen followed by GST-pull down assays and co-immunoprecipitation. In HEK293 cells stably expressing $\text{Na}_v1.5$, transfection of *MOGI* can increase the $\text{Na}_v1.5$ -mediated peak current without affecting any kinetic changes of sodium channel. These results suggested that *MOGI* is a helper protein for $\text{Na}_v1.5$ transporting to the plasma membrane (Wu et al 2008).

1.5.10 Fibroblast Growth Factor Homologous Factor 1B (*FHF1B* or *FGF12-1b*)

Fibroblast growth factor (FGF) family is one of the largest families of polypeptide growth factors functioning in both the adult and the embryos (Olsen et al 2003). One of the family members, *FGF12-1b* (also known as *FHF1B* (fibroblast growth factor homologous factor 1B)), is expressed in the heart (Abriel et al 2000). It is reported that *FGF12-1b* interacted with $\text{Na}_v1.5$ at intracellular C-terminus motif of amino acid 1773-1832 (Goetz et al 2009, Liu et al 2003). Several LQTS and BrS mutations such as

E1784K, D1790G, and Y1795H and Y1795C in *SCN5A* are located in this *FGF12-1b* binding motif. In HEK293 cells co-expressing *FGF12-1b* and Na_v1.5, the steady-state inactivation curve shifted toward hyperpolarized value without any change in the peak current density. However, *FGF12-1b* does not modulate or interact with D1790G mutant Na_v1.5 (Liu et al 2003).

1.5.11 14-3-3 η Protein

14-3-3 proteins are highly conserved proteins with a molecular weight of 28-33 kDa in all eukaryotic organisms (Aitken 2006). Several family members of 14-3-3 proteins are found in mammals – β , γ , ϵ , σ , ζ , τ and η (Morrison 2009). The yeast two-hybrid and co-immunoprecipitation experiments indicate that 14-3-3 η interacts with the intracellular N-terminus of Na_v1.5. The immunostaining in COS-7 cells expressing human Na_v1.5 and 14-3-3 η demonstrated that these two proteins were co-localized at the intercalated disk of myocytes. The same result was confirmed in isolated rabbit cardiomyocytes. Co-expression of 14-3-3 did not change the peak sodium current in COS-7 cells, but shifted the inactivation curve towards negative potential and delayed the recovery from inactivation. This result indicates that 14-3-3 does not regulate the trafficking of Na_v1.5 but modified its kinetics (Allouis et al 2006).

1.5.12 Ubiquitin-Protein Ligases of the *Nedd4/Nedd4-Like* Family

Intracellular and extracellular protein degradation processes are different. During extracellular degradation, the extracellular proteins are engulfed by vesicles and then fused with primary lysosomes (Glickman and Ciechanover 2002). However, during the

intracellular protein degradation, it undergoes the two-steps ubiquitin-proteasome proteolytic pathway: 1) tagging of the proteins with ubiquitin molecules, and 2) degradation of the tagged proteins by the 26S proteasome complexes. Ubiquitin can be recycled during this process (Glickman and Ciechanover 2002). Besides protein degradation, ubiquitin can also regulate protein trafficking to cell membranes (Staub and Rotin 2006).

Ubiquitin is a small protein with only 76 amino acid residues (Hershko and Ciechanover 1998). The *Nedd4/Nedd4*-like family of E3 ubiquitin-protein ligase contains a 40-residue domain that binds to various proteins with their PY motifs (Rotin and Kumar 2009). Almost all voltage-gated sodium channels have this PY motif on their intracellular C-terminus except for $\text{Na}_v1.4$, $\text{Na}_v1.9$, and Na_x (Fotia et al 2004). It is observed that I_{Na} was reduced by *Nedd4-2* mediated ubiquitylation in *Xenopus* oocytes (Abriel et al 2000). Since the total $\text{Na}_v1.5$ protein did not decrease in the presence of *Nedd4-2*, it is unlikely that the reduction of I_{Na} was $\text{Na}_v1.5$ protein degradation by *Nedd4-2*. Instead, $\text{Na}_v1.5$ proteins are trapped inside the cells by *Nedd4-2* rather than pushed to the membrane (Rougier et al 2005).

1.6 Anti-Arrhythmic Medications and Their Side Effects.

1.6.1 Quinidine

Quinidine, a class I anti-arrhythmia drug, used to be one of the most frequently prescribed anti-arrhythmic drugs, but has side effects that may lead to arrhythmias (Grace and Camm 1998). The pharmacokinetic study of quinidine revealed that the half life of quinidine in humans ranges between 3 and 19 hours (Grace and Camm 1998). In cardiac

cells, quinidine can block fast inward sodium currents and various potassium channels (Balser et al 1991, Wwidmann 1955). The anti-arrhythmic effect of quinidine was thought to be caused by the inhibition of the repolarizing delayed rectifier current, which is composed of three components including slow, rapid and ultrarapid currents (Deal et al 1996, Wang et al 1995c). Quinidine functions to inhibit the rapidly activating component (Carmeliet 1993, Woosley et al 1993).

Initially, quinidine was used for patients with atrial fibrillation (AF), and then was widely used as anti-arrhythmic medication (Brodsky et al 1996). However, it was later found that the application of quinidine has a potential risk of causing syncope and sudden death, which are due to ventricular tachycardia (VT) (Selzer and Wray 1964). The arrhythmia induced by quinidine treatment often happened right after treatment was started, and about 1.5%-8% of patients developed torsade de pointes (TdP) with quinidine treatment especially in patients with AF (Roden et al 1986, Roden 1994). Patients who developed TdP when treated with quinidine usually have abnormally longer corrected QT interval on ECG (Roden et al 1986).

1.6.2 Mexiletine

Mexiletine is another class I antiarrhythmic drug which plays an important role in treating cardiac arrhythmias (Sheets et al 2010). Voltage-gated sodium channels possess different types of inactivation, including fast, slow and ultra-slow (Goldin 2008). The slow inactivating component current $I_{Na,P}$ is only 1% of the peak current $I_{Na,T}$ and considered the main target for antiarrhythmic drugs such as mexiletine and ranolazine (Saint 2008).

Like other antiarrhythmic drugs, mexiletine can also promote arrhythmias (Brugada and Wellens 1988). However, a series of test of different antiarrhythmic drugs indicated that mexiletine might have the lowest risk of proarrhythmic action (Dhein et al 1993).

1.6.3 Ranolazine

Ranolazine is an investigative anti-arrhythmia drug in phase III trials, and believed to block four different voltage-gate sodium channels including $\text{Na}_v1.1$, $\text{Na}_v1.5$, $\text{Na}_v1.7$ and $\text{Na}_v1.8$ (Antzelevitch et al 2011). The effect of ranolazine in treating arrhythmias is the blockage of multiple channels such as late sodium current ($I_{\text{Na,L}}$), the late rectifying potassium channel, and the late L-type calcium channel. It is known that the inhibition of potassium channel will prolong the action potential duration (APD) and the inhibition of sodium channel and calcium channel will shorten the APD. The opposite effects of ranolazine on APD explain the modest prolongation effect on QTc in patients (Reddy et al 2010). Similar to quinidine, the QTc increase effect of ranolazine might bring the problem of developing drug-induced TdP. However, no such symptoms were observed during ranolazine clinical trials (Reddy et al 2010). It is reported that only less than 2% patients experienced the common side effects of ranolazine such as dizziness, nausea, constipation and headache (Chaitman et al 2004, Morrow et al 2007, Stone et al 2006).

Mutagenesis study demonstrated that mutation F1760A in $\text{Na}_v1.5$ significantly reduced the blockage effect of ranolazine on both peak and sustained Na^+ current. It is indicated that ranolazine interacted with the previously defined local anesthetic (LA) receptor binding site on $\text{Na}_v1.5$ (Fredj et al 2006). One group reported that ranolazine

blocked $\text{Na}_v1.5$ through modulating the mechanosensitivity of this voltage-gate channel by partitioning the lipid bilayer of the membrane (Beyder et al 2012). $\text{Na}_v1.5$ is mechanosensitive in both cardiac myocytes and a heterologous system such as transfected HEK cells, and is regulated by cytoskeleton and membrane lipid bilayer elasticity (Lundbaek et al 2004, Undrovinas et al 1995). The interruption of lipid bilayer inhibits the mechanosensitivity of $\text{Na}_v1.5$ (Beyder et al 2012).

1.6.4 Other Anti-Arrhythmic Drugs

Although newer drugs were developed and showed more clinically effective for cardiac arrhythmia treatment, the side effect of these newer drugs brought concerns to physicians. These newer drugs include flecainide, encainide, and moricizine, and were found to cause ventricular premature beats after myocardial infarction and lead to mortality in patients (Echt et al 1991). The lethal side effects brought attention to scientists, and the study of how to reduce the side effects of the medications could be more important than alleviating the symptoms.

1.7 Cardiac Excitation-Contraction Coupling (ECC) and Ca^{2+} Handling in Cardiac Cells

1.7.1 The Importance of Ca^{2+} in Cardiomyocytes

Cardiac excitation-contraction coupling is the process of the contraction of the cardiac cells to the contraction of the heart, which propels out blood to the body. Throughout this process, Ca^{2+} ion plays an important role in translating the cell electrical excitation signal to the contraction of myofilaments. Thus, the mishandling of Ca^{2+} may

cause cardiac dysfunction such as arrhythmias (Bers 2002). In the past several decades, alterations in cytosolic Ca^{2+} homeostasis were considered as the main mechanism for cell death. Ca^{2+} paradox is the hypercontracture and death of cardiomyocytes caused by Ca^{2+} restoration after a perfusion of Ca^{2+} -free buffer (Piper 2000). Hypercontraction can cause cardiac cell death, and the inhibition of hypercontraction using 2,3-butanedione monoxime (BDM) during reperfusion can prevent the further damage of the cell tissues (Garcia-Dorado et al 1992).

Ca^{2+} is a crucial element in all kinds of organisms, and plays an important role in numerous biological functions. It is known that the intracellular free Ca^{2+} concentration ($\sim 10^{-7}$ M) is much lower than the extracellular Ca^{2+} . This high Ca^{2+} gradient provides abundant Ca^{2+} available to be imported into cells, where these Ca^{2+} ions can function as second messengers (Chin and Means 2000).

1.7.2 The Process of Excitation-Contraction Coupling (ECC)

In order to initiate the cardiac ECC, Na^{+} ions need to enter the cardiac cells through voltage. Then, a relatively small amount of Ca^{2+} enters the cell through depolarization-activated Ca^{2+} channels such as L-type Ca^{2+} channel (Figure 1). This small amount of Ca^{2+} then open *RYR2* on sarcoplasmic reticulum (SR) membrane and release the Ca^{2+} storage in SR. This process is called Ca^{2+} induced Ca^{2+} release (CICR). The rapid intracellular Ca^{2+} increase allows the binding of Ca^{2+} to the protein troponin complex (TN-C) which attaches to sarcomere, the myofilament repeat subunit in striated muscle (Knollmann and Roden 2008). The binding of Ca^{2+} to TN-C induces a conformational change and exposes the myosin binding sites (thick filament) on actin (thin filament).

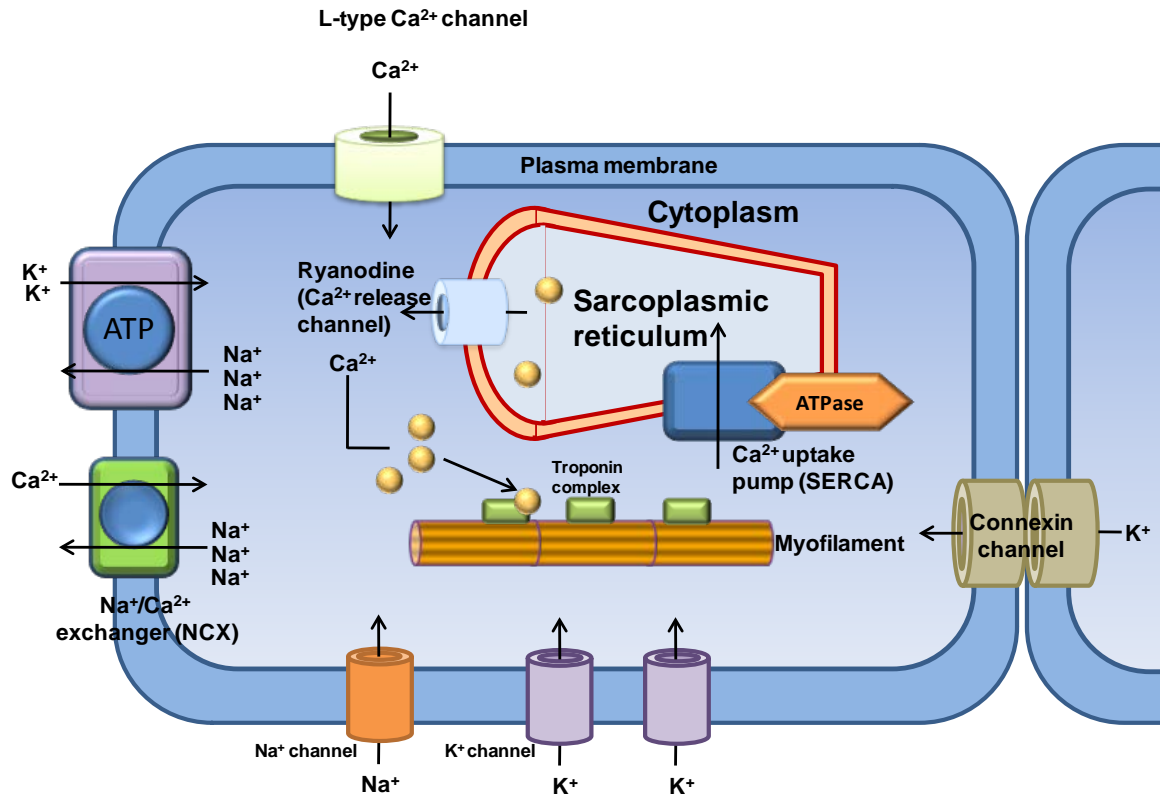


Figure 1. Schematic Diagram of Cardiac Excitation-Contraction Coupling (ECC) Events in Ventricular Myocytes. In order to initiate ECCs, K^+ ions enter into the cell from a neighboring cell through connexin channels and open the voltage gated Na^+ channels, which leads to the depolarization of the membrane. The depolarization of the membrane causes Na^+ channel inactivation and opens both K^+ channels and L-type Ca^{2+} channels. The entry of Ca^{2+} ions releases sarcoplasmic reticulum (SR) Ca^{2+} into cytosol. This rapid increase of cytosolic Ca^{2+} ions will bind to the troponin complex and activate the myofilament contraction. During the repolarization process, the cell will remove cytosolic Ca^{2+} either through $\text{Na}^+/\text{Ca}^{2+}$ exchanger (NCX) or Ca^{2+} -uptake pumps on SR. The cytosolic Na^+ is excluded through the Na^+/K^+ pump.

Following the conformational change leads to movement and binding between myosin and actin and results in the muscle contraction. This is the physiological process that how the electrical stimulus is translated to the striated muscle contraction (Sandow 1952).

1.7.3 Cardiac Ion Channels and Cardiac Action Potential

In a cardiac cell, an action potential (AP) refers to the rapid rise and fall of a cell electrical membrane potential. The cardiac action potential is electrical activity in the heart and is crucial for the electrical conduction in the heart (Grant 2009). The AP contains five phases (Figure 2), including the upstroke (0), early repolarization (1), plateau (2), final repolarization (3) and resting phases (4), all of which are generated by different selective ion channels on the membranes (Table III) (Grant 2009).

1.7.4 The Cellular Relaxation and the Removal of Cytosolic Ca^{2+}

In order to exclude the increased Ca^{2+} in cytosol, Ca^{2+} ions have to be transported out of the cell or be pumped back to SR in order to allow cell relaxation (Bers 2002). A SR Ca^{2+} -ATPase called *SERCA* on SR membrane pumps the rapidly increased Ca^{2+} back into SR. $\text{Na}^+/\text{Ca}^{2+}$ exchanger (NCX) allows three Na^+ enter the cell and exclude one Ca^{2+} outside the cell. This is the main path for Ca^{2+} transport out of the cytosol (Pogwizd et al 2001). There are two more pathways to exclude extra Ca^{2+} : sarcolemmal Ca^{2+} -ATPase and mitochondrial Ca^{2+} uniporter (Bassani et al 1994).

1.7.5 Dysfunction of $\text{Na}^+/\text{Ca}^{2+}$ Exchanger Causes Ca^{2+} Overload and Arrhythmias

$\text{Na}^+/\text{Ca}^{2+}$ exchanger (NCX), an important protein linking Ca^{2+} and Na^+ in the cell,

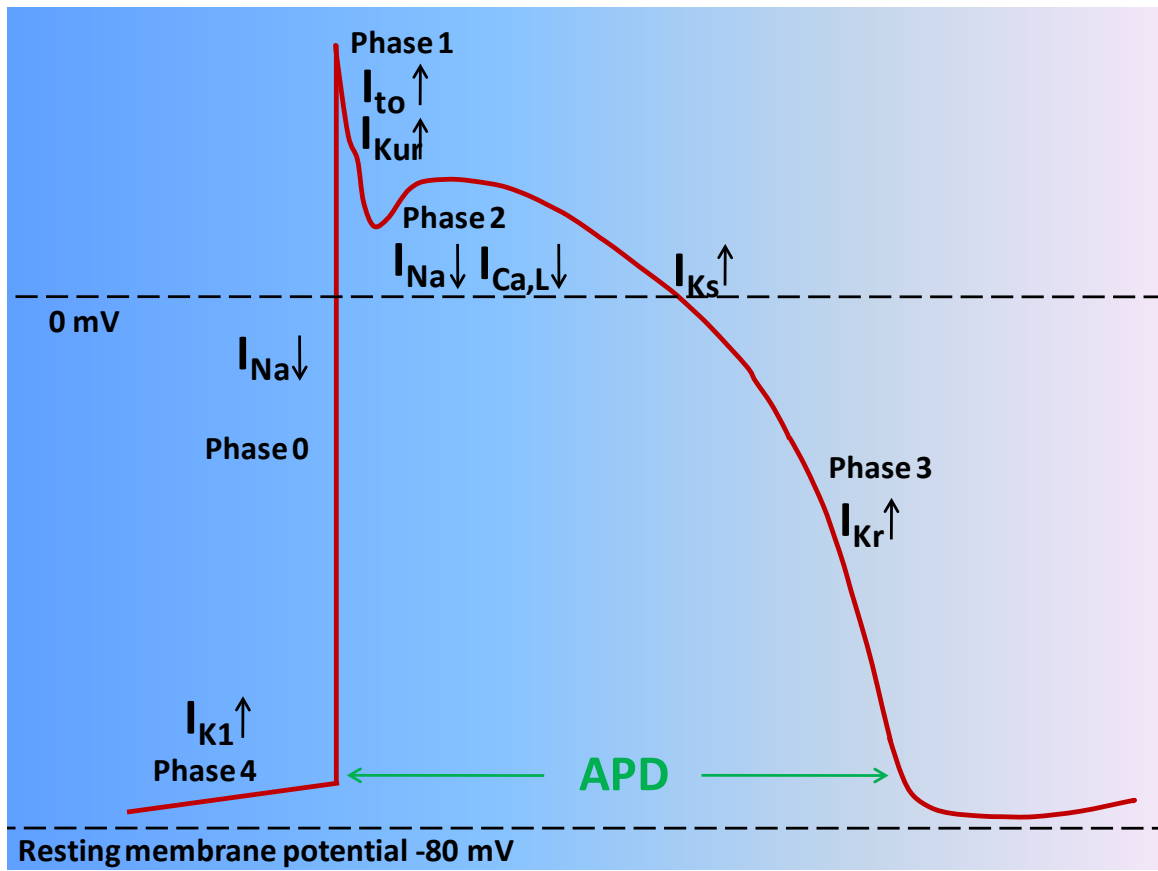


Figure 2. A Schematic Diagram Showing that Different Ionic Currents Contribute to Different Phases of a Cardiac Action Potential. During phase 0, the rapid inward sodium current I_{Na} initiates the upstroke of the action potential through $Na_v1.5$ channels. This phase is followed by the inactivation of Na^+ channels and the efflux of K^+ ions. Next, the action potential enters into a plateau phase (2) in which the inward movement of Na^+ and Ca^{2+} and the outward movement of K^+ are balanced. The final repolarization phase 3 is achieved by fast delayed rectifier, which is an outward K^+ current.

Table III. Ionic Currents and Different Phases of AP

Currents	Channel Gene	AP Phase	Description
I_{Na}	SCN5A	0 & 2	Sodium current
I_{to}	KCND2/3, KCNA4 KCNA7, KCNC4	1	Transient outward current
I_{Kur}	KCN5A, KCNC1	1	Ultrarapid delayed rectifier
$I_{Ca,L}$	CACNA1C	2	L-type calcium current
I_{NCX}	NCX1.1	2	Influx of Na^+ through NCX
I_{Kr}	KCNH2	3	Fast delayed rectifier
I_{Ks}	KCNQ1	3	Slow delayed rectifier
I_{K1}	KCNJ2/12	4	Inward rectifier

is a bi-directional membrane ion transporter (Jeffs et al 2007). There are two modes in NCX: the forward mode and reverse mode. The direction of the mode of NCX is determined mainly by intracellular and extracellular concentrations of Na^+ and Ca^{2+} (Blaustein and Lederer 1999). Under normal physiological conditions, NCX functions in the forward mode, which allows three Na^+ ions enter the cell and one Ca^{2+} moves out of the cell (McNaughton 1991). However, during the ischemia condition, the shortage of ATPs decreases the ability of Na^+ extrusion through the energy-dependent Na^+/K^+ -ATPase, which further causes the intracellular Na^+ overload (Murphy et al 1991). Another study also showed that the inhibition of Na^+/K^+ -ATPase may cause elevation of $[\text{Na}^+]$ and SR Ca^{2+} overload (Sedej et al 2010). It is believed that the elevated $[\text{Na}^+]$ leads to the reduced function of the NCX forward mode, which means that less Ca^{2+} ions are excluded through NCX and therefore leads to SR Ca^{2+} overload (Sedej et al 2010). SR Ca^{2+} overload has been experimentally proven to be the main cause for delayed afterdepolarizations (DADs) (Lederer and Tsien 1976, Marban et al 1986). DAD is the depolarization occurring after depolarization and related to initiation arrhythmias (Fink et al 2011, Pogwizd and Bers 2004).

1.7.6 Intracellular Ca^{2+} Transient and the Development of Ca^{2+} Transient Measurement

Ca^{2+} , an important signaling ion in the cytosol, regulates the cardiac cell contraction through binding to the Ca^{2+} binding protein troponin complex on myofilaments. The affinity between Ca^{2+} ions and Ca^{2+} binding proteins depends on the dynamic intracellular Ca^{2+} concentration, referred to as Ca^{2+} transient (Wier 1990).

Therefore, Ca^{2+} transient in striated muscle cells has provoked great interests of many scientists.

During the development of methods for the measurement of Ca^{2+} transient, fura-2 was proven to be an efficient Ca^{2+} fluorescent indicator in individual ventricular cells (Grynkiewicz et al 1985). Fura-2-acetoxymethyl ester (Fura-2/AM) is a membrane permeable Ca^{2+} indicator. Once entering into the cells, the cellular esterases will remove the acetoxymethyl groups on Fura-2/AM, and then Fura-2, the real working Ca^{2+} fluorescent indicator, is generated. The ratio of fluorescence at 340 nm and 380 nm (340/380) is proportional to the intracellular Ca^{2+} concentration (Grynkiewicz et al 1985).

CHAPTER II.

CARDIAC EXPRESSION OF *SCN5A* SNP R1193Q IN TRANSGENIC MICE PROLONGS QT INTERVAL

2.1 Abstract

Type 3 LQTS (LQT3) is associated with mutations in the cardiac sodium channel gene *SCN5A*. Some LQT3 mutations generate persistent, late sodium currents ($I_{Na,L}$). A single nucleotide polymorphism (SNP), *i.e.*, R1193Q, was previously reported in a patient with drug-induced LQTS and further shown to be present in 0.2% of the general Caucasian population and nearly 12% of the Chinese population. SNP R1193Q mutation destabilizes inactivation gating of the cardiac sodium channel and generates $I_{Na,L}$ that is expected to prolong the cardiac action potential duration (APD) and the QT interval on electrocardiogram (ECG). In order to study this mutation, our lab created a transgenic mouse line carrying human R1193Q mutant *SCN5A*. Using telemetry ECG analysis, I found that cardiac-specific expression of R1193Q results in prolongation of QT interval

in transgenic mice (106.3 ± 9.47 ms, $n = 7$) compared to control groups of wild type mice (81.6 ± 14.12 ms, $n = 5$, $p < 0.001$) and transgenic wild type mice (78.0 ± 7.26 ms, $n = 6$, $p < 0.001$), demonstrating that R1193Q confers risk of prolonged QT interval, which potentially could be pro-arrhythmic. Moreover, in the presence of quinidine, R1193Q transgenic mice showed a higher incidence of premature atrial contractions (PACs), premature ventricular contractions (PVCs) and sinus atrial exit block (SAEB) than littermate wild type control mice and transgenic wild type mice.

In this study, I show that cardiac-specific expression of human R1193Q mutant *SCN5A* results in prolongation of QT interval in transgenic mice, which unequivocally demonstrates that R1193Q confers risk of prolonged QT interval, which is pro-arrhythmic. Moreover, in the presence of quinidine, R1193Q transgenic mice (TG-RQ) showed a higher incidence of premature ventricle contractions (PVCs) or premature atrial contractions (PACs) and AV block than littermate wild type control mice. These results suggest that R1193Q may increase the risk for drug-induced arrhythmias. Considering the high frequency of R1193Q in the general population, it may become necessary to perform population-wide screening for the variant to identify high risk individuals.

2.2 Introduction

Long QT syndrome (LQTS) is an a cardiac disorder characterized by prolonged QT interval on surface electrocardiogram (ECG), syncope and sudden death as a result of life-threatening ventricular tachycardia, specifically *torsade de pointes* (Wang et al 2004). Among them, type-3 long QT syndrome is caused by mutations in cardiac sodium channel gene *SCN5A* encoding type 5 voltage gated sodium channel α subunit, $Na_v1.5$

(Wang et al 1995a). Nav1.5 is a large integral membrane protein which mediates the rapid upstroke of action potential in cardiac cells (George et al 1995).

Acquired LQTS is generally drug-induced and frequently caused by therapeutic drug effects on ion channels involved in genetic forms of LQTS, such as blockage of the cardiac potassium channels (Heist and Ruskin 2010). The missense mutation R1193Q was first identified in one of seven acquired LQTS patients. The electrophysiological study demonstrated that this mutation destabilizes inactivation gating and generates a persistent, non-inactivating sodium current in both transfected human kidney (HEK293) cells and *Xenopus* oocytes (Wang et al 2004). This SNP R1193Q presents in 0.2% in Caucasian general population and 12% in Chinese population (Hwang et al 2005, Wang et al 2004). Later, one group reported that *SCN5A* R1193Q polymorphism in a Chinese family was associated with progressive cardiac conduction defects and LQTS (Sun et al 2008).

Because some carriers with R1193Q have prolonged QTc, that my derivate in acquired LQTS and some have apparently normal QTc on surface ECG, it is necessary to demonstrate whether R1193Q confers a risk of QTc prolongation under action of drugs that can have the potential of prolonging the QT interval. The purpose of this study is to evaluate the ECG characteristic in transgenic mice carrying the high prevalence SNP R1193Q mutation, and the drug effects of quinidine, a class I anti-arrhythmic agent which also has class III properties, on this LQTS mouse model.

2.3 Materials and Methods

2.3.1 Preparation of Experimental Animals

This study was conducted in accordance with the guideline approved by the Cleveland Clinic Foundation Institutional Animal Care and Use Committee and was conformed to NIH guidelines.

The strategy for generating transgenic mice carrying SNP R1193Q in *SCN5A* (TG-RQ) is similar to that used for developing transgenic mice which overexpress wild type *SCN5A* (TG-WT) (Tian et al 2004) or mutant *SCN5A* with the N1325S mutation (TG-NS) (Tian et al 2004, Tian and Wang 2006, Zhang et al 2011). In brief, a cDNA fragment of 6.2 kb human *SCN5A* (*hSCN5A*) with SNP R1193Q was subcloned behind the cardiac specific mouse myosin heavy chain- α (α -mMHC) promoter (5.4kb), and before a 0.6 kb human growth hormone polyadenylation signal sequence (*hGH pIA*), resulting in a mMHC-*hSCN5A* construct. This construct was digested with *Not I*. A 12.4 kb *Not I* fragment was purified by agarose gel electrophoresis and injected into fertilized eggs derived from the CBA/B6 mouse strain to yield founder mice. Founder mice were then bred to wild type mice to generate heterozygous TG-RQ mice. The experimental control mice in this study are non-transgenic wild type mice (denoted as NTG) or TG-WT as described previously (Tian et al 2004, Tian and Wang 2006, Tian et al 2007, Zhang et al 2011).

Genotyping of positive TG-RQ mice was identical to that used for identifying TG-WT or TG-NS mice as previously described (Tian et al 2004, Tian and Wang 2006, Zhang et al 2007, Zhang et al 2011). In brief, mouse genomic DNA was isolated from clipped tail tissue samples when the pups were 10 days or younger. The tail tissue samples were collected in a 1.5 ml tube by adding 600 μ l freshly prepared 50 mM NaOH. In order to fully digest the tissue samples, the mixture was heated on a heat block at 95°C

for one hour. After digestion, the mixture was placed on ice for 5 minutes and 50 µl of Tris-HCl buffer (pH = 8.0) was added. The mixture contained mouse genomic DNA and was ready to be used as DNA template for PCR-based genotyping. The primers for genotyping of TG-RQ mice were identical to those used for genotyping TG-WT and TG-NS mice and included 5'-TGT CCG GCG CTG TCC CTC TG-3' (P1, forward) and 5'-CTC ATG CCC TCA AAT CGT GAC AGA-3' (P2, reverse) (Tian et al 2004).

2.3.2 Western Blot Analysis

Western blot analysis was performed to estimate the expression level of Nav1.5 in cardiac tissue samples from transgenic mice. Total protein extracts were extracted from the homogenized hearts using lysis buffer containing 20 mM Tris-HCl (pH = 8.0), 100 mM NaCl, 1 mM EDTA and 0.5% NP-40. The concentration of protein extracts was measured using the Bio-Rad protein assay kit (Bio-Rad, Hercules, CA) and all samples were diluted to the same concentration of 10 µg/µl. The protein extracts (100 µg) were separated by an 8% SDS-PAGE prepared with National Diagnostics ProtoGel solution (National Diagnostics, Atlanta, GA). After the separation, proteins were transferred to polyvinylidene difluoride membranes (Immun-blot PVDF membrane) (Bio-Rad, Hercules, CA) at 4 °C and 40V overnight. The membrane was blocked in 5% non-fat milk in PBST (phosphate-buffered saline, 0.05% (v/v) tween 20, pH=7.4) and then probed with an anti-rabbit Nav1.5 antibody (1:1000 dilution), followed by incubation with a horseradish peroxidase-conjugated secondary antibody (Santa Cruz, Santa Cruz, CA). The protein signal was visualized using the ECL Western blotting detection kit and Hyperfilm ECL (GE Healthcare, Pittsburgh, PA). The membrane was striped and blocked

with 5% non-fat milk in PBST, and was probed again using an anti-GAPDH antibody (Millipore, Billerica, MA), which serves as a loading control.

2.3.3 Semi-Quantitative Real-Time PCR (RT-PCR) Analysis

Total RNA samples were isolated from heart tissue samples from both NTG and TG-RQ mice in order to determine the expression level of *SCN5A* mRNA. Excised mouse hearts were placed into liquid nitrogen right after being washed with PBST. Total RNA samples were isolated using TRIzol reagent (Life Technologies, Grand Island, NY). For each heart sample, 1 ml of TRIzol reagent was applied, and the heart tissue was homogenized manually. After isolation, the RNA was immediately transcribed into cDNA using Stratagene's RT-PCR kit (Agilent Technologies, Santa Clara, CA). Double-stranded cDNA was synthesized from 10 µg of total RNA. The semi-quantitative RT-PCR was used to quantify the RNA level. PCR primers were designed to amplify a region from exon 5 to 7 of the human *SCN5A* gene. The sequence of the forward primer is 5'- TGG AAC TGG CTG GAC TTT AGT GTG -3', and the reverse primer is 5'-TGG TGC CGT TGA GCG CTG TGA AG -3'. RT-PCR analysis with 18S rRNA primers was used as internal control. The number of cycles for semi-quantitative RT-PCR was optimized for each sample to obtain data in the linear range for amplification. The PCR profile was 25 cycles for *SCN5A* and 18 cycles for 18S rRNA. The PCR products were separated by a 1.5% agarose gel and analyzed.

2.3.4 Telemetry ECG Recordings

Telemetry Electrocardiogram (ECG) Data from TG-RQ and control mice were

acquired using Data Sciences telemetry system (TA10ETA-F20 transmitter, Data Sciences International) with a receiver placed under each mouse cage. Mice (25-32g, 6-10 months) were anesthetized with 20 mg/ml of Avertin (0.025 ml/g mice) (Sigma-Aldrich, St. Louis, MO). The abdomen hair was removed and the telemetry transmitter was then implanted into the mouse peritoneal cavity. The negative and the positive leads on the telemetry transmitter were surgically placed on the right shoulder and chest, respectively. The mice were observed for the first 48 hours after surgery, and ECG data were collected at least 48 hours after surgery using Data Sciences DATA Acquisition ECG software (Data Science International, St. Paul, MN). The QT interval was corrected for the RR interval using Bazett's formula by $QTc = QT_o/(RR)^{1/2}$ (Bazett 1920, Tian et al 2004, Zhang et al 2007) or the formula of $QTc = QT_o/(RR/100)^{1/2}$ as described previously (Mitchell et al 1998).

2.3.5 Echocardiographic Assessment of Cardiac Structure and Function in Transgenic Mice

The echocardiographic data were collected from TG-RQ and control mice (8-10 month) as described previously (Zhang et al 2006). Each mouse had at least one echocardiography with the same handler. Echocardiography was performed using a high-frame rate (> 200 fps) echocardiography machine (GE Medicare, Milwaukee, WI) with 14-MHz transducer coupled with an Applio ultrasopund machine (Toshiba, Japan).

2.3.6 Data Analysis

All the results were expressed as mean \pm S.E.M., and the differences between

means were calculated by Student's paired t-test. A *P* value of 0.05 or less is considered to be statistically significant.

2.4 Results

2.4.1 Generation and Identification of Transgenic Mice with Cardiac Specific Overexpression of Mutant Human *SCN5A* Gene with SNP R1193Q

To determine whether SNP R1193Q in cardiac sodium channel gene *SCN5A* increases risk of LQTS, we generated TG-RQ transgenic mice with cardiac selective expression of mutant *SCN5A* with SNP R1193Q under the control of the mouse α -myosin heavy chain promoter, a cardiac-specific promoter (Figure 3A). Semi-quantitative real-time PCR analysis showed that TG-RQ mice expressed 5-fold more *SCN5A* mRNA in the heart tissue than control NTG mice (Figure 3B). Similarly, western blot analysis showed that TG-RQ mice expressed more than 3-fold more $\text{Na}_v1.5$ protein in the heart than control NTG mice (Figure 3C). These results suggest that TG-RQ mice successfully overexpress mutant *SCN5A* with SNP R1193Q in the hearts.

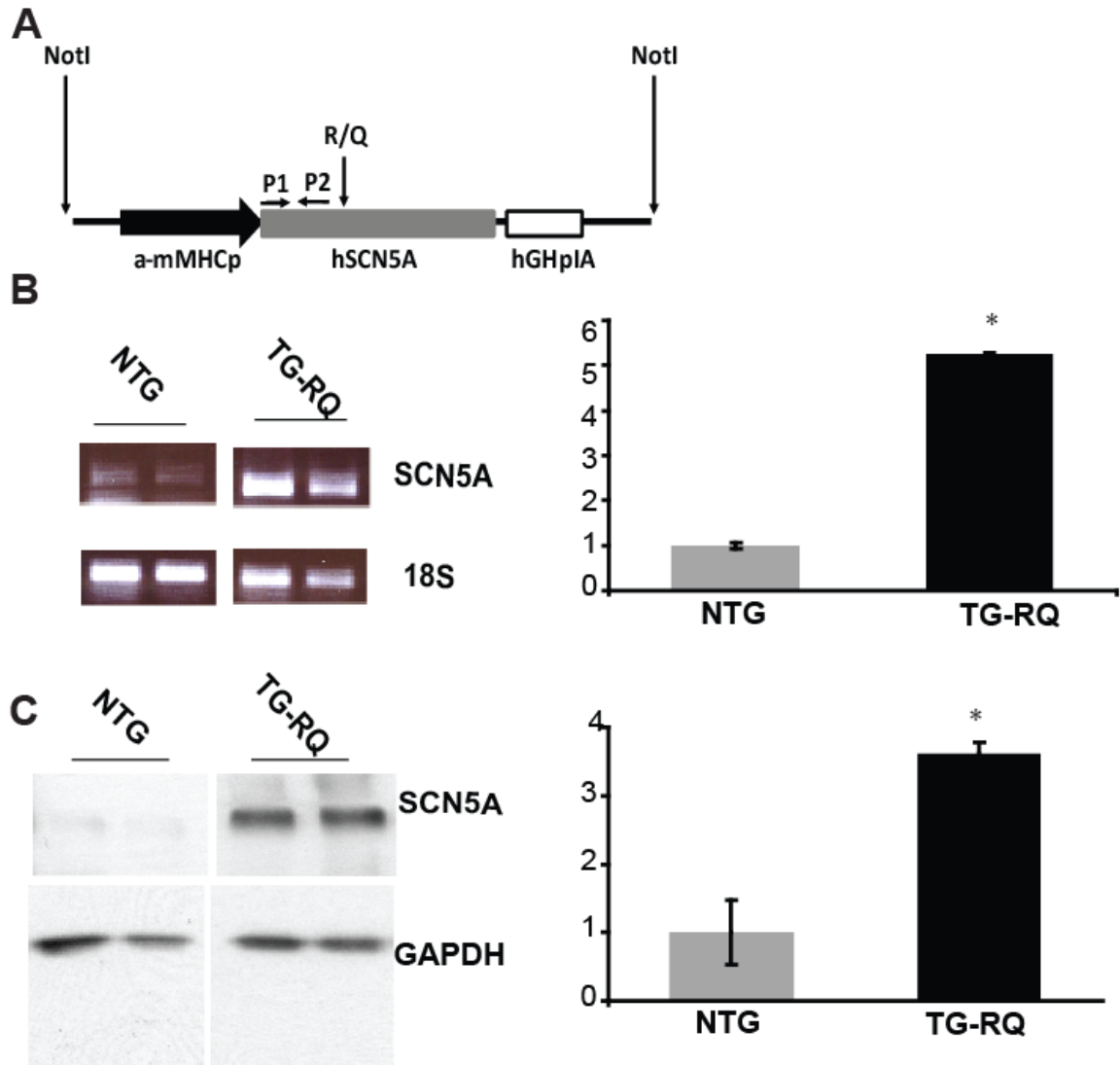


Figure 3. Generation and Genotyping of TG-RQ Mice. (A) Transgenic construct for the engineering of transgene, RQ (*SCN5A*) (human *SCN5A* with acquired LQTS-associated SNP R1193Q), into the mouse genome. (B) Semi real-time PCR analysis was performed using heart tissue samples from non-transgenic mice and TG-RQ mice to estimate the *SCN5A* mRNA expression level in mouse hearts. *SCN5A* mRNA expression level in TG-RQ mice is 5-fold more than NTG. (C) Western blot analysis was performed using mouse hearts to estimate the protein expression level of *SCN5A*. *SCN5A* protein expression level is 3-fold more than NTG.

2.4.2 Development of Long-QT Syndrome in TG-RQ Mice

I recorded ECGs from conscious and unrestrained mice using the telemetry monitoring system. Representative ECG traces for NTG, TG-WT and TG-RQ mice are shown in Figure 4A. The major ECG parameters were measured and compared among different groups of mice. Average QTc in TG-RQ mice was 106.3 ± 9.47 ms (n=7), which was significantly longer than that in either NTG mice (81.6 ± 14.12 ms, n=5) ($P < 0.001$) or TG-WT mice (78.0 ± 7.26 ms, n=6) ($P < 0.001$) (Figure 4B). These results suggest that *SCN5A* SNP R1193Q increases QTc in mice. Similar significant differences were obtained when QTc was calculated using either the Bazett's formula by $QTc = QT/(RR)^{1/2}$ (Bazett 1920, Tian et al 2004, Zhang et al 2007) or the formula of $QTc = QT/(RR/100)^{1/2}$ as described previously (Mitchell et al 1998).

The PR interval in TG-RQ mice (16.4 ± 1.55 ms) was similar to that in TG-WT mice (18.6 ± 2.37 ms) ($P > 0.05$), but significantly shorter than that in NTG mice (31.5 ± 2.70 ms, $P < 0.001$) (Figure 4B). The QRS complex in all three groups of mouse lines had no significant differences (Figure 4B).

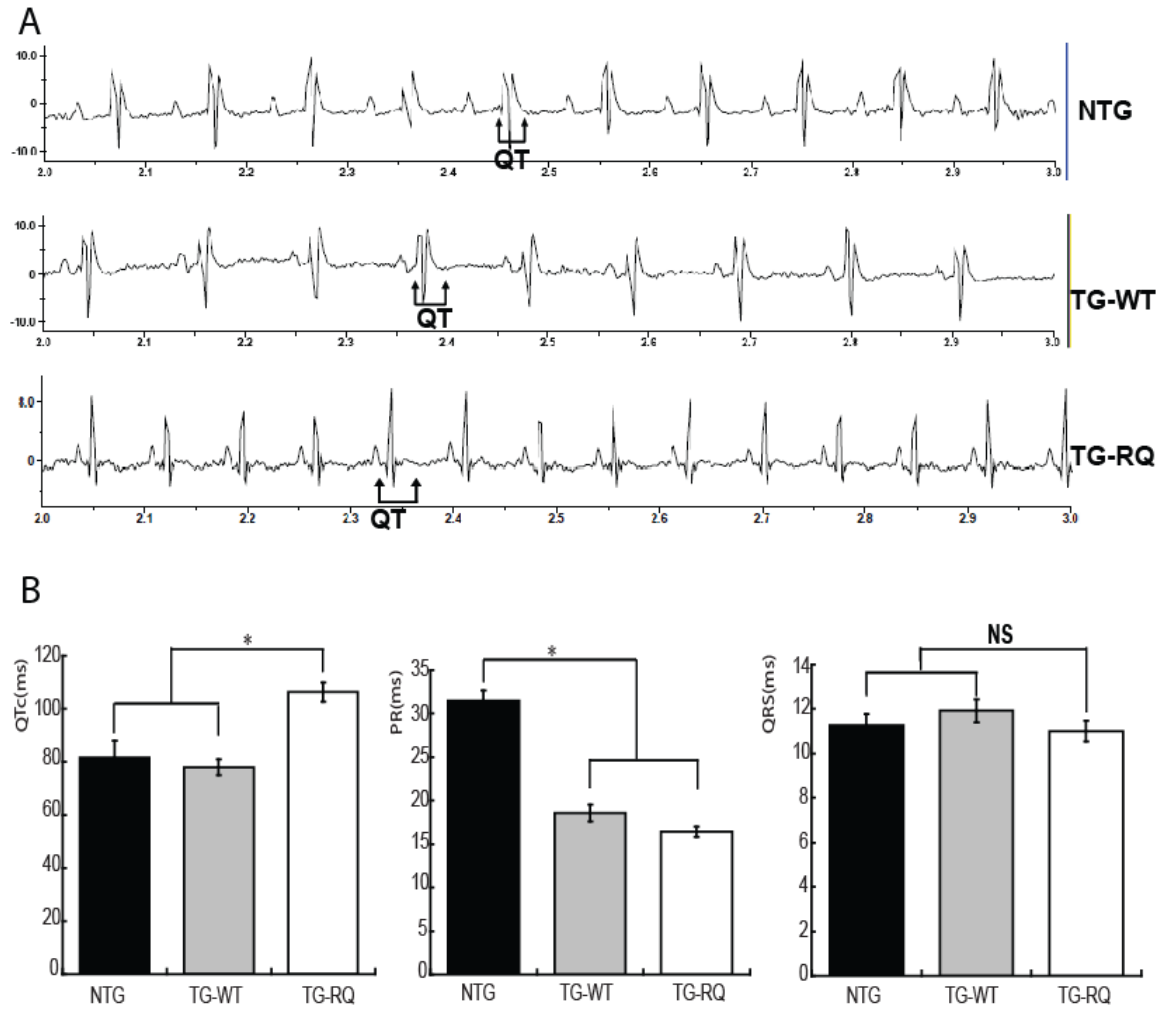


Figure 4. ECG Recordings of Non-transgenic (NTG), Transgenic Wild-type (TG-WT) and Transgenic R1193Q (TG-RQ) Mice. (A) Representative sample ECG traces from non-transgenic (NTG), TG-WT and TG-RQ mice. (B) Summary of ECG data analysis. QT intervals were corrected for heart rate as indicated as QTc. Statistical significance from control is denoted with an asterisk (*), whereas non-significance is indicated as NS.

2.4.3 Quinidine Prolonged QTc, and Increased the Frequencies of PACs, PVCs and Sinus Atrial Exit Block in TG-RQ Mice

SCN5A SNP R1193Q was identified in an acquired LQTS patient upon administration of quinidine(Wang et al 2004). Therefore, I tested whether quinidine could further increase QTc in TG-RQ mice. TG-RQ and control NTG mice were treated with 25 mg/kg body weight of quinidine (i.p.), and ECGs were recorded using the telemetry ECG monitoring system. As shown in Figure 5, quinidine treatment significantly increased QTc in both TG-RQ and NTG mice 5 minutes after quinidine treatment, although quinidine diminished the QTc differences between these two groups. After quinidine treatment, QTc increased from 106.3 ± 9.47 ms to 128.1 ± 5.7 ms ($n = 7$, $P < 0.05$) in TG-RQ mice, and from 81.6 ± 14.12 ms to 115.7 ± 6.2 ms ($n = 5$, $P < 0.01$) in NTG mice. TG-RQ mice remained to have significantly longer QTc 15 minutes and 25 minutes after treatment compared to control mice.

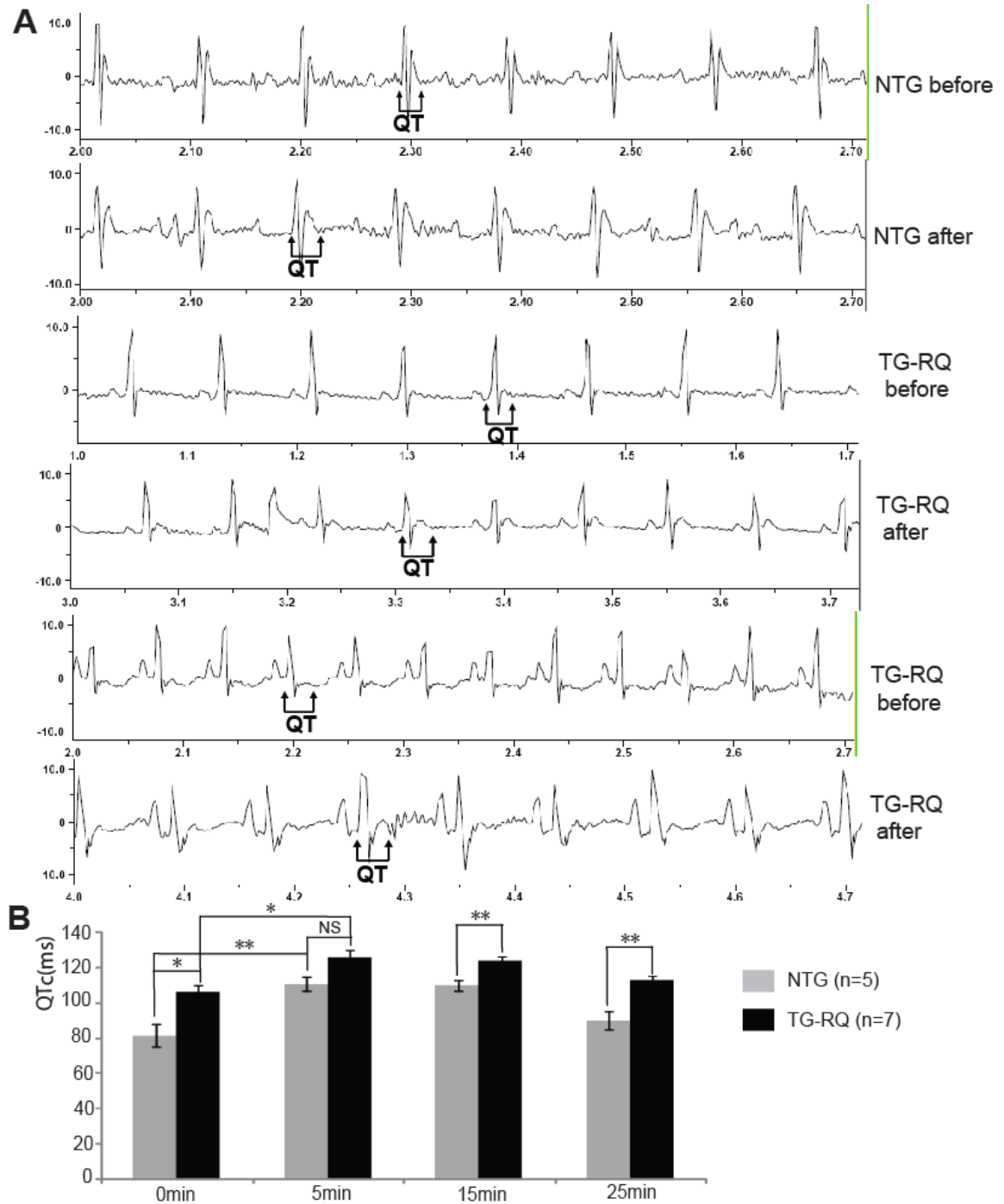


Figure 5. Quinidine Treatment Prolonged QTc in Both NTG (n=5) and TG-RQ Mice (n=7). (A) Representative ECG traces before and after quinidine treatment in both NTG and TG-RQ mice. (B) Comparison of QTc before and after quinidine treatment. Quinidine treatment significantly prolonged QTc in both NTG and TG-RQ mice. *, $P < 0.05$; **, $P < 0.01$; NS, not significant.

Representative ECG traces in TG-RQ mice after quinidine treatments are shown in Figure 6. The analysis of ECGs showed frequent premature atrial contractions (PACs), premature ventricular contractions (PVCs) and sinus atrial exit block (SAEB, or sinus node pause). The frequencies of PACs, PVCs and SAEB one hour before and after quinidine treatments were summarized in Table IV. Before quinidine treatments, no NTG mice ($n = 5$) showed any pro-arrhythmic ECG patterns, whereas three of seven TG-RQ mice showed PACs, PVCs, and SAEBs. However, after the application of quinidine, one NTG mouse showed a low frequency of PACs/PVCs, whereas five of seven TG-RQ mice developed PACs and PVCs. The frequencies of PACs and PVCs were much higher after quinidine treatments than before the treatments in TG-RQ mice. Moreover, three of seven TG-RQ mice developed SAEBs more than 25 times in one hour.

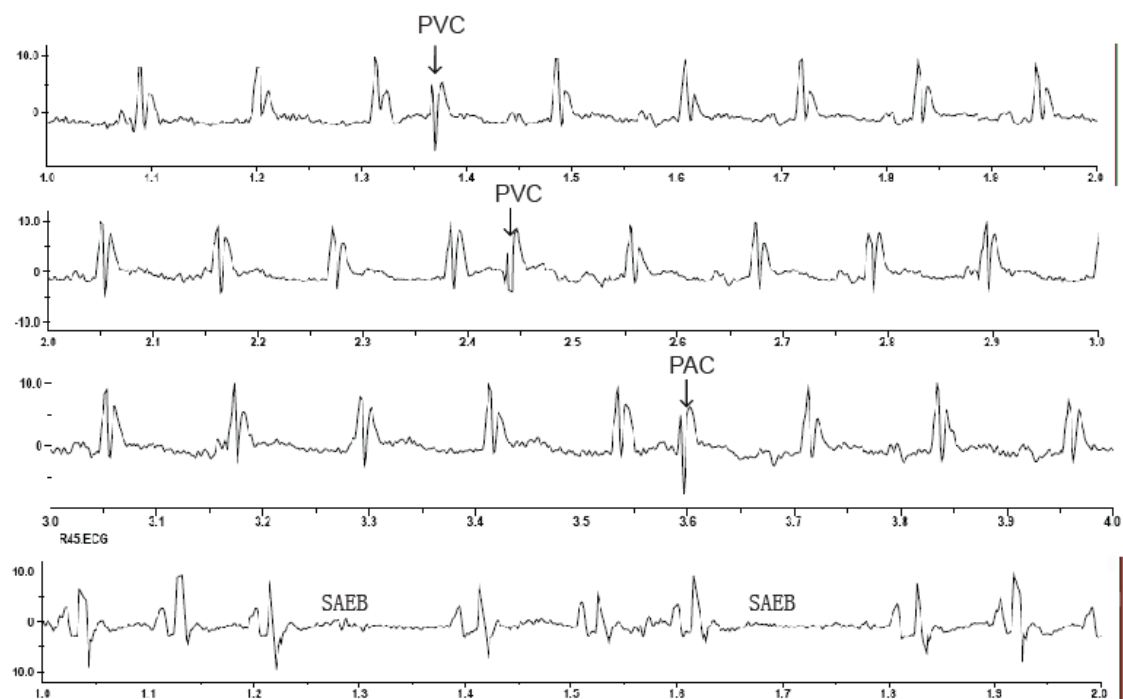


Figure 6. Quinidine Treatment Induced Increased PVCs, PACs, and SAEB in TG-RQ Mice.

Table IV. Effects of Quinidine Treatment on PACs, PVCs and SAEB in TG-RQ Mice and Control NTG Mice

Mouse ID#	Before Quinidine	After Quinidine	
	Number of PACs and PVCs	Number of PACs and PVCs	Number of SAEB
NTG 1	0	2	0
NTG 2	0	0	0
NTG 3	0	0	0
NTG 4	0	0	0
NTG 5	0	0	0
TG-RQ 1	0	4	26
TG-RQ 2	2	6	0
TG-RQ 3	2	9	0
TG-RQ 4	2	16	0
TG-RQ 5	0	5	2
TG-RQ 6	0	0	> 30
TG-RQ 7	0	0	> 30

Notes: The number of PACs, PVCs and SAEB in a period of one hour before and after quinidine treatment was counted manually and summarized.

2.4.4 Echocardiographic Assessment of Cardiac Structure and Function in the Mice

Because TG-NS mice developed dilated cardiomyopathy and heart failure at advanced ages as in human carriers with *SCN5A* mutation N1325S (Zhang et al 2011), echocardiography for TG-RQ mice was also performed, too. Basic echocardiographic parameters were compared between TG-RQ mice and control NTG mice (Table V). There were no significant structural differences between TG-RQ mice and NTG mice with regard to left ventricular fractional shortening (LVFS), systolic left ventricular end dimension (LVEDS), systolic intraventricular septum thickness (IVSS), left ventricular systolic posterior wall thickness (LVPWS), and other major echocardiographic parameters (Table V). These results suggest that *SCN5A* SNP R1193Q does not cause major structural changes in the heart.

Table V. Echocardiographic Assessment of Cardiac Function in TG-RQ Mice

Parameter	NTG (n=7)	TG-RQ (n=7)	P Value
HR (bpm)	638.3 \pm 0.7	672.4 \pm 0.5	0.59
IVSD (mm)	1.1 \pm 0.08	0.9 \pm 0.03	0.14
IVSS (mm)	1.8 \pm 0.08	1.6 \pm 0.04	0.09
LVIDD (mm)	3.3 \pm 0.1	3.1 \pm 0.1	0.41
LVIDS (mm)	1.5 \pm 0.1	1.5 \pm 0.1	0.8
LVPWD (mm)	1.0 \pm 0.09	0.9 \pm 0.06	0.65
LVPWS (mm)	1.5 \pm 0.08	1.5 \pm 0.05	0.73
LVFS(%)	57.0 \pm 2.4	51.0 \pm 3.3	0.18

Notes: HR - heart rate; IVSD - left ventricular septum wall thickness in diastole; IVSS-left ventricular septal wall thickness in systole; LVEDD - left ventricular cavity size in diastole; LVEDS - left ventricular cavity size in systole; LVPWD - left ventricular posterior wall thickness in diastole; LVPWS - left ventricular posterior wall thickness in systole; LVFS - left ventricular fractional shortening, percent change in left ventricular cavity dimensions with systolic contraction. The mice used for echocardiography were at the age of 8 - 10 months.

2.5 Discussion

SNP R1193Q of *SCN5A* is a relatively high frequent variant in the general population, accounting for 0.2% the Caucasian population and 12% of the Chinese population (Hwang et al 2005, Wang et al 2004). SNP R1193Q was identified in one patient with drug-induced LQTS and follow-up electrophysiological studies demonstrated that it had similar functional effect on cardiac sodium channels as other types of LQTS-causing mutations such as N1325S, R1644H, and DelKPQ (Huang et al 2006, Wang et al 2004). Specifically, R1193Q can generate a late non-inactivation sodium current through an increased rate of dispersed reopening, which is predicted to prolong the cardiac action potential duration and QTc on ECGs (Huang et al 2006, Wang et al 2004). However, genetic evidence for the association between SNP R1193Q and prolongation of QTc was not particularly strong. In this study, our lab established TG-RQ transgenic mice with cardiac specific expression of mutant human mutant *SCN5A* gene with the R1193Q SNP in mice. Telemetry ECG recordings showed that SNP R1193Q significantly increase QTc in TG-RQ mice compared to comparable control TG-WT or NTG mice (Figure 4). These data provide strong *in vivo* genetic data to support the hypothesis that SNP R1193Q of *SCN5A* can prolong QTc on surface ECGs.

One carrier with SNP R1193Q developed acquired LQTS after administration of quinidine (Wang et al 2004). In this study, we found that quinidine increased QTc from TG-RQ mice (Figure 5). These data support that data from the human patient that quinidine can further prolong QTc from R1193Q carriers. Because quinidine increased QTc from both TG-RQ mice and control NTG mice (Figure 5), the relationship between genotype R1193Q and quinidine is additive with regard to the QTc phenotype, meaning

no epigenetic interaction between the two. We previously reported that although quinidine inhibited the peak sodium current from both wild type and R1193Q mutant sodium channels, but did not block the persistent late sodium current, which is more relevant to prolongation of QTc (Wang et al 2004). Therefore, quinidine may prolong QTc in TG-RQ mice or NTG mice by blocking outward potassium currents. The data from TG-RQ mice reinforce the notion that acquired LQTS represents a latent form of inherited LQTS because they share the similar genetic basis, but may manifest to the full LQTS upon additive effects of quinidine and other medications as well as other environmental factors (Wang et al 2004). A precaution should be taken when prescribing quinidine or other QT-prolonging drugs to patients carrying SNP R1193Q.

In addition to in an acquired LQTS patient, SNP R1193Q was also identified in several patients with typical LQTS, Brugada syndrome, cardiac conduction disease, and sudden unexpected nocturnal death syndrome, and in a South Korean patient with LQTS, dilated cardiomyopathy, and sinus node pause (Huang et al 2006, Hwang et al 2005, Kwon et al 2012, Matsusue et al 2012, Qiu et al 2009, Skinner et al 2005, Sun et al 2008). Interestingly, I observed frequent SAEB or sinus node pause after administration of quinidine (Figure 6), a clinical feature observed in a Korean patient. No features related to dilated cardiomyopathy and Brugada syndrome were observed. No polymorphic ventricular tachyarrhythmia and sudden death were detected in TG-RQ mice, although an increased frequency of PACs and PVCs were found after administration of quinidine (Table IV). It remains to be determined whether human carriers with SNP R1193Q have increased PACs or PVCs.

There are a few limitations with the present study. The first limitation is related to

the transgenic overexpression technology. Because LQTS-associated *SCN5A* mutations are gain of functions mutations including R1193Q that generate a persistent late sodium current, it is justified to overexpress R1193Q to investigate its effect on cardiac physiology. However, one disadvantage is that the observed phenotypes may be related to overexpression of sodium channels. For example, the shortened PR interval, development of PACs and PVCs, and depressed T waves may be due to overexpression of sodium channels because these phenotypes were observed in TG-WT mice, too (Zhang et al 2007). Although utilization of TG-WT mice as control may eliminate these non-mutation specific effect, these factors need to be considered during interpretation of the data. Second, transgenic overexpression studies may exaggerate the mutant phenotype due to a higher number of the mutant *SCN5A* than the number of endogenous wild type *SCN5A*. Future studies with a knock-in model of R1193Q may be needed to mimic the human situation where there is only one copy of mutant *SCN5A* and one copy of the wild type gene.

In conclusion, cardiac specific overexpression of mutant *SCN5A* with SNP1193Q led to increased QTc in transgenic mice (TG-RQ) compared to mice with cardiac specific overexpression of wild type *SCN5A* or NTG. Quinidine treatment can further increase QTc in TG-RQ, although it also increased QTc in control NTG control. Our data provide strong genetic evidence that R1193 can increase risk of LQTS and quinidine can further exaggerate the QT phenotype. Considering that 60,000 Americans and 156 million Chinese people are potential carriers of SNP R1193Q, this functional variant may be a significant risk factor for LQTS in the general population, in particular, under conditions of other QT-prolonging medications.

CHAPTER III

LQTS MUTATION N1325S IN *SCN5A* CAUSES DISRUPTION OF CYTOSOLIC CALCIUM HOMEOSTASIS IN MOUSE VENTRICULAR MYOCYTES

3.1 Abstract

The gain-of-function mutation N1325S in cardiac sodium channel gene *SCN5A* produces the late sodium current ($I_{Na,L}$) and is associated with type 3 long QT syndrome (LQT3), ventricular tachyarrhythmia (VT) and dilated cardiomyopathy (DCM) in both human and mice. An increased rate of apoptosis was also found in the hearts of transgenic mice expressing N1325S mutant human *SCN5A* (TG-NS). We hypothesized that $I_{Na,L}$ their recoveries from caffeine applications, and Na^+/Ca^{2+} exchanger (NCX) dysfunction in isolated TG-NS myocytes. Then, it was concluded that the loss of NCX activity confines cytosolic Ca^{2+} removal to SR Ca^{2+} reuptake and, thereby, prolongs Ca^{2+} recovery. To our knowledge, this is the first time to link the sodium channel mutation to abnormal Ca^{2+} handling. But there've been brought a lot of doubts about the linkage between $I_{Na,L}$

and the abnormal Ca^{2+} transient by some reviewers. In order to further support the linkage between gain-of-function sodium channel mutations with abnormal Ca^{2+} handling, I have applied a late sodium current blocker, ranolazine, to isolated TG-NS myocytes in this study. The blockage of $I_{\text{Na,L}}$ by ranolazine markedly reduced irregularity of the Ca^{2+} transients and the recovery time from caffeine effect (indicated as T90r) in TG-NS myocytes. The rescue effect of ranolazine to abnormal Ca^{2+} handling provides additional evidence that a sodium channel mutation is the cause for abnormal Ca^{2+} handling in cardiomyocytes, which provides important insights into the pathogenic mechanisms of LQTS, VT and DCM.

3.2 Introduction

In cardiac cells, the transient opening of Na^+ channels gives rise to the inward current which is responsible for the upstroke of the cardiac action potential (AP) and initiation of excitation-contraction coupling (Li et al 1997, Liu et al 1992). After opening, most Na^+ channels quickly enter an inactivated state. However, a small fraction of Na^+ channel either fails to inactivate or to reopen during the plateau of the AP when the channels are normally closed. As a result, the outside Na^+ ions continue to flow into the cell, and the influx of Na^+ produces persistent or late Na^+ currents ($I_{\text{Na,L}}$). Then, $I_{\text{Na,L}}$ slows the repolarization of the AP and therefore increases the action potential duration (APD), proliferating heterogeneity of repolarization, and promoting the formation of early after-depolarizations (Kiyosue and Arita 1989).

It is known that under an ischemia and/or reperfusion condition, where Na^+ channel activation is impaired, $I_{\text{Na,L}}$ contributes to a rise of myocardial Na^+ content in the

cells (Barrington et al 1997, Williams and Lisanti 2004). The increase of intracellular $[Na^+]$ can lead to intracellular Ca^{2+} overload via the dysfunction of Na^+/Ca^{2+} exchanger (NCX), and these observations are consistent with the findings that an enhanced $I_{Na,L}$ can lead to a Na^+ -dependent Ca^{2+} overload (Fraser et al 2006, Pieske et al 2002, Song et al 2006, Wang et al 2008).

N1325S mutation in the cardiac sodium channel gene *SCN5A* is associated with type 3 long QT syndrome (LQT3), which was originally identified in a 96-member family in 1995 (Wang et al 1995a). In order to study this mutation, our lab has created a transgenic mouse model in two different lines (TG-NSL3 and TG-NSL12) that overexpress this NS mutation in the heart with different copy numbers. At the same time, a control model in two different lines (TG-WTL5 and TG-WTL10) that carry a similar copy number of wild type *SCN5A* in the heart was also generated. The resulting TG-NS phenotype of prolonged APDs in isolated ventricular cells, increased QTc, a high incidence of both ventricular tachyarrhythmias (VT) and sudden death has been reported previously (Tian et al 2004). Then follow-up studies in these TG-NS mice revealed co-development of dilated cardiomyopathy (DCM) and increased apoptosis and fibrosis (Zhang et al 2011). After these findings, in order to determine the mechanistic basis for this association, the Ca^{2+} handling was tested in isolated ventricular myocytes. The existence of cytosolic Ca^{2+} irregularities from TG-NS ventricular myocytes but not from TG-WT hearts is consistent with previous results that the heterogeneity of APD waveforms was effectively reduced in the presence of the L-type Ca^{2+} channel blocker, verapamil (Yong et al 2007). The major findings in isolated TG-NS ventricular myocytes include increased intracellular $[Na^+]$, Na^+/Ca^{2+} exchanger dysfunction, and abnormal

Ca²⁺ handling. These findings are the first to demonstrate a direct link between *SCN5A* mutations and abnormal Ca²⁺ handling in cardiomyocytes. This potential link offers possible mechanisms into the high rate of apoptosis and fibrosis in TG-NS mice heart tissue and the existence of extracardiac diseases such as DCM. However, the up-regulation of some important Ca²⁺ handling proteins such as NCX, RyR2 and L-type Ca²⁺ channel in adult TG-NS mice hearts indicates the remodeling of the cardiomyocytes in the presence of N1325S mutation. In order to strengthen the direct linkage between this gain-of-function *SCN5A* mutation and abnormal Ca²⁺ handling, a late sodium current blocker, ranolazine (Antzelevitch et al 2011, Fredj et al 2006, Zaza et al 2008), was applied to the isolated myocytes. The rescue effect of ranolazine to the abnormal Ca²⁺ transient signals in TG-NS myocytes built a stronger bond between N1325S mutation and cytosolic Ca²⁺ irregularity. The possibility that the Ca²⁺ mishandling is caused by the remodeling of adult TG-NS myocytes is also diminished due to the ranolazine rescue effect.

3.3 Methods and Materials

All experiments were conducted in accordance with the guidelines of the Cleveland Clinic Foundation Institutional Review Board on Animal Subjects and conformed to NIH guidelines. The generation and genotyping of TG-NSL3, TG-NSL12, TG-WTL5 and TG-WTL10 transgenic mice have been described previously (Tian et al 2004, Zhang et al 2007).

3.3.1 Isolation of Mouse Ventricular Myocytes

The isolation procedure of ventricular myocytes is similar to what has been previously reported (Tian et al 2004, Yong et al 2007). The mouse was heparinized with 150 U (0.15ml of 1000 U/ml) of heparin via intraperitoneal (IP) injection 20 minutes before neck dislocation sacrifice. Then the mouse chest was quickly opened, and the heart was removed and washed with ice cold surgery buffer containing (in mM): 200, NaCl; 10, KCl; 5, MgCl₂; 2, KH₂PO₄; 22, glucose; 50, HEPE; 4, CaCl₂; 12.5, pyruvic acid; pH 7.25 with NaOH. Next, under the microscope, the aorta of the heart was mounted on a syringe needle for Langendorff apparatus with a constant perfusion buffer flow rate of 1.5ml/minute, and the aorta was secured with silk suture. The procedure should be finished within 5 minutes after the mouse was sacrificed. Before surgery, the Langendorff perfusion system was filled with perfusion solutions and cleared of air bubbles in order to prevent bubbles from entering the aorta during perfusion. The perfusion solutions were saturated with 95% O₂:5% CO₂ and warmed to 37°C using a heated water bath. The cannulated heart was first washed with 100 ml first step Ca²⁺ containing perfusion buffer containing (in mM) 118, NaCl; 4.8, KCl; 2, CaCl₂; 2.5, MgCl₂; 1.2 KH₂PO₄; 11, glucose; 13.8, NaHCO₃; 4.9, pyruvic acid; PH 7.2. During this stage, a healthy and successful perfused heart should exhibit strong contraction and the blood in the heart chamber would be flooded out. After 3-minutes of washing with Ca²⁺ containing perfusion buffer, the heart was transferred to another perfusion system containing 60 ml second step Ca²⁺-free perfusion buffer. Then 45 mg of type II collagenase (Worthington, Lakewood, NJ) was added to second step Ca²⁺-free perfusion buffer once the heart stopped beating. Three minutes after adding collagenase, 1 mg of protease (Type XXIV, Sigma-Aldrich, St. Louis, MO) was added. Two sets of 0.1 mM CaCl₂ was added 5 minutes (5 µl) and 10

minutes (10 μ l) after applying collagenase. About 25 minutes after second step perfusion, the ventricle should appear yellowish and soft, and the digestion perfusion completed. The heart was placed in warm ($\sim 35^{\circ}\text{C}$) KB media buffer to reduce “ Ca^{2+} paradox” (Isenberg and Klockner 1982), and the atrial appendages were carefully removed. Gentle titration was performed in order to loosen the cells from the heart tissue. After titration, a series of incremental increases in Ca^{2+} was made to a final Ca^{2+} concentration of 1.8 mM. The cells are rested at room temperature for one hour before recordings.

The cells were split into two sets in order to test the rescue effects of ranolazine. The ranolazine was dissolved in PBST:DMSO (95:5) to 10 mM and saved as stock. One set of cells were incubated in 10 μM of ranolazine when “resting”, the other set of cell were incubated with same amount of blank PBST:DMSO (95:5) solvent that was used to dissolve ranolazine.

3.3.2 Measurements of Ca^{2+} Transient Signals

The Ca^{2+} transient signals were recorded according to the protocols reported previously (Lalli et al 2001, Ritter et al 2000, Rota et al 2005). Myocytes were loaded with 1 μM fura-2 acetoxymethyl ester (Fura-2-AM, Teflabs, Austin, TX) for 10 minutes at room temperature in the dark. Then the cells were centrifuged, and the buffer containing fura-2 was removed. Next, the cells were re-suspended in 3-4 ml of HEPE buffer and put in the dark.

Before measurement, cells were transferred to the Biopetechs chamber (Biopetechs, Butler, PA) for which the temperature was set at 28°C . The initial field stimulation was set at 0.5 Hz and 5 ms duration. Ca^{2+} transients were measured using the same excitation

(340/380 nm) and emission (510 nm) spectra from the spectrofluorometer. As an index of Ca^{2+} changes, the ratio of the emitted fluorescence at the wavelength of 340 nm over 380 nm (F/F_o) was obtained. The steady-state Ca^{2+} transient signals were recorded at a pacing frequency at 0.5 Hz in the absence of caffeine. The relative sarcoplasmic reticulum (SR) Ca^{2+} contents were estimated by the amplitudes of Ca^{2+} transient after the application of 10 mM caffeine. The stimulation was stopped before adding caffeine. The resulting caffeine-induced Ca^{2+} transient (the amplitude from baseline to peak of the signal) was considered as a qualitative index of the SR Ca^{2+} content. The time for a caffeine-induced Ca^{2+} transient to recover by 90% from peak to baseline (T90r) was considered as the effectiveness of the SR and NCX in the myocytes to remove cytosolic Ca^{2+} back to SR or out of the cytoplasm.

3.4 Results

Irregular Ca^{2+} Transients in TG-NS Cardiomyocytes Can be Rescued by Late Sodium Current Blocker Ranolazine

According to the intracellular $[\text{Na}^+]$ measurement done by Dr. Yong in our lab, it was confirmed that the intracellular $[\text{Na}^+]$ in TG-NS myocytes was higher than in TG-WT myocytes. An increase in $[\text{Na}^+]$ can potentially lead to Ca^{2+} overload in the cells, perhaps through disrupting the cell's ability to internally regulate Na^+ and Ca^{2+} ionic homeostasis. Using Fura-2 AM method to estimate the intracellular Ca^{2+} from both TG-NS and TG-WT myocytes, an irregular Ca^{2+} handling was also observed in TG-NS myocytes which had longer recovery time when pacing at 0.5 Hz. Besides, the time to 90% recovery (T90r) of caffeine-induced Ca^{2+} transient signals was also longer in TG-NS

cells.

In order to link the abnormal Ca^{2+} transient signals in TG-NS myocytes to the presence of gain-of-function mutant $\text{Na}_v1.5$, a late sodium blocker, ranolazine, was applied to the isolated TG-NS myocytes. Ranolazine is a blocker of the late sodium current caused by LQT3 mutation (Fredj et al 2006, Zaza et al 2008). The ranolazine treatment was performed in both isolated TG-NSL3 (Figure 7) and TG-NSL12 (Figure 8) myocytes. After 1 hour of ranolazine treatment, the Ca^{2+} transient signal has significant reduction ($P < 0.05$) in recovery time (T90r) (Figure 7E and Figure 8E) from caffeine effect with little or no changes in the transient amplitudes. Before ranolazine treatment, the myocytes in both TG-NSL3 (Figure 7A) and TG-NSL12 (Figure 8A) did not respond to the stimulation and the interval between each signal was irregular. However, in the presence of ranolazine, most isolated myocytes can respond to the stimulation (Figure 7C and Figure 8C) in the absence of caffeine. These results indicate that although ranolazine cannot reduce the higher SR Ca^{2+} storage significantly in TG-NS myocytes, it can reduce the time required for the removal of Ca^{2+} from the cytosol. This is consistent with the previous results that the SR Ca^{2+} content is not higher in TG-NS myocytes compared with TG-WT, but T90r is longer for TG-NS myocytes.

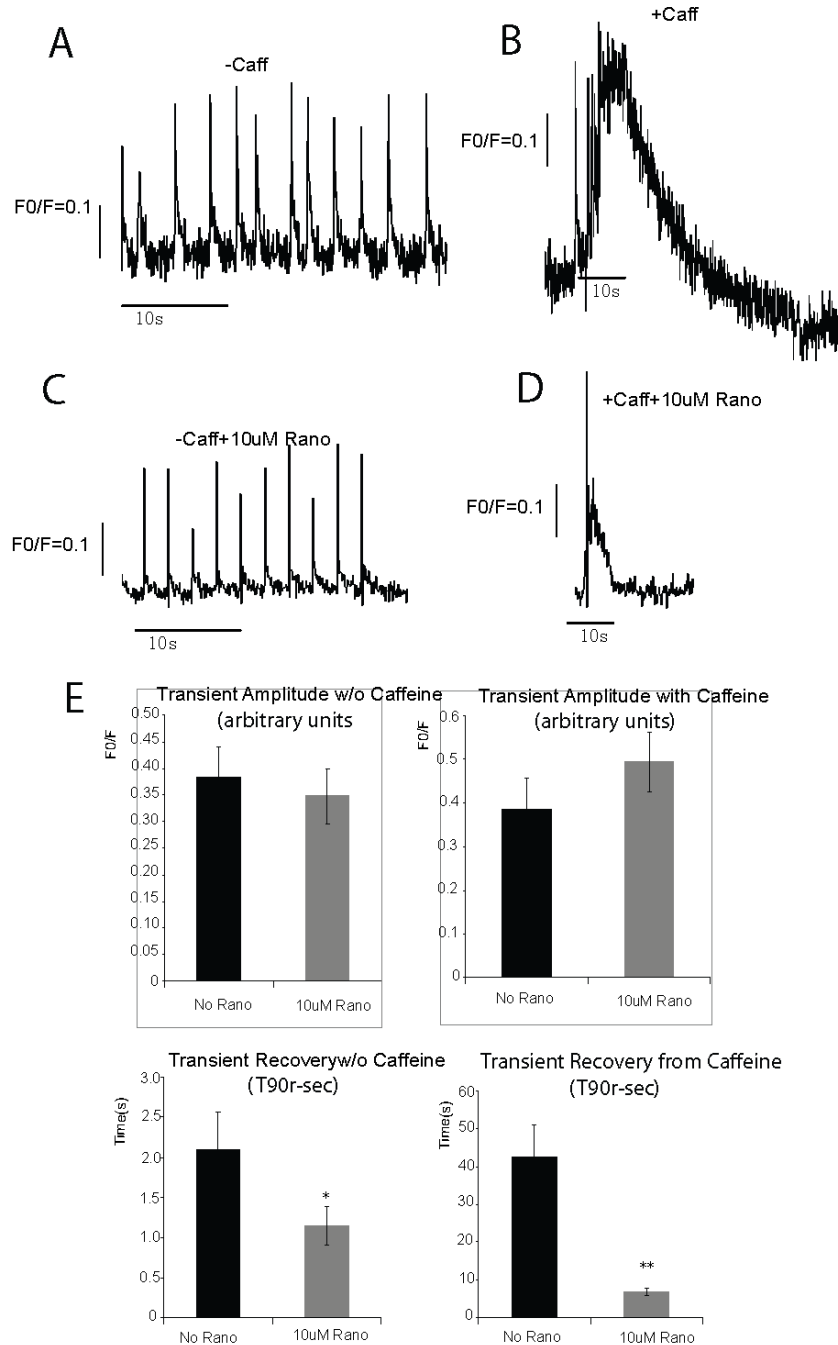


Figure 7. Ca^{2+} Transients Signals in Isolated TG-NSL3 Mice Myocytes (age=6-10 months, n=14). (A & B) Representative Ca^{2+} transient recording in isolated TG-NSL3 myocytes with (B) and without (A) 10 mM of caffeine. (C & D) Representative Ca^{2+} transient recording in isolated TG-NSL3 myocytes treated with 10 μM of ranolazine for 1 hour with (D) and without (C) 10 mM of caffeine. (E) Summary of data from all the recordings. The time needed for recovery of caffeine-induced transient signal is significantly shortened after 10 μM of ranolazine treatment. *, $P < 0.05$ and **, $P < 0.01$ indicates statistical significance.

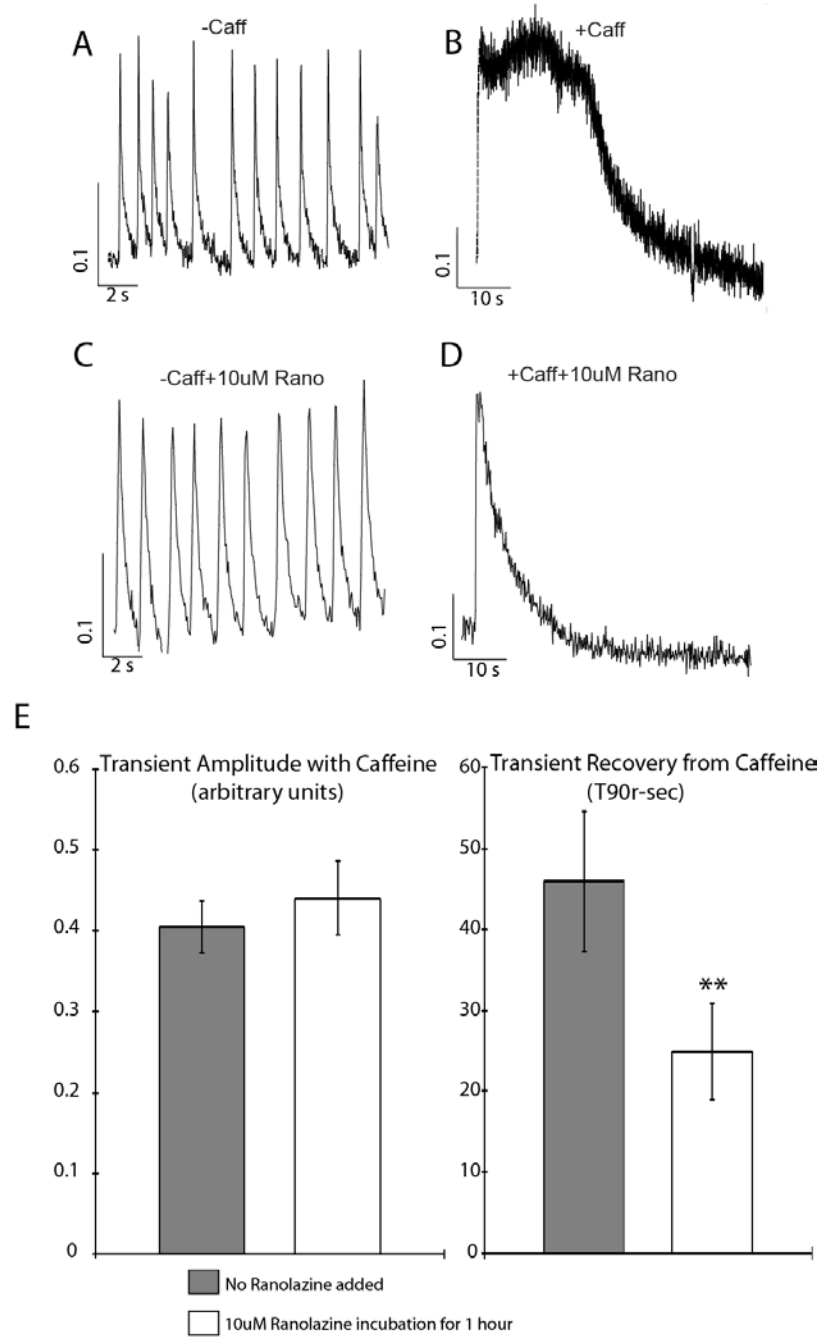


Figure 8. Ca^{2+} Transients Signals in Isolated TG-NSL12 Mice Myocytes (age=6-10 months, n=24). (A & B) Representative Ca^{2+} transient recording in isolated TG-NSL12 myocytes with (B) and without (A) 10mM caffeine. (C & D) Representative Ca^{2+} transient recordings from isolated TG-NSL12 myocytes treated with 10 μM of ranolazine for 1 hour with (D) and without (C) 10 mM of caffeine. (E) Summary of data from all the recordings. The time needed for recovery of caffeine-induced transient signal is significantly shortened after 10 μM of ranolazine treatment. *, $P < 0.05$ and **, $P < 0.01$ indicates statistical significance.

3.5 Discussion

Previously, our lab has demonstrated that the LQTS-causing mutation N1325S in cardiac sodium channel gene *SCN5A* led to abnormal cytosolic Ca^{2+} transient signals in isolated single TG-NS ventricular myocytes. Then we have performed a series of experiments showing the intracellular $[\text{Na}^+]_i$ increase and the dysfunction of $\text{Na}^+/\text{Ca}^{2+}$ exchanger (NCX). These results gave us a potential mechanism that the abnormal Ca^{2+} handling in TG-NS cells is caused by this *SCN5A* gain-of-function mutation via dysfunction of NCX. To the best of our knowledge, this is the first study that provides a direct link between a *SCN5A* mutation and abnormal intracellular Ca^{2+} transient signaling. The comparison between TG-NSL12 and TG-WTL10 mice which express the wild-type human *SCN5A* gene and have the a similar copy number of the transgene revealed that only TG-NS myocytes showed this abnormal Ca^{2+} handling. Besides, another transgenic mouse line which carries less copy numbers of this mutant transgene, TG-NSL3, also exhibited irregularities in Ca^{2+} transient signals, albeit with less severity. All these observations indicate that it is the mutation N1325S, rather than the overexpression of *SCN5A*, that caused the Ca^{2+} transient abnormality.

Our lab has also studied the expression level of the important Ca^{2+} handling proteins in TG-NS mouse hearts using Western blot analysis. The up-regulation of L-type Ca^{2+} channel protein, NCX and RyR2 in the presence of N1325S mutation suggests the remodeling of TG-NS myocytes. The changes in the Ca^{2+} handling proteins weaken the linkage between *SCN5A* mutation and abnormal Ca^{2+} handling we have set based on intracellular $[\text{Na}^+]$ increase and NCX dysfunction. In order to further investigate the relationship between this gain-of-function mutation and the abnormal Ca^{2+} handling in

the TG-NS myocytes, we introduced the LQTS drug, ranolazine, to block the late sodium current produced by N1325S mutation. After 1 hour of 10 μ M ranolazine treatment, the abnormal Ca^{2+} transient signal in the isolated TG-NSL3 and TG-NSL12 ventricular myocytes can be successfully rescued. This rescue effect further strengthened the direct linkage between N1325S mutation and abnormal Ca^{2+} handling.

In the previous study of Ca^{2+} transient signals in TG-NS ventricular myocytes, the most remarkable Ca^{2+} transient irregularity in TG-NS cells was in response to caffeine application though the amplitudes of the caffeine-induced Ca^{2+} transients did not have significant differences when compared to TG-WT cells. The prolongation of the recovery rate was often characterized by oscillations or “re-excitations” in TG-NS cells, and this characterization was also observed in HL-1 cells expressing N1325S mutant human *SCN5A* gene. These results suggested that the Ca^{2+} abnormalities in TG-NS ventricular myocytes may not stem from an “excess” of SR Ca^{2+} ion content but rather from a weakened ability to recover the cytosolic Ca^{2+} concentration to baseline. According to Ca^{2+} handling study in cardiac cells, the decline of intracellular Ca^{2+} ions during a caffeine-induced SR- Ca^{2+} release is almost entirely due to the extrusion of the Ca^{2+} via NCX (Altamirano et al 2006, Picht et al 2007). The interesting finding is that the expression of NCX-1 is increased in TG-NS mouse hearts, which seems to be contradictory to our findings in Ca^{2+} handling. Whereas, it is believed that NCX-1 expression level increase is a response to this chronic elevation of cytosolic Ca^{2+} in TG-NS myocytes. In the presence of N1325S mutant *SCN5A* gene, both intracellular Na^+ and Ca^{2+} increase. It is hypothesized that the excess of Na^+ and Ca^{2+} forces an adaptive response of the TG-NS cells in which the NCX is impossible to work in its proper way.

The lack of NCX current in TG-NS myocytes gives us a strong support to our hypothesis. As a result, in order to compensate dysfunction of NCX, more NCX-1 will be expressed in TG-NS myocytes.

Based on the result of our experiments, the ranolazine treatment to isolated TG-NSL3 and TG-NSL12 ventricular myocytes can significantly reduce the recovery time of caffeine-induced Ca^{2+} transients. It suggests that one hour, 10 μM ranolazine treatment is enough to recover the NCX function. The excess Na^+ entry caused by $\text{I}_{\text{Na,L}}$ is reduced using this late sodium blocker ranolazine, and the application of ranolazine can improve Ca^{2+} homeostasis.

In conclusion, this study has established the link between the existence of cytosolic Ca^{2+} inhomogeneity in TG-NS ventricular murine myocytes and the presence of a gain-of-function LQTS mutation N1325S in human cardiac sodium channel gene *SCN5A*, which is known to generate late sodium current $\text{I}_{\text{Na,L}}$. The application of $\text{I}_{\text{Na,L}}$ blocker ranolazine is proved to successfully rescue the abnormal Ca^{2+} handling in TG-NS mouse ventricular myocytes. This finding along with the intracellular Ca^{2+} abnormality in the presence of *SCN5A* mutation N1325S may provide a molecular mechanism for development of VT and DCM in both TG-NS mice and human patients with *SCN5A* mutations.

CHAPTER IV

LATE SODIUM CURRENT PRODUCED BY GAIN-OF-FUNCTION LQTS MUTATIONS IN CARDIAC SODIUM CHANNEL LEADS TO ABNORMAL CALCIUM HANDLING IN CARDIAC CELLS

4.1 Abstract

N1325S mutation in the cardiac sodium channel gene *SCN5A* produces late sodium currents ($I_{Na,L}$) and is associated with type-3 long QT syndrome (LQTS), ventricular tachyarrhythmias (VT) and dilated cardiomyopathy (DCM) in both human and mice. However, the underlying molecular mechanisms that originated from $I_{Na,L}$ need to be further explored. In this study, I have successfully correlated the mutant *SCN5A* with abnormal Ca^{2+} transient signals in transfected HL-1 cells. In HL-1 cells expressing N1325S mutant human *SCN5A*, the caffeine-induced Ca^{2+} transient signal showed significant prolonged recovery time from caffeine effects compared with cells expressing wild type human sodium channel $Na_v1.5$. This result indicates the reduced ability to

re-uptake the cytosolic Ca^{2+} of SR or to remove extra intracellular Ca^{2+} out of the cell in the presence of mutant $\text{Na}_v1.5$. Based on these observations, I hypothesized that $\text{I}_{\text{Na,L}}$ leads to cytosolic Ca^{2+} abnormalities. In order to test my hypothesis, I treated the cells with late sodium current blockers, ranolazine and mexiletine, and test if the abnormal Ca^{2+} handling can be rescued. The experiment results confirmed that both blockers was able to shorten the time required to remove the cytosolic Ca^{2+} from caffeine effects with no significant reduction in peak Ca^{2+} response. In order to further test my hypothesis, I then selected several other *SCN5A* mutations that can either cause LQTS or Brugada syndrome for *SCN5A* mutation classification. In this experiment, I measured the Ca^{2+} transients and time of recovery from caffeine in these mutations. After measurements, the results were compared in different types of $\text{Na}_v1.5$ mutations. The mutation classification results further indicated the correlation between the late sodium current and the weakened ability of the cell to reduce the cytosolic Ca^{2+} . Taken together, this study first correlates sodium mutations with Ca^{2+} handling in cardiac cells, and it can provide us important insights into the pathogenic mechanisms of LQTS, VT and DCM.

4.2 Introduction

The transient opening of Na^+ channels in cardiac cells gives rise to the inward current responsible for the upstroke of the cardiac action potential (AP) and the initiation of excitation-contraction coupling (Kiyosue and Arita 1989, Li et al 1997, Liu et al 1992). The changes in cardiac AP are composed of 5 phases from 0 to 4 and the opening of sodium channel contributes to rapid depolarization phase 0 and the plateau phase 2. After opening, sodium channels enter an inactivated state. However, gain-of-function mutant

sodium channels will stay at the inactivated state during the plateau (phase 2) of the AP when the wild type channels are usually closed. The abnormal prolonged inactivated state of the sodium channels will allow the continuous flow of Na^+ into the cell and results in persistent late sodium current ($I_{\text{Na,L}}$). Accordingly, the presence of $I_{\text{Na,L}}$ slows down the repolarization of the cell and therefore increases action potential duration (APD) (Liu et al 1992).

It is known that under ischemia/reperfusion conditions, sodium channel activation in cardiac cells is impaired, and that leads to $I_{\text{Na,L}}$. Consequently, $I_{\text{Na,L}}$ will cause the rise of myocardial Na^+ content (Barrington et al 1997, Williams et al 2007). The increase of intracellular Na^+ content can lead to increased Ca^{2+} via $\text{Na}^+/\text{Ca}^{2+}$ exchanger (NCX), which is consistent with the findings that $I_{\text{Na,L}}$ leads to a Na^+ -dependent Ca^{2+} overload (Fraser et al 2006, Pieske et al 2002, Song et al 2006, Wang et al 2008).

N1325S mutation in cardiac sodium channel *SCN5A* gene is a type-3 long QT syndrome mutation and was originally identified in a 96-member family (Wang et al 1995a). Previously, our lab generated a transgenic mouse model that overexpresses N1325S mutant human *SCN5A* in the heart (TG-NSL3 and TG-NSL12). According to the prior results, $I_{\text{Na,L}}$ produced by this gain-of-function LQTS mutation results in prolonged APDs in isolated ventricular myocytes, increased QTc on electrocardiograms and a high incidence of both ventricular tachyarrhythmias (VT) and sudden death in both TG-NSL3 and TG-NSL12 mice (Tian et al 2004). Besides, Dr. Sandro Yong in our lab has found that the Ca^{2+} transient signal is abnormal in isolated TG-NS myocytes due to the elevated intracellular Na^+ concentration and $\text{Na}^+/\text{Ca}^{2+}$ dysfunction. All these findings in TG-NS mice demonstrate a potential mechanism that can explain the pathogenesis of this

mutation. However, there is one more problem to be solved before we come up with the conclusion. In TG-NS myocytes, some important Ca^{2+} handling proteins, *e.g.*, NCX, RyR2 and L-type Ca^{2+} channel, are up-regulated in the presence of N1325S mutation (Zhang et al 2011). The up-regulation of these proteins indicates the remodeling of adult TG-NS myocytes caused by the mutant *SCN5A* transgene.

In order to overcome the adult myocytes remodeling problem, I introduced HL-1 cells, a cardiac muscle cell line derived from AT-1 mouse atrial cardiomyocyte tumor lineage, in this study (Claycomb et al 1998). In HL-1 cells expressing N1325S mutant *SCN5A* gene, the time required to remove extra cytosolic Ca^{2+} induced by caffeine is significantly prolonged compared with cells expressing wild type *SCN5A* gene. The further study of the effect for the blockage of $I_{\text{Na,L}}$ on abnormal Ca^{2+} handling provides us more evidences that $I_{\text{Na,L}}$ correlates with Ca^{2+} handling abnormality in cardiac cells expressing gain-of-function mutant $\text{Na}_v1.5$. The linkage between *SCN5A* mutation and abnormal Ca^{2+} handling offers a potential mechanism for LQTS and cardiac arrhythmias.

4.3 Materials and Methods

4.3.1 HL-1 Cardiac Cell Culture

HL-1 cardiac cell was a gift from Dr. William Claycomb (Louisiana State University, Medical Center, New Orleans, LA). According to the instruction from Dr. Claycomb, the cells were cultured in 5% CO_2 at 37°C in Claycomb media (Sigma-Aldrich, St. Louis, MO) supplemented with batch-specific 10% FBS (Sigma-Aldrich, St. Louis, MO), 100 U-100 $\mu\text{g/ml}$ penicillin-streptomycin (medium room at Lerner Research Institute, Cleveland Clinic Foundation, Cleveland, OH), 2 mM L-

glutamine (medium room at Lerner Research Institute, Cleveland Clinic Foundation, Cleveland, OH), and 0.1 mM norepinephrine (Sigma-Aldrich, St. Louis, MO). Before plating HL-1 cells, all the culture flasks and dishes were pre-treated for overnight with fibronectin/gelatin coating buffer containing 0.02% gelatin (ThermoFisher Scientific, Austin, TX) with 0.5% fibronectin (Life Technologies, Grand Island, NY).

4.3.2 Na⁺ Channel Cloning and Site-Directed Mutagenesis

Both wild type (WT) and mutant human cardiac *SCN5A* constructs were generated as described in the previous study (Wan et al 2001). All the plasmids were prepared at the same time using plasmid Maxi Prep (QIAGEN, Valencia, CA).

4.3.3 Transient Transfection of HL-1 Cell

HL-1 cardiac cells were transfected with either wild-type (WT) or mutant *SCN5A* expression plasmids along with GFP as an indicator for transfected cells using the PolyJet DNA In Vitro Transfection Reagent (SignaGen Laboratories, Gaithersburg, MD) according to the manufacturer's instructions with minor modifications to optimize the transfection efficiency. For Ca²⁺ transient measurements, HL-1 cells were plated on 12 mm diameter glass coverslips (Life Technologies, Grand Island, NY) at a density of 3×10^5 cells/ well in a 12-well culture plate (Sigma-Aldrich, St. Louis, MO). For each well, the amount of plasmid DNA and PolyJet reagent used for transfection is 1 µg and 3 µL, respectively. The transfected HL-1 cells were ready for Ca²⁺ transient measurements 48 hours after transfection.

4.3.4 Intracellular Ca^{2+} Transient Measurements

Before Ca^{2+} transient measurements, the transfected HL-1 cardiac cells were incubated with 10 μM Fura-2 acetoxymethyl ester (Fura-2/AM, TEF Labs, Austin, TX) for 10 minutes at room temperature in the dark. The cells were then washed with the fresh complemented Claycomb medium and incubated at 37°C with 5% CO_2 for 20 min to make sure that the acetoxymethyl group in Fura-2/AM is completely removed by cellular esterase. The coverslips containing HL-1 cells were then transferred to a Biotech chamber on the microscopic stage at 28°C, and initial field stimulation was set at 0.5 Hz and 5 ms duration during measurement. Ca^{2+} transient was measured simultaneously in 20-30 cells using excitation (340/380 nm) and emission (510 nm) spectra from the spectrofluorometer with a fixed test field. As an index of Ca^{2+} changes, the ratio of the emitted fluorescence at the wavelength of 340nm over 380nm (F/F_o) was calculated. Steady state Ca^{2+} transient signals were obtained at a pacing frequency of 0.25 Hz in the absence of caffeine. The relative sarcoplasmic reticulum (SR) Ca^{2+} contents of HL-1 cardiac cells expressing both WT and mutant *SCN5A* were estimated by comparing the amplitudes of Ca^{2+} transients before and after the application of 10mM caffeine, and the time needed for 90% recovery from caffeine application was calculated. The stimulation was stopped before 10 mM caffeine application. The rescue effects of late sodium current blockers were tested in the presence of 10 μM ranolazine and 10 μM mexiletine after one hour treatment at 37°C with 5% CO_2 .

4.3.5 Data Analysis

All the results were expressed as mean \pm S.E.M., and the differences between

means were calculated by student's paired t-test. A value of $P < 0.05$ was considered as statistically significant.

4.4 Results

4.4.1 N1325S Mutant Sodium Channels Lead to Irregular Ca^{2+} Handling in HL-1 Cells

In order to evaluate the effects of gain-of-function mutation N1325S in *SCN5A* gene to the cardiac Ca^{2+} handling, the HL-1 cells were transfected with wild-type (WT) or N1325S mutant *SCN5A* and used to assess the cytosolic Ca^{2+} levels using the Fura-2 AM. In excited HL-1 cells expressing the N1325S mutation, I found the premature or re-excited Ca^{2+} transient signals, which did not respond accordingly to the stimulation at a 0.25 Hz frequency. This abnormal Ca^{2+} transient signals indicate that the cytosolic Ca^{2+} in HL-1 cells expressing N1325S mutant *SCN5A* has difficulties in returning to baseline under 0.25 Hz stimulation frequency.

In order to further estimate the SR Ca^{2+} storage in mutant cells, I acutely treated the transfected cells with 10 mM caffeine. Caffeine is commonly used to estimate the content of the SR Ca^{2+} storage, Ca^{2+} release, and the rate of Ca^{2+} extrusion from the cells (Picht et al 2006). In this experiment, I observed a significant increase in the amplitude and duration of Ca^{2+} release after adding caffeine (10 mM) to the cells (Figure 9C) in HL-1 cells expressing N1325S mutant *SCN5A*. The amplitude of the Ca^{2+} transient in response to caffeine is often an index of the SR Ca^{2+} content during diastole (Lewartowski and Zdanowski 1990). In HL-1 cells expressing N1325S mutant *SCN5A*, the higher Ca^{2+} transient amplitudes comparing with HL-1 cells expressing WT *SCN5A* indicate a higher

SR Ca^{2+} content during diastole (F/F_o value: 0.53 ± 0.03 in N1325S and 0.35 ± 0.03 in WT, $P < 0.05$). At the same time, the time required for Ca^{2+} transients returning to baseline in response to caffeine is higher in cells expressing N1325S mutation than in control cells (20.5 ± 1.9 s in N1325S and 14.7 ± 0.8 s in WT, $P < 0.05$). These results indicate that compared with cells expressing WT *SCN5A*, HL-1 cells with the N1325S mutation have higher initial SR Ca^{2+} content, and slower removal of Ca^{2+} from the cytosol compared with WT cells. Besides, in some HL-1 cells expressing the N1325S mutation, there are a second caffeine-induced Ca^{2+} responses (Figure 9D). This phenomenon can be explained by re-excitation by elevated cytosolic Ca^{2+} concentrations of the cells during repolarization. The sustained high cytosolic Ca^{2+} causes the release of SR Ca^{2+} storage more than once during one excitation-contraction coupling.

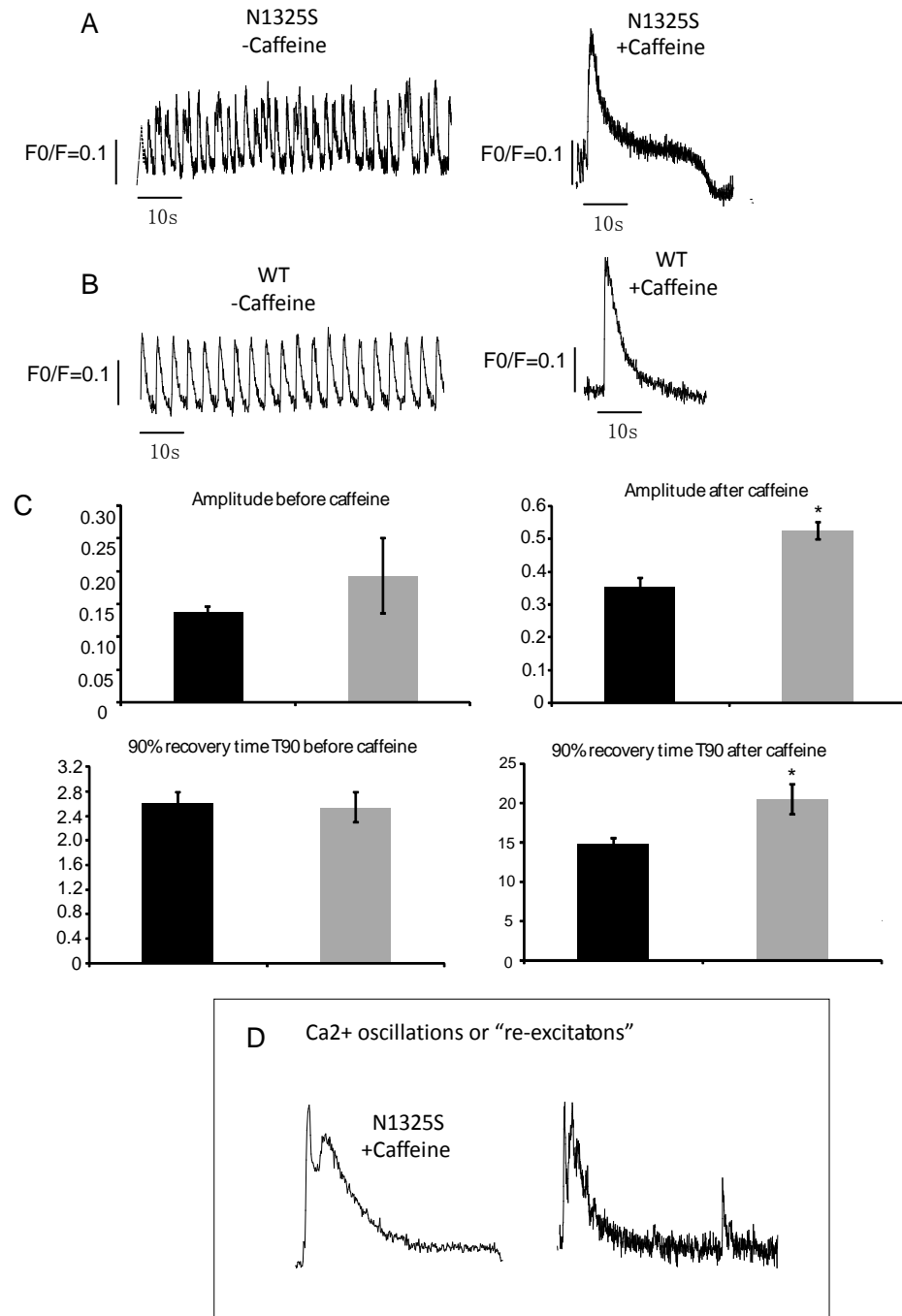


Figure 9. Ca²⁺ Transients Signals in Transfected HL-1 Cells. (A) Representative Ca²⁺ transient recordings in HL-1 cells expressing N1325S mutation in *SCN5A* gene with (right) and without (left) 10 mM of caffeine. (B) Representative Ca²⁺ transient recordings in HL-1 cells expressing wild type *SCN5A* gene with (right) and without (left) 10 mM caffeine. (C) Summary of data from all the recordings. The caffeine-induced peak Ca²⁺ response is higher in N1325S HL-1 cells (upper right). The time needed for recovery from caffeine effect is also significantly prolonged in HL-1 cells expressing N1325S mutant *SCN5A* gene. (D) Representative Ca²⁺ transient signals with re-excitation after adding caffeine. *, $P < 0.05$ indicates statistical significance.

4.4.2 Ranolazine Can Reduce the SR Ca^{2+} Content and Strengthen the Ability of Removing Extra Cytosolic Ca^{2+} in HL-1 Cells Expressing N1325S Mutant *SCN5A*

N1325S mutation is a gain-of-function mutation in *SCN5A* that can produce persistent late sodium currents (Tian et al 2004). In the isolated myocytes from transgenic mice carrying N1325S mutation (TG-NS), the intracellular Na^+ concentration is higher compared with non-transgenic (NTG) and transgenic wild type (TG-WT) mice. During the excitation-contraction coupling in the cardiac cells, Ca^{2+} ions are extruded from the cells mainly via the $\text{Na}^+/\text{Ca}^{2+}$ exchanger in order to reduce the cytosolic Ca^{2+} after diastole (Bers 2002). In our TG-NS mouse myocytes, the lack of Ni^{2+} -sensitive current indicated that $\text{Na}^+/\text{Ca}^{2+}$ exchanger is dysfunctional (Yong S, unpublished data). These two findings in our TG-NS mice provided a direct link between a *SCN5A* mutation and the abnormal intracellular Ca^{2+} signaling. However, the up-regulation of some Ca^{2+} handling proteins such as NCX, RyR2 and L-type Ca^{2+} channel indicated the remodeling of the cardiac cells in adult TG-NS mice (Zhang et al 2011). The lack of mature cardiac cell phenotype in neonatal cardiomyocytes limits the use of isolated neonatal myocytes in TG-NS mice. In this study, the introduction of HL-1 cells overcame the remodeling problem in adult TG-NS mice.

To correlate the effects of late sodium current and abnormal Ca^{2+} handling, the cells were treated with 10 μM of ranolazine (Figure 10) to block the late sodium currents. Ranolazine is a investigative anti-arrhythmic drug in phase III trials. It has been approved that ranolazine can successfully block the late sodium currents caused by LQT3 mutations in the *SCN5A* gene (Fredj et al 2006, Zaza et al 2008). After 1 hour of

ranolazine treatment, I observed that the Ca^{2+} transient signal showed significant reduction from 20.5 ± 1.9 s to 12.9 ± 1.7 s ($P < 0.05$) in recovery time (T90) (Figure 10F) from caffeine effect with little or no changes in the transient amplitudes (Figure 10D). Besides, in the presence of ranolazine, most abnormal transient signals can also be rescued to normal and can respond to the stimulation accordingly (Figure 10A and 10B). These results indicate that although ranolazine cannot reduce the higher SR Ca^{2+} storage significantly in N1325S mutant HL-1 cells (Figure 10D), it can reduce the time required for the removal of Ca^{2+} from the cytosol (Figure 10F). Therefore, according to my results, the treatment of ranolazine itself is not enough to reduce the SR Ca^{2+} content significantly. However, the shortening of time that is required for the removal of Ca^{2+} from cytosol can explain the potential mechanism why ranolazine is an effective treatment for LQT3 patients. Consequently, after successful blockage of late sodium currents by ranolazine, the elevated intracellular Na^+ concentration is reduced, and the dysfunction of NCX is rescued. Note that during the excitation-contraction coupling in the cardiac cells, Ca^{2+} ions are extruded from the cells mainly via the $\text{Na}^+/\text{Ca}^{2+}$ exchanger in order to reduce the cytosolic Ca^{2+} after diastole (Bers 2002). The re-gaining function of NCX increases the ability of the cell to extrude cytosolic Ca^{2+} .

Furthermore, ranolazine treatment was not able to decrease the caffeine-induced peak Ca^{2+} responses (Figure 10D). One of the excitation-contraction coupling model proposed that the SR Ca^{2+} is stored in two compartments: an uptake compartment and a release compartment (Euler 1999). Thus, the caffeine-induced peak Ca^{2+} response may not be determined by the total SR Ca^{2+} content, but the Ca^{2+} content available to be released in the release compartment. The ranolazine treatment for one hour is not enough

to break the “balance” between uptake compartment and release compartment Ca^{2+} content in SR, thus it would not change the peak Ca^{2+} response in the presence of 10 mM caffeine.

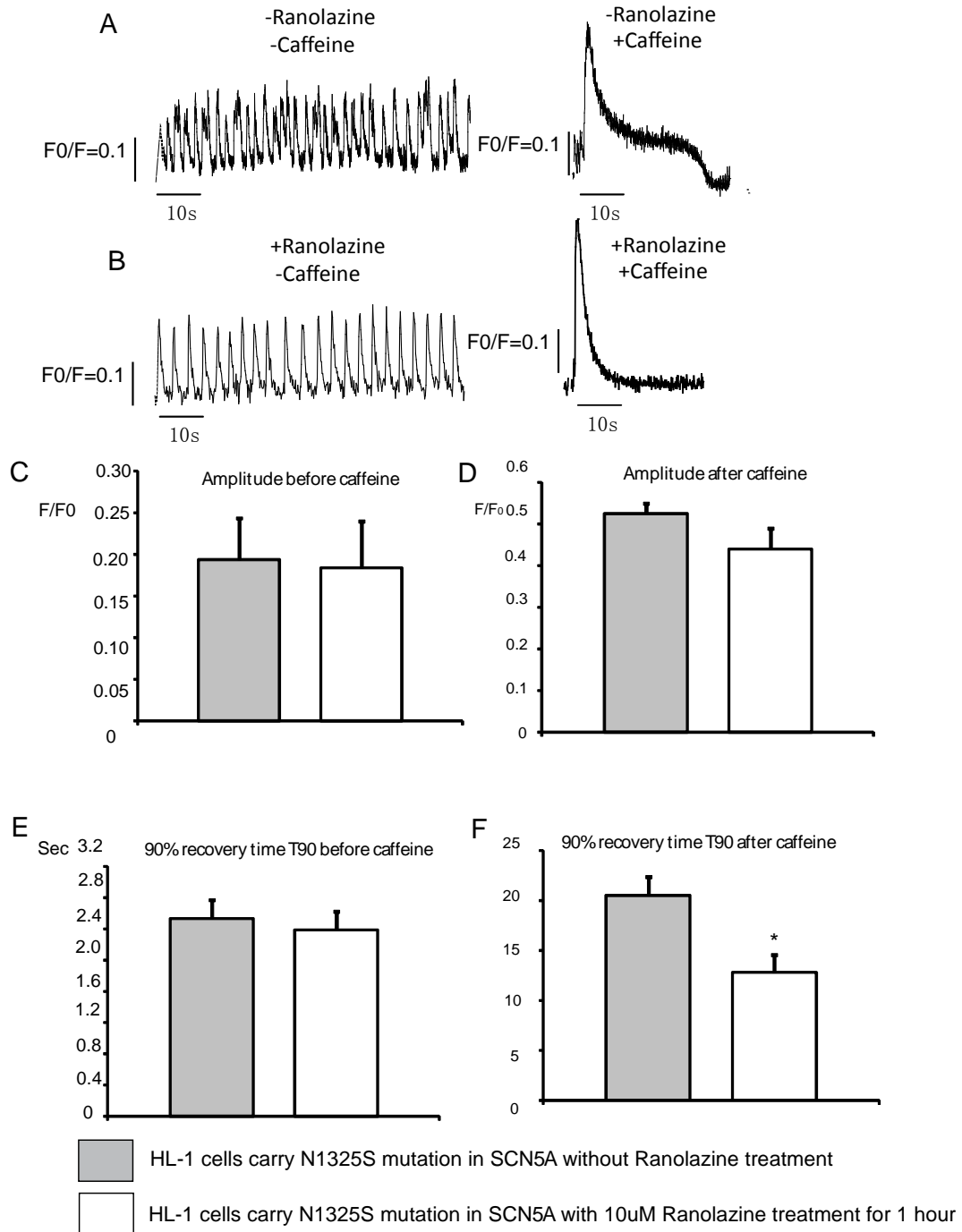


Figure 10. Effect of Ranolazine Treatments in HL-1 Cells Expressing the N1325S Mutation. (A) Representative Ca^{2+} transient recordings in HL-1 cells carrying the N1325S mutation before (left) and after (right) caffeine. (B) Representative Ca^{2+} transient recording in HL-1 cells carrying the N1325S mutation in the presence of 10 μM of ranolazine treatment before (left) and after (right) caffeine. (C-F) Summary of data from all the recordings. The time needed for the removal of cytosolic Ca^{2+} after caffeine is shortened after ranolazine treatment. *, $P < 0.05$ indicates statistical significance.

4.4.3 Mexiletine Can Reduce the SR Ca^{2+} Content in HL-1 Cells Expressing N1325S Mutant *SCN5A*

In this study, another late sodium current blocker mexiletine was also tested in N1325S mutant HL-1 cells. Mexiletine can abbreviate the QT interval in LQT3 patients (Sicouri et al 1997). Our lab previously reported that mexiletine was able to successfully block the late sodium current in isolated TG-NS myocytes (Tian et al 2004). Mexiletine can also suppress ventricular fibrillation (VF) and ventricular tachycardia (VT) in TG-RQ mice (Tian et al 2004). In this study, I identified that similar to ranolazine, in the presence of 10 μM of mexiletine, the recovery time from caffeine is significantly reduced by ~50% from more than 20 seconds to 10.6 ± 1.4 s ($P < 0.05$) (Figure 11F). And also similar to ranolazine, mexiletine treatment is also not able to reduce the caffeine-induced Ca^{2+} peak response (Figure 11E). And the cells can respond to the stimulation better after treatment (Figure 11A and 11B).

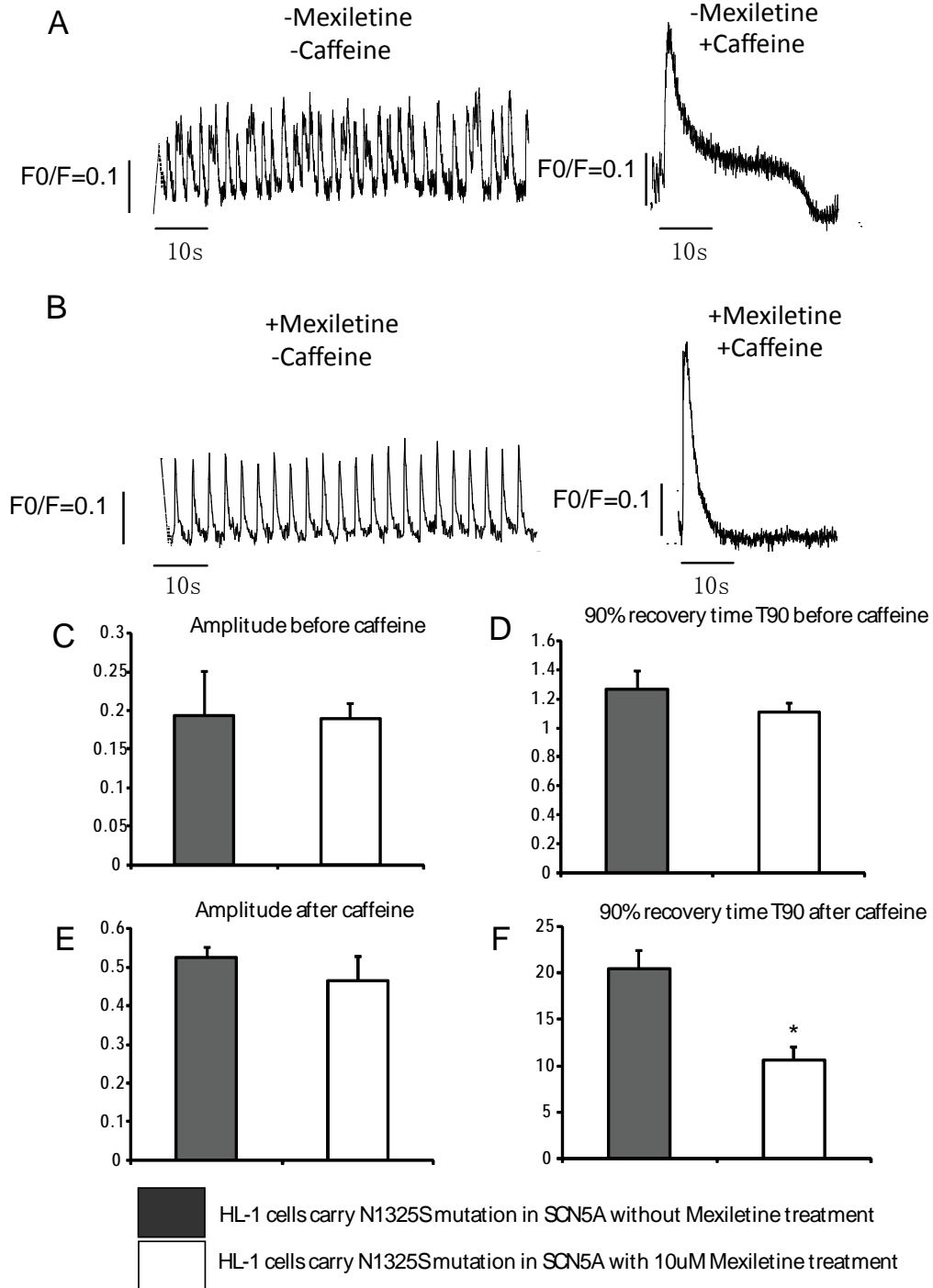


Figure 11. Effect of Mexiletine Treatments in HL-1 Cells Expressing the N1325S Mutation. (A) Representative Ca^{2+} transient recordings in HL-1 cells carrying the N1325S mutation before (left) and after (right) caffeine. (B) Representative Ca^{2+} transient recording in HL-1 cells carrying the N1325S mutation in the presence of 10 μM of mexiletine treatment before (left) and after (right) caffeine. (C-F) Summary of data from all the recordings. The time needed for the removal of cytosolic Ca^{2+} after caffeine is shortened after mexiletine treatment. *, $P < 0.05$ indicates statistical significance.

4.4.4 Classification of Different *SCN5A* Mutations

Since LQTS mutation N1325S showed these Ca^{2+} transient signal specific features in both isolated myocytes and transfected HL-1 cells, I was wondering if other gain-of-function mutations in *SCN5A* will display the same phenotype or it is just N1325S specific phenomenon. In the next series of experiments, I have selected other two LQTS mutations in *SCN5A* gene, E1784K and Δ KPQ, which also produce late sodium currents like N1325S mutation (Dumaine et al 1996, Wei et al 1999). At the same time, I selected two Brugada syndrome mutations, A1924T and L567Q, which do not produce the late sodium current (Rook et al 1999, Wan et al 2001). In this experiment, I only evaluated the effects from caffeine effects to estimate the content of SR Ca^{2+} storage and the recovery time required to remove extra cytosolic Ca^{2+} (Figure 12). After statistical analysis, I found that both E1784K and Δ KPQ mutations can significantly prolong the recovery time from caffeine, and the prolongation of E1784K mutation is almost 10 times as much as wild type sodium channel (Figure 12C). The caffeine-induced peak Ca^{2+} response in N1325S, Δ KPQ, E1784K and A1924T are all significantly higher than HL-1 cells transfected with WT *SCN5A* (Figure 12B). According to my results, the caffeine-induced peak Ca^{2+} response is not correlated with the presence of LQTS mutations (Figure 12B). The reason behind this could be explained by the two SR compartments theory(Euler 1999). During excitation-contraction coupling, the cells expressing LQTS mutant *SCN5A* experience a spontaneous Ca^{2+} oscillation, and no sufficient time for the cells to transfer the uptake compartment Ca^{2+} to release compartment in SR. As a result, the Ca^{2+} content in release compartment is limited and not be able to reflect the total SR Ca^{2+} content. This theory about SR Ca^{2+} storage can

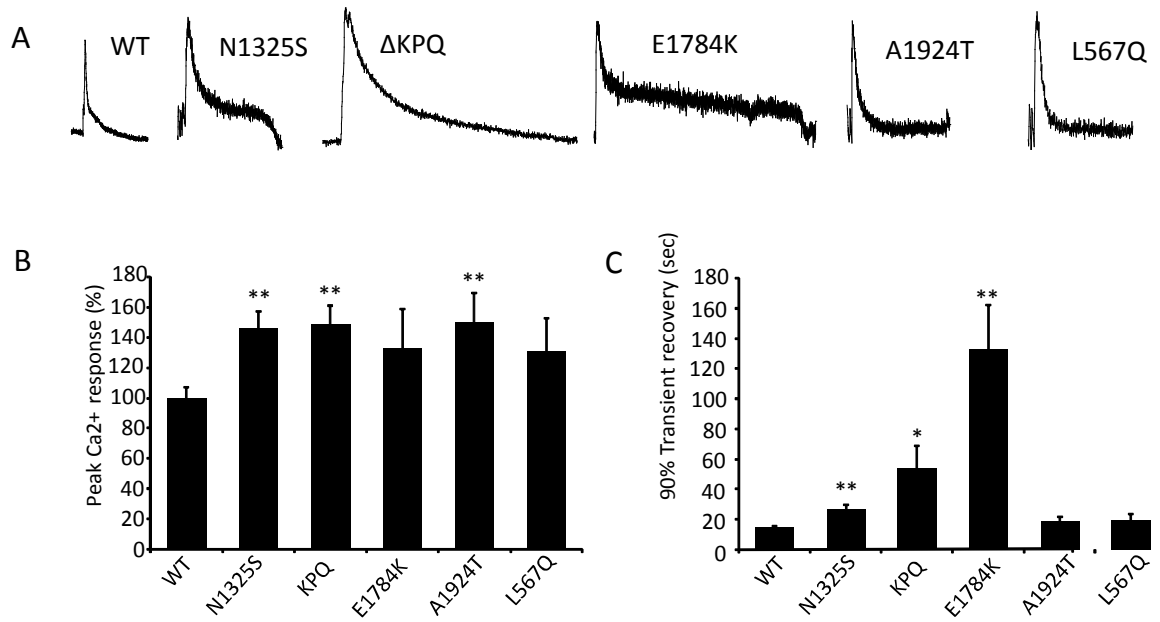


Figure 12. Effects of Different *SCN5A* Mutations on Ca^{2+} Transients. (A) Representative Ca^{2+} signal response induced by 10 mM of caffeine. (B) The peak Ca^{2+} response in different mutations related to wild type *SCN5A* (100%). Three mutations, N1325S, ΔKPQ and A1924T have higher peak Ca^{2+} response compared with wild type sodium channels. (C) Time required for 90% recovery in the intracellular Ca^{2+} from caffeine effect. Three mutations, N1325S, ΔKPQ and E1784K which are all LQTS mutations producing late sodium currents need significantly longer 90% transient recovery time. *, $P < 0.05$ and **, $P < 0.01$ indicate statistical significance.

explain why the caffeine-induced peak Ca^{2+} response is not always higher in LQTS mutant cells. Except for Na^{2+} content, the amount of Ca^{2+} in SR release compartment is affected by other factors or it is a result of complex factors.

4.4.5 Ranolazine Effect in Various *SCN5A* Mutations

In order to further test the relationship between different types of *SCN5A* mutations and Ca^{2+} handling, the ranolazine effect in these mutations was also tested (Figure 13). After one hour, 10 μM of ranolazine treatment, the Ca^{2+} transient signals were collected in HL-1 cells transfected with different *SCN5A* mutations and wild-type *SCN5A*. As I expected, the 90% transient recovery time from caffeine was significantly reduced in the mutations (N1325S, ΔKPQ and E1784K) that can produce certain amount of late sodium currents (Figure 13C). The shortening of recovery time from caffeine is especially dramatic in E1784K mutation, from 132.67 seconds ($n=8$) to an average of 13.877 seconds ($n=10$). At the same time, the peak Ca^{2+} response from caffeine in E1784K mutation is more than 300% compared with wild-type *SCN5A* (Figure 13B). This significantly higher peak Ca^{2+} response from caffeine in E1784K mutation indicates an increase of release Ca^{2+} content in SR after ranolazine treatment. One of the Brugada mutations, L567Q, also showed significantly increased peak Ca^{2+} response in the presence of caffeine, but the mechanism behind this is not clear and need to be further explored (Figure 13B).

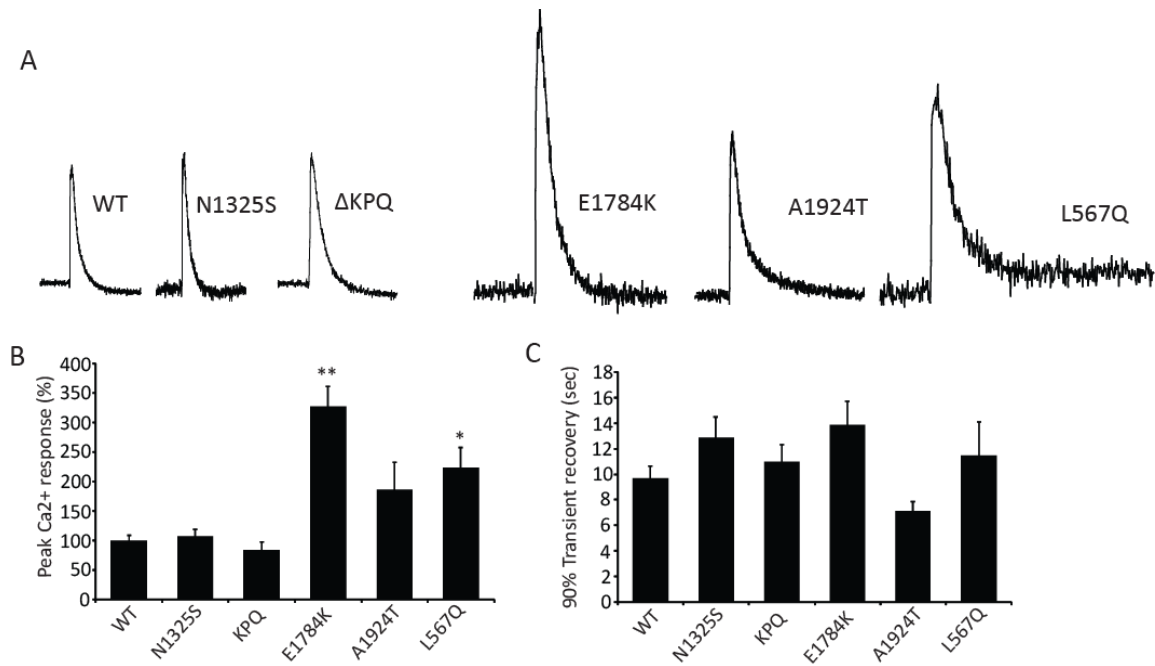


Figure 13. Effect of Ranolazine in Various *SCN5A* Mutations. (A) Representative Ca^{2+} signal induced by 10 mM caffeine after 1 hour, 10 μM ranolazine treatment. (B) The peak Ca^{2+} response in different mutations related to wild type *SCN5A* (100%) after ranolazine treatment. One of the LQTS mutations, E1784K, has significantly increased response compared with WT. One of the Brugada mutations, L567Q, has dramatically stronger caffeine response compared with WT. (C) Time required for 90% recovery in the intracellular Ca^{2+} from caffeine effect. After one hour, 10 μM ranolazine treatment, all the LQTS mutations studied in this experiment showed no significant differences compared with WT. *, $P < 0.05$ and **, $P < 0.01$ indicate statistical significance.

4.5 Discussion

In this study, I introduced transfected HL-1 cells for Ca^{2+} handling study related to $\text{Na}_v1.5$ mutations for the first time. The results in this study demonstrate that gain-of-function LQTS causing mutation, N1325S, in cardiac sodium channel gene *SCN5A* leads to abnormal cytosolic Ca^{2+} transient signal in HL-1 cells. This Ca^{2+} handling study correlates the sodium mutations with abnormal intracellular Ca^{2+} in the cardiac cells. The electrophysiological study of transgenic mice is time consuming, and the isolation for adult mice cardiomyocytes depends on the quality of the collagenase from the commercial companies. The introduction of HL-1 cells will solve the adult myocytes remodeling problems because HL-1 cells are easy to be transfected and can retain the adult cardiomyocyte phenotype in culture.

In this study, I found that the caffeine-induced peak Ca^{2+} transients in HL-1 cells expressing N1325S mutant *SCN5A* were increased, and the recovery time from caffeine is significantly prolonged in mutant cells. The presence of Ca^{2+} oscillations or “re-excitations” in N1325S HL-1 cells suggests that the abnormal Ca^{2+} handling may not stem from the higher content of SR Ca^{2+} content, but from a reduced ability to remove the cytosolic Ca^{2+} back to SR or out of the cells. Therefore, the prolonged reduction of cytosolic Ca^{2+} can cause another Ca^{2+} induce Ca^{2+} release (CICR) and give a second peak when adding caffeine. This result indicates the linkage between *SCN5A* mutation and abnormal Ca^{2+} , the following series of experiments I had designed would further strengthen the correlation between these two.

In order to investigate whether late sodium currents produced by N1325S mutation play a critical role in abnormal intracellular Ca^{2+} transient signals, I treated the cells with

late sodium current blockers, ranolazine and mexiletine. Following the treatment of 10 μM of ranolazine or mexiletine, the recovery time from caffeine effects is significantly shortened with no change in amplitudes. This suggested that a reduction of excessive Na^+ entry caused by late sodium currents will reduce the intracellular Na^+ concentration and quicken the removal of cytosolic Ca^{2+} back to SR or out of the cells. The comparison of different *SCN5A* mutations on Ca^{2+} handling indicates that the SR Ca^{2+} content was not necessarily affected by late sodium currents because not only did N1325S, ΔKPQ and E1784K mutations increase the caffeine-induced peak Ca^{2+} response, but A1924T mutation also increased the peak Ca^{2+} response. A1924T mutation is a Brugada mutation causing negative shift of inactivation curve, I_{Na} increase and a larger action potential overshoot (Rook et al 1999). The overall impact on intracellular Na^+ concentration is unknown. However, according to my results, the ability of removing extra cytosolic Ca^{2+} is correlated to the presence of late sodium currents produced by *SCN5A* mutations because only mutations that produce $I_{\text{Na,L}}$ have significantly prolonged recovery time from caffeine.

Since the first mutation in *SCN5A* related to cardiac arrhythmia was identified in 1995 (Wang et al 1995b), various mutations in this gene have been found and associated with numerous arrhythmia syndromes, such as LQT3, Brugada syndrome, progressive cardiac conduction defect (PCCD), sick sinus node syndrome (SSS), atrial fibrillation (AF) and DCM. The molecular pathology of these mutations is still not fully understood. Ca^{2+} is a crucial element in all kinds of organisms, and it plays an important role in numerous biological functions. It is known that the intracellular free Ca^{2+} concentration ($\sim 10^{-7}$ M) is much lower than the extracellular Ca^{2+} . This high Ca^{2+} gradient provides

abundant Ca^{2+} available to be imported into cells, where these Ca^{2+} ions can function as second messengers (Chin and Means 2000). Thus, the abnormal Ca^{2+} handling in some *SCN5A* mutations could play an important role in the development of cardiac arrhythmia.

In conclusion, this study has established the correlation between gain-of-function sodium mutations and abnormal cytosolic Ca^{2+} handling in cardiac cells. I believe that the late sodium current is the cause for Ca^{2+} inhomogeneity caused by the N1325S mutation. I further showed that in the presence of late sodium current blocker, ranolazine or mexiletine, the prolonged recovery time from caffeine can be shortened. The advantage of this study over the isolated TG-NS adult myocytes is the introduction of HL-1 cells. HL-1 cells diminished the remodeling responses such as a higher apoptosis rate and up-regulations of Ca^{2+} handling proteins in aging TG-NS mouse hearts. The finding that abnormal intracellular Ca^{2+} transient signals are associated with gain-of-function LQTS *SCN5A* mutation may provide a molecular mechanism for the development of VT and DCM.

BIBLIOGRAPHY

Abbott GW, Sesti F, Splawski I, Buck ME, Lehmann MH, Timothy KW *et al* (1999). MiRP1 forms IKr potassium channels with HERG and is associated with cardiac arrhythmia. *Cell* **97**: 175-187.

Abriel H, Kamynina E, Horisberger JD, Staub O (2000). Regulation of the cardiac voltage-gated Na⁺ channel (H1) by the ubiquitin-protein ligase Nedd4. *FEBS Lett* **466**: 377-380.

Abriel H, Kass RS (2005). Regulation of the voltage-gated cardiac sodium channel Nav1.5 by interacting proteins. *Trends Cardiovasc Med* **15**: 35-40.

Abriel H (2007). Cardiac sodium channel Nav1.5 and its associated proteins. *Arch Mal Coeur Vaiss* **100**: 787-793.

Ahern CA, Zhang JF, Wookalis MJ, Horn R (2005). Modulation of the cardiac sodium channel NaV1.5 by Fyn, a Src family tyrosine kinase. *Circ Res* **96**: 991-998.

Aitken A (2006). 14-3-3 proteins: a historic overview. *Semin Cancer Biol* **16**: 162-172.

Akai J, Makita N, Sakurada H, Shirai N, Ueda K, Kitabatake A *et al* (2000). A novel SCN5A mutation associated with idiopathic ventricular fibrillation without typical ECG findings of Brugada syndrome. *FEBS Lett* **479**: 29-34.

Allouis M, Le Bouffant F, Wilders R, Pérez D, Schott JJ, Noireaud J *et al* (2006). 14-3-3 is a regulator of the cardiac voltage-gated sodium channel Nav1.5. *Circ Res* **98**: 1538-1546.

Altamirano J, Li Y, DeSantiago J, Piacentino V, Houser SR, Bers DM (2006). The inotropic effect of cardioactive glycosides in ventricular myocytes requires Na⁺-Ca²⁺ exchanger function. *J Physiol* **575**: 845-854.

Andavan GS, Lemmens-Gruber R (2011). Voltage-gated sodium channels: mutations, channelopathies and targets. *Curr Med Chem* **18**: 377-397.

Antzelevitch C, Pollevick GD, Cordeiro JM, Casis O, Sanguinetti MC, Aizawa Y *et al* (2007). Loss-of-function mutations in the cardiac calcium channel underlie a new clinical entity characterized by ST-segment elevation, short QT intervals, and sudden cardiac death. *Circulation* **115**: 442-449.

Antzelevitch C, Burashnikov A, Sicouri S, Belardinelli L (2011). Electrophysiologic basis for the antiarrhythmic actions of ranolazine. *Heart Rhythm* **8**: 1281-1290.

Asahi M, Nakayama H, Tada M, Otsu K (2003). Regulation of sarco(endo)plasmic reticulum Ca²⁺ adenosine triphosphatase by phospholamban and sarcolipin: implication for cardiac hypertrophy and failure. *Trends Cardiovasc Med* **13**: 152-157.

Baba S, Dun W, Boyden PA (2004). Can PKA activators rescue Na⁺ channel function in epicardial border zone cells that survive in the infarcted canine heart. *Cardiovasc Res* **64**: 260-267.

Balijepalli RC, Kamp TJ (2008). Caveolae, ion channels and cardiac arrhythmias. *Prog Biophys Mol Biol* **98**: 149-160.

Balser JR, Bennett PB, Hondeghem LM, Roden DM (1991). Suppression of time-dependent outward current in guinea pig ventricular myocytes: actions of quinidine and amiodarone. *Circ Res* **69**: 519-529.

Baroudi G, Carbonneau E, Pouliot V, Chahine M (2000). SCN5A mutation (T1620M) causing Brugada syndrome exhibits different phenotypes when expressed in *Xenopus* oocytes and mammalian cells. *FEBS Lett* **467**: 12-16.

Barrington PL, Martin RL, Zhang K (1997). Slowly inactivating sodium currents are reduced by exposure to oxidative stress. *J Mol Cell Cardiol* **29**: 3251-3265.

Bassani JW, Bassani RA, Bers DM (1994). Relaxation in rabbit and rat cardiac cells: species-dependent differences in cellular mechanisms. *J Physiol* **476**: 279-293.

Baulac S, Gourfinkel-An I, Picard F, Rosenberg-Bourgin M, Prud'homme JF, Baulac M *et*

al (1999). A second locus for familial generalized epilepsy with febrile seizures plus maps to chromosome 2q21-q33. *Am J Hum Genet* **65**: 1078-1085.

Bazett HC (1920). An analysis of the time relations of electrocardiograms. *Heart* **7**: 353-370.

Beggs AH (1997). Dystrophinopathy, the expanding phenotype. Dystrophin abnormalities in X-linked dilated cardiomyopathy. *Circulation* **95**: 2344-2347.

Bender AC, Morse RP, Scott RC, Holmes GL, Lenck-Santini PP (2012). SCN1A mutations in Dravet syndrome: Impact of interneuron dysfunction on neural networks and cognitive outcome. *Epilepsy Behavior: E&B* **23**: 177-186.

Bennett PB, Yazawa K, Makita N, George AL, Jr. (1995). Molecular mechanism for an inherited cardiac arrhythmia. *Nature* **375**: 683-685.

Benson DW, Wang DW, Dymment M, Knilans TK, Fish FA, Strieper MJ *et al* (2003). Congenital sick sinus syndrome caused by recessive mutations in the cardiac sodium channel gene (SCN5A). *J Clin Invest* **112**: 1019-1028.

Bers DM (2002). Cardiac excitation-contraction coupling. *Nature* **415**: 198-205.

Beyder A, Strege PR, Reyes S, Bernard CE, Terzic A, Makielski J *et al* (2012).

Ranolazine decreases mechanosensitivity of the voltage-gated sodium ion channel NaV1.5: a novel mechanism of drug action. *Circulation* **125**: 2698-2706.

Bezzina C, Veldkamp MW, van Den Berg MP, Postma AV, Rook MB, Viersma JW *et al* (1999). A single Na(+) channel mutation causing both long-QT and Brugada syndromes. *Circ Res* **85**: 1206-1213.

Bezzina CR, Tan HL (2002). Pharmacological rescue of mutant ion channels. *Cardiovasc Res* **55**: 229-232.

Bezzina CR, Rook MB, Groenewegen WA, Herfst LJ, van der Wal AC, Lam J *et al* (2003). Compound heterozygosity for mutations (W156X and R225W) in SCN5A associated with severe cardiac conduction disturbances and degenerative changes in the conduction system. *Circ Res* **92**: 159-168.

Binder WH, Barragan V, Menger FM (2003). Domains and rafts in lipid membranes. *Angew Chem Int Ed Engl* **42**: 5802-5827.

Blangy H, Sadoul N, Coutelour JM, Rebmann JP, Joseph M, Scherrer C *et al* (2005). Prevalence of Brugada syndrome among 35,309 inhabitants of Lorraine screened at a preventive medicine centre. *Arch Mal Coeur Vaiss* **98**: 175-180.

Blaustein MP, Lederer WJ (1999). Sodium/calcium exchange: its physiological

implications. *Physiol Rev* **79**: 763-854.

Braun AP, Schulman H (1995). The multifunctional calcium/calmodulin-dependent protein kinase: from form to function. *Annu Rev Physiol* **57**: 417-445.

Brink PA, Ferreira A, Moolman JC, Weymar HW, van der Merwe PL, Corfield VA (1995). Gene for progressive familial heart block type I maps to chromosome 19q13. *Circulation* **91**: 1633-1640.

Brodsky MA, Chun JG, Podrid PJ, Douban S, Allen BJ, Cygan R (1996). Regional attitudes of generalists, specialists, and subspecialists about management of atrial fibrillation. *Arch Intern Med* **156**: 2553-2562.

Brown DA, London E (1998). Structure and origin of ordered lipid domains in biological membranes. *J Membr Biol* **164**: 103-114.

Brugada J, Brugada R, Antzelevitch C, Towbin J, Nademanee K, Brugada P (2002). Long-term follow-up of individuals with the electrocardiographic pattern of right bundle-branch block and ST-segment elevation in precordial leads V1 to V3. *Circulation* **105**: 73-78.

Brugada P, Wellens HJ (1988). Arrhythmogenesis of antiarrhythmic drugs. *Am J Cardiol* **61**: 1108-1111.

Brugada P, Brugada J (1992). Right bundle branch block, persistent ST segment elevation and sudden cardiac death: a distinct clinical and electrocardiographic syndrome. A multicenter report. *J Am Coll Cardiol* **20**: 1391-1396.

Burgess DL, Kohrman DC, Galt J, Plummer NW, Jones JM, Spear B *et al* (1995). Mutation of a new sodium channel gene, *Scn8a*, in the mouse mutant 'motor endplate disease'. *Nat Genet* **10**: 461-465.

Camacho JA, Hensellek S, Rougier JS, Blechschmidt S, Abriel H, Benndorf K *et al* (2006). Modulation of Nav1.5 channel function by an alternatively spliced sequence in the DII/DIII linker region. *J Biol Chem* **281**: 9498-9506.

Cantrell AR, Smith RD, Goldin AL, Scheuer T, Catterall WA (1997). Dopaminergic modulation of sodium current in hippocampal neurons via cAMP-dependent phosphorylation of specific sites in the sodium channel alpha subunit. *J Neurosci* **17**: 7330-7338.

Carmeliet E (1993). Use-dependent block of the delayed K⁺ current in rabbit ventricular myocytes. *Cardiovasc Drugs Ther* **7**: 599-604.

Casini S, Tan HL, Bhuiyan ZA, Bezzina CR, Barnett P, Cerbai E *et al* (2007). Characterization of a novel SCN5A mutation associated with Brugada syndrome reveals

involvement of DIIS4-S5 linker in slow inactivation. *Cardiovasc Res* **76**: 418-429.

Chaitman BR, Pepine CJ, Parker JO, Skopal J, Chumakova G, Kuch J *et al* (2004). Effects of ranolazine with atenolol, amlodipine, or diltiazem on exercise tolerance and angina frequency in patients with severe chronic angina: a randomized controlled trial. *JAMA* **291**: 309-316.

Chambers JC, Zhao J, Terracciano CM, Bezzina CR, Zhang W, Kaba R *et al* (2010). Genetic variation in SCN10A influences cardiac conduction. *Nat Genet* **42**: 149-152.

Chang CC, Acharfi S, Wu MH, Chiang FT, Wang JK, Sung TC *et al* (2004). A novel SCN5A mutation manifests as a malignant form of long QT syndrome with perinatal onset of tachycardia/bradycardia. *Cardiovasc Res* **64**: 268-278.

Chauhan VS, Tuvia S, Buhusi M, Bennett V, Grant AO (2000). Abnormal cardiac Na(+) channel properties and QT heart rate adaptation in neonatal ankyrin(B) knockout mice. *Circ Res* **86**: 441-447.

Chen J, Chien KR (1999). Complexity in simplicity: monogenic disorders and complex cardiomyopathies. *J Clin Invest* **103**: 1483-1485.

Chen L, Marquardt ML, Tester DJ, Sampson KJ, Ackerman MJ, Kass RS (2007). Mutation of an A-kinase-anchoring protein causes long-QT syndrome. *Proc Natl Acad*

Sci U S A **104**: 20990-20995.

Chen Q, Kirsch GE, Zhang D, Brugada R, Brugada J, Brugada P *et al* (1998). Genetic basis and molecular mechanism for idiopathic ventricular fibrillation. *Nature* **392**: 293-296.

Chen S, Chung MK, Martin D, Rozich R, Tchou PJ, Wang Q (2002). SNP S1103Y in the cardiac sodium channel gene SCN5A is associated with cardiac arrhythmias and sudden death in a white family. *J Med Genet* **39**: 913-915.

Chen T, Inoue M, Sheets MF (2005). Reduced voltage dependence of inactivation in the SCN5A sodium channel mutation delF1617. *Am J Physiol Heart Circ Physiol* **288**: H2666-2676.

Chen YH, Xu SJ, Bendahhou S, Wang XL, Wang Y, Xu WY *et al* (2003). KCNQ1 gain-of-function mutation in familial atrial fibrillation. *Science* **299**: 251-255.

Chin D, Means AR (2000). Calmodulin: a prototypical calcium sensor. *Trends Cell Biol* **10**: 322-328.

Claycomb WC, Lanson NA, Jr., Stallworth BS, Egeland DB, Delcarpio JB, Bahinski A *et al* (1998). HL-1 cells: a cardiac muscle cell line that contracts and retains phenotypic characteristics of the adult cardiomyocyte. *Proc Natl Acad Sci U S A* **95**: 2979-2984.

Collier JJ, White SM, Claycomb WC, Scott DK (2002). Insulin represses and chronic hyperglycemia stimulates adrenomedullin gene expression in HL-1 cultured cardiac myocytes. *Diabetes* **51**.

Cordeiro JM, Barajas-Martinez H, Hong K, Burashnikov E, Pfeiffer R, Orsino AM *et al* (2006). Compound heterozygous mutations P336L and I1660V in the human cardiac sodium channel associated with the Brugada syndrome. *Circulation* **114**: 2026-2033.

Couchonnal LF, Anderson ME (2008). The role of calmodulin kinase II in myocardial physiology and disease. *Physiology (Bethesda)* **23**: 151-159.

Cunha SR, Mohler PJ (2006). Cardiac ankyrins: Essential components for development and maintenance of excitable membrane domains in heart. *Cardiovasc Res* **71**: 22-29.

Curran ME, Splawski I, Timothy KW, Vincent GM, Green ED, Keating MT (1995). A molecular basis for cardiac arrhythmia: HERG mutations cause long QT syndrome. *Cell* **80**: 795-803.

Das S, Makino S, Melman YF, Shea MA, Goyal SB, Rosenzweig A *et al* (2009). Mutation in the S3 segment of KCNQ1 results in familial lone atrial fibrillation. *Heart Rhythm* **6**: 1146-1153.

de Meeus A, Stephan E, Debrus S, Jean MK, Loiselet J, Weissenbach J *et al* (1995). An isolated cardiac conduction disease maps to chromosome 19q. *Circ Res* **77**: 735-740.

Deal KK, England SK, Tamkun MM (1996). Molecular physiology of cardiac potassium channels. *Physiol Rev* **76**: 49-67.

Deschênes I, Baroudi G, Berthet M, Barde I, Chalvidan T, Denjoy I *et al* (2000). Electrophysiological characterization of SCN5A mutations causing long QT (E1784K) and Brugada (R1512W and R1432G) syndromes. *Cardiovasc Res* **46**: 55-65.

Dhar Malhotra J, Chen C, Rivolta I, Abriel H, Malhotra R, Mattei LN *et al* (2001). Characterization of sodium channel alpha- and beta-subunits in rat and mouse cardiac myocytes. *Circulation* **103**: 1303-1310.

Dhein S, Müller A, Gerwin R, Klaus W (1993). Comparative study on the proarrhythmic effects of some antiarrhythmic agents. *Circulation* **87**: 617-630.

Dib-Hajj SD, Tyrrell L, Black JA, Waxman SG (1998). Na_v1.9, a novel voltage-gated Na channel, is expressed preferentially in peripheral sensory neurons and down-regulated after axotomy. *Proc Natl Acad Sci U S A* **95**: 8963-8968.

Dib-Hajj SD, Tyrrell L, Escayg A, Wood PM, Meisler MH, Waxman SG (1999). Coding sequence, genomic organization, and conserved chromosomal localization of the mouse

gene Scn11a encoding the sodium channel NaN. *Genomics* **59**: 309-318.

Dobrzynski H, Boyett MR, Anderson RH (2007). New insights into pacemaker activity: promoting understanding of sick sinus syndrome. *Circulation* **115**: 1921-1932.

Dumaine R, Wang Q, Keating MT, Hartmann HA, Schwartz PJ, Brown AM *et al* (1996). Multiple mechanisms of Na⁺ channel--linked long-QT syndrome. *Circ Res* **78**: 916-924.

Echt DS, Liebson PR, Mitchell LB, Peters R, Obias-Manno D, Barker AH *et al* (1991). Mortality and morbidity in patients receiving encainide, flecainide, or placebo. The cardiac arrhythmia suppression trial. *N Engl J Med* **324**: 781-788.

Euler DE (1999). Cardiac alternans: mechanisms and pathophysiological significance. *Cardiovasc Res* **42**: 583-590.

Fahmi AI, Patel M, Stevens EB, Fowden AL, John JE, 3rd., Lee K *et al* (2001). The sodium channel beta-subunit SCN3b modulates the kinetics of SCN5a and is expressed heterogeneously in sheep heart. *J Physiol* **537**: 693-700.

Fatkin D, Otway R, Vandenberg JI (2007). Genes and atrial fibrillation: a new look at an old problem. *Circulation* **116**: 782-792.

Fink M, Noble PJ, Noble D (2011). Ca²⁺-induced delayed afterdepolarizations are

triggered by dyadic subspace Ca^{2+} affirming that increasing SERCA reduces aftercontractions. *Am J Physiol Heart Circ Physiol* **301**: H921-935.

Fotia AB, Ekberg J, Adams DJ, Cook DI, Poronnik P, Kumar S (2004). Regulation of neuronal voltage-gated sodium channels by the ubiquitin-protein ligases Nedd4 and Nedd4-2. *J Biol Chem* **279**: 28930-28935.

Fraser H, Belardinelli L, Wang L, Light PE, McVeigh JJ, Clanachan AS (2006). Ranolazine decreases diastolic calcium accumulation caused by ATX-II or ischemia in rat hearts. *J Mol Cell Cardiol* **41**: 1031-1038.

Fredj S, Sampson KJ, Liu H, Kass RS (2006). Molecular basis of ranolazine block of LQT-3 mutant sodium channels: evidence for site of action. *Br J Pharmacol* **148**: 16-24.

Frohnwieser B, Chen LQ, Schreibmayer W, Kallen RG (1997). Modulation of the human cardiac sodium channel alpha-subunit by cAMP-dependent protein kinase and the responsible sequence domain. *J Physiol* **498**: 309-318.

Garcia-Dorado D, Théroux P, Duran JM, Solares J, Alonso J, Sanz E *et al* (1992). Selective inhibition of the contractile apparatus. A new approach to modification of infarct size, infarct composition, and infarct geometry during coronary artery occlusion and reperfusion. *Circulation* **85**: 1160-1174.

Gellens ME, George AL, Jr., Chen LQ, Chahine M, Horn R, Barchi RL *et al* (1992). Primary structure and functional expression of the human cardiac tetrodotoxin-insensitive voltage-dependent sodium channel. *Proc Natl Acad Sci U S A* **89**: 554-558.

George AL, Jr., Gellens ME, Kallen RG, Barchi RL (1990). Molecular cloning and chromosomal location of two human muscle voltage-gated sodium channels. *Soc Neurosci Abst* **16**: 184.

George AL, Jr., Knops JF, Han J, Finley WH, Knittle TJ, Tamkun MM *et al* (1994). Assignment of a human voltage-dependent sodium channel alpha-subunit gene (SCN6A) to 2q21-q23. *Genomics* **19**: 395-397.

George AL, Jr., Varkony TA, Drabkin HA, Han J, Knops JF, Finley WH *et al* (1995). Assignment of the human heart tetrodotoxin-resistant voltage-gated Na⁺ channel α -subunit gene (SCN5A) to band 3p21. *Cytogenet Cell Genet* **68**: 67-70.

Glickman MH, Ciechanover A (2002). The ubiquitin-proteasome proteolytic pathway: destruction for the sake of construction. *Physiol Rev* **82**: 373-428.

Goetz R, Dover K, Laezza F, Shtraizent N, Huang X, Tchetchik D *et al* (2009). Crystal structure of a fibroblast growth factor homologous factor (FHF) defines a conserved surface on FHF for binding and modulation of voltage-gated sodium channels. *J Biol Chem* **284**: 17883-17896.

Goldin AL (2008). Mechanisms of sodium channel inactivation. *Curr Opin Neurobiol* **13**: 284-290.

Gollob MH, LJones D, Krahn AD, Gong LDXQ, Shao Q, Liu X *et al* (2006). Somatic mutations in the connexin 40 gene (GJA5) in atrial fibrillation. *N Engl J Med* **354**: 2677-2688.

Grace AA, Camm AJ (1998). Quinidine. *N Engl J Med* **338**: 35-45.

Grant AO, Carboni MP, Neplioueva V, Starmer CF, Memmi M, Napolitano C *et al* (2002). Long QT syndrome, Brugada syndrome, and conduction system disease are linked to a single sodium channel mutation. *J Clin Invest* **110**: 1201-1209.

Grant AO (2009). Cardiac ion channels. *Circ Arrhythm Electrophysiol* **2**: 185-194.

Grynkiewicz G, Poenie M, Tsien RY (1985). A new generation of Ca²⁺ indicators with greatly improved fluorescence properties. *J Biol Chem* **260**: 3440-3450.

Hallaq H, Yang Z, Viswanathan PC, Fukuda K, Shen W, Wang DW *et al* (2006). Quantitation of protein kinase A-mediated trafficking of cardiac sodium channels in living cells. *Cardiovasc Res* **72**: 250-261.

Han JA, Lu CM, Brown GB, Rado TA (1991). Direct amplification of a single dissected chromosomal segment by polymerase chain reaction: a human brain sodium channel gene is on chromosome 2q22-q23. *Proc Natl Acad Sci U S A* **88**: 335-339.

Hanlon MR, Wallace BA (2002). Structure and function of voltage-dependent ion channel regulatory beta subunits. *Biochemistry* **41**: 2886-2894.

Hedley PL, Jørgensen P, Schlamowitz S, Moolman-Smook J, Kanters JK, Corfield VA *et al* (2009). The genetic basis of Brugada syndrome: a mutation update. *Hum Mutat* **30**: 1256-1266.

Heist EK, Ruskin JN (2010). Drug-induced arrhythmia. *Circulation* **122**: 1426-1435.

Hershko A, Ciechanover A (1998). The ubiquitin system. *Annu Rev Biochem* **67**: 425-479.

Herzog RI, Liu C, Waxman SG, Cummins TR (2003). Calmodulin binds to the C terminus of sodium channels Nav1.4 and Nav1.6 and differentially modulates their functional properties. *J Neurosci* **23**: 8261-8271.

Hodgson-Zingman DM, Karst ML, Zingman LV, Heublein DM, Darbar D, Herron KJ *et al* (2008). Atrial natriuretic peptide frameshift mutation in familial atrial fibrillation. *N Engl J Med* **359**: 158-165.

Hong K, Piper DR, Diaz-Valdecantos A, Brugada J, Oliva A, Burashnikov E *et al* (2005). De novo KCNQ1 mutation responsible for atrial fibrillation and short QT syndrome in utero. *Cardiovasc Res* **68**: 433-440.

Huang H, Zhao J, Barrane FZ, Champagne J, Chahine M (2006). Nav1.5/R1193Q polymorphism is associated with both long QT and Brugada syndromes. *Can J Cardiol* **22**: 309-313.

Hwang HW, Chen JJ, Lin YJ, Shieh RC, Lee MT, Hung SI *et al* (2005). R1193Q of SCN5A, a Brugada and long QT mutation, is a common polymorphism in Han Chinese. *J Med Genet* **42**: e7.

Isenberg G, Klockner U (1982). Calcium tolerant ventricular myocytes prepared by preincubation in a "KB medium". *Pflugers Arch* **395**: 6-18.

Isom LL, De Jongh KS, Patton DE, Reber BF, Offord J, Charbonneau H *et al* (1992). Primary structure and functional expression of the beta 1 subunit of the rat brain sodium channel. *Science* **256**: 839-842.

Isom LL, Ragsdale DS, De Jongh KS, Westenbroek RE, Reber BF, Scheuer T *et al* (1995). Structure and function of the beta 2 subunit of brain sodium channels, a transmembrane glycoprotein with a CAM motif. *Cell* **83**: 433-442.

Itoh H, Shimizu M, Takata S, Mabuchi H, Imoto K (2005). A novel missense mutation in the SCN5A gene associated with Brugada syndrome bidirectionally affecting blocking actions of antiarrhythmic drugs. *J Cardiovasc Electrophysiol* **16**: 686-693.

Jefferis GJ, Meloni BP, Bakker AJ, Knuckey NW (2007). The role of the Na(+)/Ca(2+) exchanger (NCX) in neurons following ischaemia. *J Clin Neurosci* **14**: 507-514.

Jeong SY, Goto J, Hashida H, Suzuki T, Ogata K, Masuda N *et al* (2000). Identification of a novel human voltage-gated sodium channel alpha subunit gene, SCN12A. *Biochem Biophys Res Commun* **267**: 262-270.

Jespersen T, Gavillet B, van Bemmelen MX, Cordonier S, Thomas MA, Staub O *et al* (2006). Cardiac sodium channel Na(v)1.5 interacts with and is regulated by the protein tyrosine phosphatase PTPH1. *Biochem Biophys Res Commun* **648**: 1455-1462.

Juang JM, Huang SK, Tsai CT, Chiang FT, Lin JL, Lai LP *et al* (2003). Characteristics of Chinese patients with symptomatic Brugada syndrome in Taiwan. *Cardiology* **99**: 182-189.

Kane GC, Liu XK, Yamada S, Olson TM, Terzic A (2005). Cardiac KATP channels in health and disease. *J Mol Cell Cardiol* **38**: 937-943.

Kapplinger JD, Tester DJ, Alders M, Benito B, Berthet M, Brugada J *et al* (2010). An international compendium of mutations in the SCN5A-encoded cardiac sodium channel in patients referred for Brugada syndrome genetic testing. *Heart Rhythm* **7**: 33-46.

Kearney JA, Plummer NW, Smith MR, Kapur J, Cummins TR, Waxman SG *et al* (2001). A gain-of-function mutation in the sodium channel gene Scn2a results in seizures and behavioral abnormalities. *Neuroscience* **102**: 307-317.

Kerr NC, Holmes FE, Wynick D (2004). Novel isoforms of the sodium channels Nav1.8 and Nav1.5 are produced by a conserved mechanism in mouse and rat. *J Biol Chem* **279**: 24826-24833.

Kim J, Ghosh S, Liu H, Tateyama M, Kass RS, Pitt GS (2004). Calmodulin mediates Ca²⁺ sensitivity of sodium channels. *J Biol Chem* **279**: 45004-45012.

Kiyosue T, Arita M (1989). Late sodium current and its contribution to action potential configuration in guinea pig ventricular myocytes. *Circ Res* **64**: 389-397.

Klabunde RE (2012). *Cardiovascular physiology concepts*, 2 edn. Lippincott Williams & Wilkins: Baltimore, MD

Knollmann BC, Roden DM (2008). A genetic framework for improving arrhythmia therapy. *Nature* **451**: 929-936.

Ko SH, Lenkowski PW, Lee HC, Mounsey JP, Patel MK (2005). Modulation of Na(v)1.5 by beta1-- and beta3-subunit co-expression in mammalian cells. *Pflugers Arch* **449**: 403-412.

Kohrman DC, Smith MR, Goldin AL, Harris J, Meisler MH (1996). A missense mutation in the sodium channel Scn8a is responsible for cerebellar ataxia in the mouse mutant jolting. *J Neurosci* **16**: 5993-5999.

Kwon HW, Lee SY, Kwon BS, Kim GB, Bae EJ, Kim WH *et al* (2012). Long QT syndrome and dilated cardiomyopathy with SCN5A p.R1193Q polymorphism: cardioverter-defibrillator implantation at 27 months. *Pacing Clin Electrophysiol* **35**: e243-246.

Kyndt F, Probst V, Potet F, Demolombe S, Chevallier JC, Baro I *et al* (2001). Novel SCN5A mutation leading either to isolated cardiac conduction defect or Brugada syndrome in a large French family. *Circulation* **104**: 3081-3086.

Lalli MJ, Yong J, Prasad V, Hashimoto K, Plank D, Babu GJ *et al* (2001). Sarcoplasmic reticulum Ca(2+) atpase (SERCA) 1a structurally substitutes for SERCA2a in the cardiac sarcoplasmic reticulum and increases cardiac Ca(2+) handling capacity. *Circ Res* **89**: 160-167.

Lederer WJ, Tsien RW (1976). Transient inward current underlying arrhythmogenic effects of cardiotonic steroids in Purkinje fibres. *J Physiol* **263**: 73-100.

Lei M, Huang CL, Zhang Y (2008). Genetic Na⁺ channelopathies and sinus node dysfunction. *Prog Biophys Mol Biol* **98**: 171-178.

Lemaitre G, Walker B, Lambert S (2003). Identification of a conserved ankyrin-binding motif in the family of sodium channel α subunits. *J Biol Chem* **278**: 27333-27339.

Lewartowski B, Zdanowski K (1990). Net Ca²⁺ influx and sarcoplasmic reticulum Ca²⁺ uptake in resting single myocytes of the rat heart: comparison with guinea-pig. *J Mol Cell Cardiol* **22**: 1221-1229.

Li CZ, Wang XD, Wang HW, Bian YT, Liu YM (1997). Four types of late Na channel current in isolated ventricular myocytes with reference to their contribution to the lastingness of action potential plateau. *Sheng Li Xue Bao* **49**: 241-248.

Li L, Desantiago J, Chu G, Kranias EG, Bers DM (2000). Phosphorylation of phospholamban and troponin I in beta-adrenergic-induced acceleration of cardiac relaxation. *Am J Physiol Heart Circ Physiol* **278**: H769-779.

Liu CJ, Dib-Hajj SD, Renganathan M, Cummins TR, Waxman SG (2003). Modulation of the cardiac sodium channel Nav1.5 by fibroblast growth factor homologous factor 1B. *J*

Biol Chem **278**: 1029-1036.

Liu H, Sun HY, Lau CP, Li GR (2007). Regulation of voltage-gated cardiac sodium current by epidermal growth factor receptor kinase in guinea pig ventricular myocytes. *J Mol Cell Cardiol* **42**: 760-768.

Liu YM, DeFelice LJ, Mazzanti M (1992). Na channels that remain open throughout the cardiac action potential plateau. *Biophys J* **63**: 654-662.

London B, Michalec M, Mehdi H, Zhu X, Kerchner L, Sanyal S *et al* (2007). Mutation in glycerol-3-phosphate dehydrogenase 1 like gene (GPD1-L) decreases cardiac Na⁺ current and causes inherited arrhythmias. *Circulation* **116**: 2260-2268.

Luca F, Alfio Q, Alessandro V (2009). *Cardiovascular Mathematics: Modeling and simulation of the circulatory system*. springer.

Lundbaek JA, Birn P, Hansen AJ, Søgaaard R, Nielsen C, Girshman J *et al* (2004). Regulation of sodium channel function by bilayer elasticity: the importance of hydrophobic coupling. Effects of Micelle-forming amphiphiles and cholesterol. *J Gen Physiol* **123**: 599-621.

Lupoglazoff JM, Cheav T, Baroudi G, Berthet M, Denjoy I, Cauchemez B *et al* (2002). Homozygous SCN5A mutation in long-QT syndrome with functional two-to-one

atrioventricular block. *Circ Res* **89**: E16-21.

Maier SK, Westenbroek RE, Yamanushi TT, Dobrzynski H, Boyett MR, Catterall WA *et al* (2003). An unexpected requirement for brain-type sodium channels for control of heart rate in the mouse sinoatrial node. *Proc Natl Acad Sci U S A* **100**: 3507-3512.

Makielski JC, Ye B, Valdivia CR, Pagel MD, Pu J, Tester DJ *et al* (2003). A ubiquitous splice variant and a common polymorphism affect heterologous expression of recombinant human SCN5A heart sodium channels. *Circ Res* **93**: 821-828.

Makiyama T, Akao M, Tsuji K, Doi T, Ohno S, Takenaka K *et al* (2005). High risk for bradyarrhythmic complications in patients with Brugada syndrome caused by SCN5A gene mutations. *J Am Coll Cardiol* **46**: 2100-2106.

Makiyama T, Akao M, Shizuta S, Doi T, Nishiyama K, Oka Y *et al* (2008). A novel SCN5A gain-of-function mutation M1875T associated with familial atrial fibrillation. *J Am Coll Cardiol* **52**: 1326-1334.

Malhotra JD, Koopmann MC, Kazen-Gillespie KA, Fettman N, Hortsch M, Isom LL (2002). Structural requirements for interaction of sodium channel beta 1 subunits with ankyrin. *J Biol Chem* **277**: 26681-26688.

Malhotra JD, Thyagarajan V, Chen C, Isom LL (2004). Tyrosine-phosphorylated and

nonphosphorylated sodium channel beta1 subunits are differentially localized in cardiac myocytes. *J Biol Chem* **279**: 40748-40754.

Marban E, Robinson SW, Wier WG (1986). Mechanisms of arrhythmogenic delayed and early afterdepolarizations in ferret ventricular muscle. *J Clin Invest* **78**: 1185-1192.

Marfatia KA, Harreman MT, Fanara P, Vertino PM, Corbett AH (2001). Identification and characterization of the human MOG1 gene. *Gene* **266**: 45-56.

Martin MS, Tang B, Papale LA, Yu FH, Catterall WA, Escayg A (2007). The voltage-gated sodium channel Scn8a is a genetic modifier of severe myoclonic epilepsy of infancy. *Hum Mol Genet* **16**: 2892-2899.

Matsusue A, Kashiwagi M, Hara K, Waters B, Sugimura T, Kubo S (2012). An autopsy case of sudden unexpected nocturnal death syndrome with R1193Q polymorphism in the SCN5A gene. *Leg Med (Tokyo)* **14**: :317-319.

McNair WP, Ku L, Taylor MR, Fain PR, Dao D, Wolfel E *et al* (2004). SCN5A mutation associated with dilated cardiomyopathy, conduction disorder, and arrhythmia. *Circulation* **110**: 2163-2167.

McNaughton PA (1991). Fundamental properties of the Na-Ca exchange. An overview. *Ann N Y Acad Sci* **639**: 2-9.

Meadows LS, Isom LL (2005). Sodium channels as macromolecular complexes: implications for inherited arrhythmia syndromes. *Cardiovasc Res* **67**: 448-458.

Medeiros-Domingo A, Kaku T, Tester DJ, Iturralde-Torres P, Itty A, Ye B *et al* (2007). SCN4B-encoded sodium channel beta4 subunit in congenital long-QT syndrome. *Circulation* **116**: 134-142.

Meyer-Kleine C, Otto M, Zoll B, Koch MC (1994). Molecular and genetic characterisation of German families with paramyotonia congenita and demonstration of founder effect in the Ravensberg families. *Human Genetics* **93**: 707-710.

Mitchell GF, Jeron A, Koren G (1998). Measurement of heart rate and Q-T interval in the conscious mouse. *Am J Physiol* **274**: H747-751.

Mohler PJ, Schott JJ, Gramolini AO, Dilly KW, Guatimosim S, duBell WH *et al* (2003). Ankyrin-B mutation causes type 4 long-QT cardiac arrhythmia and sudden cardiac death. *Nature* **421**: 634-639.

Mohler PJ, Rivolta I, Napolitano C, LeMaillet G, Lambert S, Priori SG *et al* (2004). Nav1.5 E1053K mutation causing Brugada syndrome blocks binding to ankyrin-G and expression of Nav1.5 on the surface of cardiomyocytes. *Proc Natl Acad Sci U S A* **101**: 17533-17538.

Morgan K, Stevens EB, Shah B, Cox PJ, Dixon AK, Lee K *et al* (2000). beta 3: an additional auxiliary subunit of the voltage-sensitive sodium channel that modulates channel gating with distinct kinetics. *Proc Natl Acad Sci U S A* **97**: 2308-2313.

Morrison DK (2009). The 14-3-3 proteins: integrators of diverse signaling cues that impact cell fate and cancer development. *Trends Cell Biol* **19**: 16-22.

Morrow DA, Scirica BM, Karwatowska-Prokopczuk E, Murphy SA, Budaj A, Varshavsky S *et al* (2007). Effects of ranolazine on recurrent cardiovascular events in patients with non-ST-elevation acute coronary syndromes: the MERLIN-TIMI 36 randomized trial. *JAMA* **297**: 1775-1783.

Mulley JC, Scheffer IE, Petrou S, Dibbens LM, Berkovic SF, Harkin LA (2005). SCN1A mutations and epilepsy. *Hum Mutat* **25**: 535-542.

Murphy BJ, Rogers J, Perdichizzi AP, Colvin AA, Catterall WA (1996). cAMP-dependent phosphorylation of two sites in the alpha subunit of the cardiac sodium channel. *J Biol Chem* **271**: 28837-28843.

Murphy E, Perlman M, London RE, Steenbergen C (1991). Amiloride delays the ischemia-induced rise in cytosolic free calcium. *Circ Res* **68**: 1250-1258.

Navedo MF, Cheng EP, Yuan C, Votaw S, Molkentin JD, Scott JD *et al* (2010). Increased coupled gating of L-type Ca²⁺ channels during hypertension and Timothy syndrome. *Circ Res* **106**: 748-756.

Neyroud N, Tesson F, Denjoy I, Leibovici M, Donger C, Barhanin J *et al* (1997). A novel mutation in the potassium channel gene KVLQT1 causes the Jervell and Lange-Nielsen cardioauditory syndrome. *Nat Genet* **15**: 186-189.

Nguyen SV, Claycomb WC (1999). Hypoxia regulates the expression of the adrenomedullin and HIF-1 genes in cultured HL-1 cardiomyocytes. *Biochem Biophys Res Commun* **265**: 382-386.

Nilsen KB, Nicholas AK, Woods CG, Mellgren SI, Nebuchennykh M, Aasly J (2009). Two novel SCN9A mutations causing insensitivity to pain. *Pain* **143**: 155-158.

Oberti C, Wang L, Li L, Dong J, Rao S, Du W *et al* (2004). Genome-wide linkage scan identifies a novel genetic locus on chromosome 5p13 for neonatal atrial fibrillation associated with sudden death and variable cardiomyopathy. *Circulation* **110**: 3753-3759.

Oki M, Nishimoto T (1998). A protein required for nuclear-protein import, Mog1p, directly interacts with GTP-Gsp1p, the *Saccharomyces cerevisiae* ran homologue. *Proc Natl Acad Sci U S A* **95**: 15388-15393.

Olsen SK, Garbi M, Zampieri N, Eliseenkova AV, Ornitz DM, Goldfarb M *et al* (2003). Fibroblast growth factor (FGF) homologous factors share structural but not functional homology with FGFs. *J Biol Chem* **278**: 34226-34236.

Olson TM, Keating MT (1996). Mapping a cardiomyopathy locus to chromosome 3p22-p25. *J Clin Invest* **97**: 528-532.

Olson TM, Michels VV, Ballew JD, Reyna SP, Karst ML, Herron KJ *et al* (2005). Sodium channel mutations and susceptibility to heart failure and atrial fibrillation. *JAMA* **293**: 447-454.

Olson TM, Alekseev AE, Liu XK, Park S, Zingman LV, Bienengraeber M *et al* (2006). Kv1.5 channelopathy due to KCNA5 loss-of-function mutation causes human atrial fibrillation. *Hum Mol Genet* **15**: 2185-2191.

Otway R, Vandenberg JJ, Guo G, Varghese A, Castro ML, Liu J *et al* (2007). Stretch-sensitive KCNQ1 mutation A link between genetic and environmental factors in the pathogenesis of atrial fibrillation. *J Am Coll Cardiol* **49**: 578-586.

Palade GE (1953). An electron microscope study of the mitochondrial structure. *J Histochem Cytochem* **1**: 188-211.

Papadatos GA, Wallerstein PM, Head CE, Ratcliff R, Brady PA, Benndorf K *et al* (2002).

Slowed conduction and ventricular tachycardia after targeted disruption of the cardiac sodium channel gene *Scn5a*. *Proc Natl Acad Sci U S A* **99**: 6210-6215.

Patino GA, Isom LL (2010). Electrophysiology and beyond: multiple roles of Na⁺ channel β subunits in development and disease. *Neurosci Lett* **486**: 53-59.

Picht E, DeSantiago J, Blatter LA, Bers DM (2006). Cardiac alternans do not rely on diastolic sarcoplasmic reticulum calcium content fluctuations. *Circ Res* **99**: 740-748.

Picht E, DeSantiago J, Huke S, Kaetzel MA, Dedman JR, Bers DM (2007). CaMKII inhibition targeted to the sarcoplasmic reticulum inhibits frequency-dependent acceleration of relaxation and Ca²⁺ current facilitation. *J Mol Cell Cardiol* **42**: 196-205.

Pieske B, Maier LS, Piacentino V, 3rd, Weisser J, Hasenfuss G, Houser S (2002). Rate dependence of [Na⁺]_i and contractility in nonfailing and failing human myocardium. *Circulation* **106**: 447-453.

Piper HM (2000). The calcium paradox revisited: an artefact of great heuristic value. *Cardiovasc Res* **45**: 123-127.

Plassart E, Reboul J, Rime C, Recan D, Millasseau P, Eymard B *et al* (1994). Mutations in the muscle sodium channel gene (SCN4A) in 13 French families with hyperkalemic periodic paralysis and paramyotonia congenita: phenotype to genotype correlations and

demonstration of the predominance of two mutations. *Eur J Hum Genet* **2**: 110-124.

Plummer NW, Galt J, Jones JM, Burgess DL, Sprunger LK, Kohrman DC *et al* (1998). Exon organization, coding sequence, physical mapping, and polymorphic intragenic markers for the human neuronal sodium channel gene SCN8A. *Genomics* **54**: 287-296.

Plummer NW, Meisler MH (1999). Evolution and diversity of mammalian sodium channel genes. *Genomics* **57**: 323-331.

Pogwizd SM, Schlotthauer K, Li L, Yuan W, Bers DM (2001). Arrhythmogenesis and contractile dysfunction in heart failure: Roles of sodium-calcium exchange, inward rectifier potassium current, and residual beta-adrenergic responsiveness. *Circ Res* **88**: 1159-1167.

Pogwizd SM, Bers DM (2004). Cellular basis of triggered arrhythmias in heart failure. *Trends Cardiovasc Med* **14**: 61-66.

Potet F, Mabo P, Le Coq G, Probst V, Schott JJ, Airaud F *et al* (2003). Novel brugada SCN5A mutation leading to ST segment elevation in the inferior or the right precordial leads. *J Cardiovasc Electrophysiol* **14**: 200-203.

Potts JF, Regan MR, Rochelle JM, Seldin MF, Agnew WS (1993). A glial-specific voltage-sensitive Na channel gene maps close to clustered genes for neuronal isoforms on

mouse chromosome 2. *Biochem Biophys Res Commun* **197**: 100-104.

Qiu X, Liu W, Hu D, Sun Y, Li L, Li C (2009). Patient with obstructive sleep apnea-hypopnea syndrome and SCN5A mutation (R1193Q polymorphism) associated with Brugada type 2 electrocardiographic pattern. *J Electrocardiol* **42**: 250-253.

Qu Y, Rogers J, Tanada T, Scheuer T, Catterall WA (1994). Modulation of cardiac Na⁺ channels expressed in a mammalian cell line and in ventricular myocytes by protein kinase C. *Proc Natl Acad Sci U S A* **91**: 3289-3293.

Qu Y, Isom LL, Westenbroek RE, Rogers JC, Tanada TN, McCormick KA *et al* (1995). Modulation of cardiac Na⁺ channel expression in *Xenopus* oocytes by beta 1 subunits. *J Biol Chem* **270**: 25696-25701.

Ragsdale DS, McPhee JC, Scheuer T, Catterall WA (1994). Molecular determinants of state-dependent block of Na⁺ channels by local anesthetics. *Science* **265**: 1724-1728.

Ravn LS, Aizawa Y, Pollevick GD, Hofman-Bang J, Cordeiro JM, Dixen U *et al* (2008). Gain of function in IKs secondary to a mutation in KCNE5 associated with atrial fibrillation. *Heart Rhythm* **5**: 427-435.

Reddy BM, Weintraub HS, Schwartzbard AZ (2010). Ranolazine: a new approach to treating an old problem. *Tex Heart Inst J* **37**: 641-647.

Remme CA, Wilde AA, Bezzina CR (2008). Cardiac sodium channel overlap syndromes: different faces of SCN5A mutations. *Trends Cardiovasc Med* **18**: 78-87.

Ritter M, Su Z, Xu S, Shelby J, Barry WH (2000). Cardiac unloading alters contractility and calcium homeostasis in ventricular myocytes. *J Mol Cell Cardiol* **32**: 577-584.

Roden DM, Woosley RL, Primm RK (1986). Incidence and clinical features of the quinidine-associated long QT syndrome: implications for patient care. *Am Heart J* **111**: 1088-1093.

Roden DM (1994). Risks and benefits of antiarrhythmic therapy. *N Engl J Med* **331**: 785-791.

Rook MB, Alshinawi CB, Groenewegen WA, van Gelder IC, van Ginneken AC, Jongsma HJ *et al* (1999). Human SCN5A gene mutations alter cardiac sodium channel kinetics and are associated with the Brugada syndrome. *Cardiovasc Res* **44**: 507-517.

Rossenbacker T, Carroll SJ, Liu H, Kuipéri C, de Ravel TJ, Devriendt K *et al* (2004). Novel pore mutation in SCN5A manifests as a spectrum of phenotypes ranging from atrial flutter, conduction disease, and Brugada syndrome to sudden cardiac death. *Heart Rhythm* **1**: 610-615.

Rota M, Boni A, Urbanek K, Padin-Iruegas ME, Kajstura TJ, Fiore G *et al* (2005). Nuclear targeting of Akt enhances ventricular function and myocyte contractility. *Circ Res* **97**: 1332-1341.

Rotin D, Kumar S (2009). Physiological functions of the HECT family of ubiquitin ligases. *Nat Rev Mol Cell Biol* **10**: 398-409.

Rougier JS, van Bemmelen MX, Bruce MC, Jespersen T, Gavillet B, Apothéloz F *et al* (2005). Molecular determinants of voltage-gated sodium channel regulation by the Nedd4/Nedd4-like proteins. *Am J Physiol Cell Physiol* **288**: C692-701.

Royer A, van Veen TA, Le Bouter S, Marionneau C, Griol-Charhbili V, Léoni AL *et al* (2005). Mouse model of SCN5A-linked hereditary Lenègre's disease: age-related conduction slowing and myocardial fibrosis. *Circulation* **111**: 1738-1746.

Ruan Y, Liu N, Bloise R, Napolitano C, Priori SG (2007). Gating properties of SCN5A mutations and the response to mexiletine in long-QT syndrome type 3 patients. *Circulation* **116**: 1137-1144.

Ruan Y, Liu N, Priori SG (2009). Sodium channel mutations and arrhythmias. *Nat Rev Cardiol* **6**: 337-348.

Saimi Y, Kung C (2002). Calmodulin as an ion channel subunit. *Annu Rev Physiol* **64**:

289-311.

Saint DA (2008). The cardiac persistent sodium current: an appealing therapeutic target. *Br J Pharmacol* **153**: 1133-1142.

Saitoh M, Shinohara M, Hoshino H, Kubota M, Amemiya K, Takanashi JL *et al* (2012). Mutations of the SCN1A gene in acute encephalopathy. *Epilepsia* **53**: 558-564.

Sandow A (1952). Excitation-contraction coupling in muscular response. *Yale J Biol Med* **25**: 176-201.

Schmitt JP, Kamisago M, Asahi M, Li GH, Ahmad F, Mende U *et al* (2003). Dilated cardiomyopathy and heart failure caused by a mutation in phospholamban. *Science* **299**: 1410-1413.

Schott JJ, Alshinawi C, Kyndt F, Probst V, Hoorntje TM, Hulsbeek M *et al* (1999). Cardiac conduction defects associate with mutations in SCN5A. *Nat Genet* **23**: 20-21.

Schroeter A, Walzik S, Blechschmidt S, Haufe V, Benndorf K, Zimmer T (2010). Structure and function of splice variants of the cardiac voltage-gated sodium channel Na(v)1.5. *J Mol Cell Cardiol* **49**: 16-24.

Schulze-Bahr E, Eckardt L, Breithardt G, Seidl K, Wichter T, Wolpert C *et al* (2003).

Sodium channel gene (SCN5A) mutations in 44 index patients with Brugada syndrome: different incidences in familial and sporadic disease. *Hum Mutat* **21**: 651-652.

Sedj S, Heinzl FR, Walther S, Dybkova N, Wakula P, Groborz J *et al* (2010). Na⁺-dependent SR Ca²⁺ overload induces arrhythmogenic events in mouse cardiomyocytes with a human CPVT mutation. *Cardiovasc Res* **87**: 50-59.

Selzer A, Wray HW (1964). Quinidine syncope. paroxysmal ventricular fibrillation occurring during treatment of chronic atrial arrhythmias. *Circulation* **30**: 17-26.

Shah VN, Wingo TL, Weiss KL, Williams CK, Balser JR, Chazin WJ (2006). Calcium-dependent regulation of the voltage-gated sodium channel hH1: intrinsic and extrinsic sensors use a common molecular switch. *Proc Natl Acad Sci U S A* **103**: 3592-3597.

Sheets MF, Fozzard HA, Lipkind GM, Hanck DA (2010). Sodium channel molecular conformations and antiarrhythmic drug affinity. *Trends Cardiovasc Med* **20**: 16-21.

Shim SH, Ito M, Maher T, Milunsky A (2005). Gene sequencing in neonates and infants with the long QT syndrome. *Genet Test* **9**: 281-284.

Shin DJ, Kim E, Park SB, Jang WC, Bae Y, Han J *et al* (2007). A novel mutation in the SCN5A gene is associated with Brugada syndrome. *Life Sci* **80**: 719-727.

Sicouri S, Antzelevitch D, Heilmann C, Antzelevitch C (1997). Effects of sodium channel block with mexiletine to reverse action potential prolongation in in vitro models of the long term QT syndrome. *J Cardiovasc Electrophysiol* **8**: 1280-1290.

Skinner JR, Chung SK, Montgomery D, McCulley CH, Crawford J, French J *et al* (2005). Near-miss SIDS due to Brugada syndrome. *Arch Dis Child* **90**: 528-529.

Smits JP, Koopmann TT, Wilders R, Veldkamp MW, Opthof T, Bhuiyan ZA *et al* (2005). A mutation in the human cardiac sodium channel (E161K) contributes to sick sinus syndrome, conduction disease and Brugada syndrome in two families. *J Mol Cell Cardiol* **38**: 969-981.

Song KS, Scherer PE, Tang Z, Okamoto T, Li S, Chafel M *et al* (1996). Expression of caveolin-3 in skeletal, cardiac, and smooth muscle cells. Caveolin-3 is a component of the sarcolemma and co-fractionates with dystrophin and dystrophin-associated glycoproteins. *J Biol Chem* **271**: 160-165.

Song Y, Shryock JC, Wagner S, Maier LS, Belardinelli L (2006). Blocking late sodium current reduces hydrogen peroxide-induced arrhythmogenic activity and contractile dysfunction. *J Pharmacol Exp Ther* **318**: 214-222.

Splawski I, Timothy KW, Vincent GM, Atkinson DL, Keating MT (1997a). Molecular

basis of the long-QT syndrome associated with deafness. *N Engl J Med* **336**: 1562-1567.

Splawski I, Tristani-Firouzi M, Lehmann MH, Sanguinetti MC, Keating MT (1997b). Mutations in the hminK gene cause long QT syndrome and suppress IKs function. *Nat Genet* **17**: 338-340.

Splawski I, Shen J, Timothy KW, Lehmann MH, Priori S, Robinson JL *et al* (2000). Spectrum of mutations in long-QT syndrome genes. KVLQT1, HERG, SCN5A, KCNE1, and KCNE2. *Circulation* **102**: 1178-1185.

Staub O, Rotin D (2006). Role of ubiquitylation in cellular membrane transport. *Physiol Rev* **86**: 669-677.

Stone PH, Gratsiansky NA, Blokhin A, Huang IZ, Meng L (2006). Antianginal efficacy of ranolazine when added to treatment with amlodipine: the ERICA (Efficacy of Ranolazine in Chronic Angina) trial. *J Am Coll Cardiol* **48**: 566-575.

Sun A, Xu L, Wang S, Wang K, Huang W, Wang Y *et al* (2008). SCN5A R1193Q polymorphism associated with progressive cardiac conduction defects and long QT syndrome in a Chinese family. *J Med Genet* **45**: 127-128.

Takehara N, Makita N, Kawabe J, Sato N, Kawamura Y, Kitabatake A *et al* (2004). A cardiac sodium channel mutation identified in Brugada syndrome associated with atrial

standstill. *J Intern Med* **255**: 137-142.

Tan HL, Bink-Boelkens MT, Bezzina CR, Viswanathan PC, Beaufort-Krol GC, van Tintelen PJ *et al* (2001). A sodium-channel mutation causes isolated cardiac conduction disease. *Nature* **409**: 1043-1047.

Tan HL, Kupersmidt S, Zhang R, Stepanovic S, Roden DM, Wilde AA *et al* (2002). A calcium sensor in the sodium channel modulates cardiac excitability. *Nature* **415**: 442-447.

Tang Z, Scherer PE, Okamoto T, Song K, Chu C, Kohtz DS *et al* (1996). Molecular cloning of caveolin-3, a novel member of the caveolin gene family expressed predominantly in muscle. *J Biol Chem* **274**: 2255-2261.

Tian XL, Yong SL, Wan X, Wu L, Chung MK, Tchou PJ *et al* (2004). Mechanisms by which SCN5A mutation N1325S causes cardiac arrhythmias and sudden death in vivo. *Cardiovasc Res* **61**: 256-267.

Tian XL, Wang QK (2006). Generation of transgenic mice for cardiovascular research. *Methods Mol Med* **129**: 68-81.

Tian XL, Cheng Y, Zhang T, Liao ML, Yong SL, Wang QK (2007). Optical mapping of ventricular arrhythmias in LQTS mice with SCN5A mutation N1325S. *Biochem Biophys*

Res Commun **352**: 879-883.

Tristani-Firouzi M, Jensen JL, Donaldson MR, Sansone V, Meola G, Hahn A *et al* (2002). Functional and clinical characterization of KCNJ2 mutations associated with LQT7 (Andersen syndrome). *J Clin Invest* **110**: 381-388.

Trudeau MM, Dalton JC, Day JW, Ranum LP, Meisler MH (2006). Heterozygosity for a protein truncation mutation of sodium channel SCN8A in a patient with cerebellar atrophy, ataxia, and mental retardation. *J Med Genet* **43**: 527-530.

Ueda K, Valdivia C, Medeiros-Domingo A, Tester DJ, Vatta M, Farrugia G *et al* (2008). Syntrophin mutation associated with long QT syndrome through activation of the nNOS-SCN5A macromolecular complex. *Proc Natl Acad Sci U S A* **105**: 9355-9360.

Undrovinas AI, Shander GS, Makielski JC (1995). Cytoskeleton modulates gating of voltage-dependent sodium channel in heart. *Am J Physiol* **269**: H203-214.

Valdivia CR, Ackerman MJ, Tester DJ, Wada T, McCormack J, Ye B *et al* (2002). A novel SCN5A arrhythmia mutation, M1766L, with expression defect rescued by mexiletine. *Cardiovasc Res* **55**: 279-289.

Van Norstrand DW, Valdivia CR, Tester DJ, Ueda K, London B, Makielski JC *et al* (2007). Molecular and functional characterization of novel glycerol-3-phosphate

dehydrogenase 1 like gene (GPD1-L) mutations in sudden infant death syndrome. *Circulation* **116**: 2253-2259.

Veldkamp MW, Wilders R, Baartscheer A, Zegers JG, Bezzina CR, Wilde AA (2003). Contribution of sodium channel mutations to bradycardia and sinus node dysfunction in LQT3 families. *Circ Res* **92**: 976-913.

Vincent GM (2003). *Romano-Ward Syndrome*. University of Washington: Seattle (WA).

Wagner S, Dybkova N, Rasenack EC, Jacobshagen C, Fabritz L, Kirchhof P *et al* (2006). Ca²⁺/calmodulin-dependent protein kinase II regulates cardiac Na⁺ channels. *J Clin Invest* **116**: 3127-3138.

Wallace RH, Scheffer IE, Barnett S, Richards M, Dibbens L, Desai RR *et al* (2001). Neuronal sodium-channel alpha1-subunit mutations in generalized epilepsy with febrile seizures plus. *Am J Hum Genet* **68**: 859-865.

Wan X, Chen S, Sadeghpour A, Wang Q, Kirsch GE (2001). Accelerated inactivation in a mutant Na(+) channel associated with idiopathic ventricular fibrillation. *Am J Physiol Heart Circ Physiol* **280**: H354-360.

Wang DW, Desai RR, Crotti L, Arnestad M, Insolia R, Pedrazzini M *et al* (2007). Cardiac sodium channel dysfunction in sudden infant death syndrome. *Circulation* **115**: 368-376.

Wang L, Lopaschuk GD, Clanachan AS (2008). H₂O₂-induced left ventricular dysfunction in isolated working rat hearts is independent of calcium accumulation. *J Mol Cell Cardiol* **45**: 787-795.

Wang P, Yang Q, Wu X, Yang Y, Shi L, Wang C *et al* (2010). Functional dominant-negative mutation of sodium channel subunit gene SCN3B associated with atrial fibrillation in a Chinese GeneID population. *Biochem Biophys Res Commun* **398**: 98-104.

Wang Q, Shen J, Li Z, Timothy K, Vincent GM, Priori SG *et al* (1995a). Cardiac sodium channel mutations in patients with long QT syndrome, an inherited cardiac arrhythmia. *Hum Mol Genet* **4**: 1603-1607.

Wang Q, Shen J, Splawski I, Atkinson D, Li Z, Robinson JL *et al* (1995b). SCN5A mutations associated with an inherited cardiac arrhythmia, long QT syndrome. *Cell* **80**: 805-811.

Wang Q, Curran ME, Splawski I, Burn TC, Millholland JM, VanRaay TJ *et al* (1996a). Positional cloning of a novel potassium channel gene: KVLQT1 mutations cause cardiac arrhythmias. *Nat Genet* **12**: 17-23.

Wang Q, Li Z, Shen J, Keating MT (1996b). Genomic organization of the human SCN5A

gene encoding the cardiac sodium channel. *Genomics* **34**: 9-16.

Wang Q, Chen S, Chen Q, Wan X, Shen J, Hoeltge GA *et al* (2004). The common SCN5A mutation R1193Q causes LQTS-type electrophysiological alterations of the cardiac sodium channel. *J Med Genet* **41**: e66.

Wang TJ, Larson MG, Levy D, Vasan RS, Leip EP, Wolf PA *et al* (2003). Temporal relations of atrial fibrillation and congestive heart failure and their joint influence on mortality: the Framingham Heart Study. *Circulation* **107**: 2920-2925.

Wang Z, Fermini B, Nattel S (1995c). Effects of flecainide, quinidine, and 4-aminopyridine on transient outward and ultrarapid delayed rectifier currents in human atrial myocytes. *J Pharmacol Exp Ther* **272**: 184-196.

Watanabe H, Darbar D, Kaiser DW, Jiramongkolchai K, Chopra S, Donahue BS *et al* (2009). Mutations in sodium channel beta1- and beta2-subunits associated with atrial fibrillation. *Circ Arrhythm Electrophysiol* **2**: 268-275.

Wattanasirichaigoon D, Vesely MR, Duggal P, Levine JC, Blume ED, Wolff GS *et al* (1999). Sodium channel abnormalities are infrequent in patients with long QT syndrome: identification of two novel SCN5A mutations. *Am J Med Genet* **86**: 470-476.

Wei J, Wang DW, Alings M, Fish F, Wathen M, Roden DM *et al* (1999). Congenital

long-QT syndrome caused by a novel mutation in a conserved acidic domain of the cardiac Na⁺ channel. *Circulation* **99**: 3165-3171.

Weiss R, Barmada MM, Nguyen T, Seibel JS, Cavlovich D, Kornblit CA *et al* (2002). Clinical and molecular heterogeneity in the Brugada syndrome: a novel gene locus on chromosome 3. *Circulation* **105**: 707-713.

White SM, Constantin P, Claycomb WC (2004). Cardiac physiology at the cellular level: use of cultured HL-1 cardiomyocytes for studies of cardiac muscle cell structure and function. *Am J Physiol Heart Circ Physiol* **286**: H823-829.

Wier WG (1990). Cytoplasmic [Ca²⁺] in mammalian ventricle: dynamic control by cellular processes. *Annu Rev Physiol* **52**: 467-485.

Williams IA, Xiao XH, Ju YK, Allen DG (2007). The rise of [Na(+)] (i) during ischemia and reperfusion in the rat heart-underlying mechanisms. *Pflugers Arch* **454**: 903-912.

Williams TM, Lisanti MP (2004). The Caveolin genes: from cell biology to medicine. *Ann Med* **36**: 584-595.

Wingo TL, Shah VN, Anderson ME, Lybrand TP, Chazin WJ, Balser JR (2004). An EF-hand in the sodium channel couples intracellular calcium to cardiac excitability. *Nat Struct Mol Biol* **11**: 219-225.

Woosley RL, Chen Y, Freiman JP, Gillis RA (1993). Mechanism of the cardiotoxic actions of terfenadine. *JAMA* **269**: 1532-1536.

Wu L, Yong SL, Fan C, Ni Y, Yoo S, Zhang T *et al* (2008). Identification of a new co-factor, MOG1, required for the full function of cardiac sodium channel Nav 1.5. *J Biol Chem* **283**: 6968-6978.

Wwidmann S (1955). Effects of calcium ions and local anesthetics on electrical properties of Purkinje fibres. *J Physiol* **129**: 568-582.

Yang Y, Xia M, Jin Q, Bendahhou S, Shi J, Chen Y *et al* (2004). Identification of a KCNE2 gain-of-function mutation in patients with familial atrial fibrillation. *Am J Hum Genet* **75**: 899-905.

Yang Y, Yang Y, Liang B, Liu J, Li J, Grunnet M *et al* (2010). Identification of a Kir3.4 mutation in congenital long QT syndrome. *Am J Hum Genet* **86**: 872-880.

Yarbrough TL, Lu T, Lee HC, Shibata EF (2002). Localization of cardiac sodium channels in caveolin-rich membrane domains: regulation of sodium current amplitude. *Circ Res* **90**: 443-449.

Yong SL, Ni Y, Zhang T, Tester DJ, Ackerman MJ, Wang QK (2007). Characterization of

the cardiac sodium channel SCN5A mutation, N1325S, in single murine ventricular myocytes. *Biochem Biophys Res Commun* **352**: 378-393.

Yu FH, Westenbroek RE, Silos-Santiago I, McCormick KA, Lawson D, Ge P *et al* (2003). Sodium channel beta4, a new disulfide-linked auxiliary subunit with similarity to beta2. *J Neurosci* **23**: 7577-7585.

Zaza A, Belardinelli L, Shryock JC (2008). Pathophysiology and pharmacology of the cardiac "late sodium current.". *Pharmacol Ther* **119**: 326-339.

Zhang KX, Zhu DL, He X, Zhang Y, Zhang H, Zhao R *et al* (2003). [Association of single nucleotide polymorphism in human SCN7A gene with essential hypertension in Chinese]. *Zhonghua Yi Xue Yi Chuan Xue Za Zhi* **20**: 463-467.

Zhang T, Yong S, Drink J, Popvic Z, Wang Q (2006). Late sodium currents generated by mutation N1325S in sodium channel gene SCN5A cause heart failure. *Circulation* **114**: II-65.

Zhang T, Yong SL, Tian XL, Wang QK (2007). Cardiac-specific overexpression of SCN5A gene leads to shorter P wave duration and PR interval in transgenic mice. *Biochem Biophys Res Commun* **355**: 444-450.

Zhang T, Yong SL, Drinko JK, Popović ZB, Shryock JC, Belardinelli L *et al* (2011).

LQTS mutation N1325S in cardiac sodium channel gene SCN5A causes cardiomyocyte apoptosis, cardiac fibrosis and contractile dysfunction in mice. *Int J Cardiol* **147**: 239-245.

Zhang X, Chen S, Yoo S, Chakrabarti S, Zhang T, Ke T *et al* (2008). Mutation in nuclear pore component NUP155 leads to atrial fibrillation and early sudden cardiac death. *Cell* **135**: 1017-1027.

Zhou J, Yi J, Hu N, George AL, Jr., Murray KT (2000). Activation of protein kinase A modulates trafficking of the human cardiac sodium channel in *Xenopus* oocytes. *Circ Res* **87**: 33-38.